People's Democratic Republic of Algeria
Ministry of Higher Education and Scientific Research

Batna 2 University - Mostefa Ben Boulaïd
Faculty of Technology
Electronics Department

Thesis

Advanced Electronics Laboratory

Submitted for the diploma of:

Doctorate 3rd cycle LMD
Option: Automatic

Under the Theme:

Forecasting Daily Global Solar Radiation on a Horizontal Surface Using Artificial Intelligence Methods

Submitted by:

YAHIAOUI Samah

In front of a jury composed of:

Mr. ABDESSEMED Foudil	Pr.	University of Batna2	Chairman
Ms. ASSAS Ouarda	Pr.	University of Batna2	Supervisor
Mr. CHAFAA kheireddine	Pr.	University of Batna2	Examiner
Mr. BOUZGOU Hassen	Pr.	University of Batna2	Examiner
Mr. ZEROUAL Abdelhafid	Dr.	University of Skikda	Examiner

2023\ 2024

Dedication

With heartfelt sincerity, I present this work as a dedication to all those who are dear to me,

In memory of my father.

From the depths of my thoughts, this work is dedicated to my father, the best dad in the world, who passed away prematurely. His unfailing support and constant encouragement were the pillars of my academic success. As a testament to his love, sacrifices and invaluable advice, which helped shape the person I am today. May God Almighty receive her into His holy mercy!

To my dear mother

To my mother, an inexhaustible source of support and love since I was a child, I offer my most sincere thanks. May your blessing be with me always. May you enjoy health, happiness and long life, thanks to the grace of God, the Most High.

To my husband RAZIK

To the man who shares my life and is a constant source of support, love and inspiration, I dedicate this work with infinite gratitude. Your unwavering encouragement has been a beacon in my academic and personal journey.

To my sisters(Linda and Amel), my brothers(Kais , Djarir and Djamil)

To those who have never ceased to encourage and support me, I wish even greater success in their own journeys.

To my friends

And to all those I love and who love me..

Acknowledgments

First of all, I express my gratitude to the Almighty, **ALLAH**, for having given me the health, the will, the courage and the patience to complete my training and to be able to carry out this modest work.

My warmest thanks and deepest gratitude go to **Pr.Assas Ouarda**, for having supervised my thesis. Her pertinent advices, attentiveness, kindness and patience enabled my work to come to fruition and see the light of day.

I would like to thank **Mr.Abdessemed Foudil**, professor at the University of Batna 2, for the honor of chairing this thesis jury. I would also like to thank **Mr.Chafaa Kheireddine** and **Mr.Hassen Bouzgou**, professors at the University of Batna 2, and **Mr.Zeroual Abdelhafid**, doctor at the University of Skikda, who kindly examined this work, and I would like to thank them for agreeing to serve on the jury.

Many thanks to my brother **Pr.Djarir Yahiaoui**, who gave me his moral and intellectual support throughout the process.

I would like to thank **Ms.Bouhamida Farida** and **Ms.Boussajada Fadila**for there invaluable help during the most difficult of times.

Finally, I would like to thank all those who contributed in any way to the realization of this work.

Yahiaoui Samah

Abstract

Since the creation of the earth, the sun has been an inexhaustible source of energy. For this reason, this research work is focused on exploiting this star to maximize its use by predicting solar radiation. In this work, the main objective was to improve the accuracy of solar radiation forecasts for the city of Batna, Algeria by exploiting the advanced capabilities of artificial intelligence techniques. These data span a decade (1996-2005) and are sourced from the Helio-Clim1 database. In this work, several artificial intelligence models are presented, divided into two categories: classical model, such as regression, and intelligent models, which are in turn divided into two subcategories, including individual models (Fuzzy Logic, MLP, RNN, CNN, LSTM, DT, M5, GBDT, XGBoost, CatBoost, RF, SVR and KNN) as well as hybrid models (The average, The geometric average, The harmonic average and The weighted average). The results of our analyses indicate that the multilayer neural network (MLP) model, integrating multiple meteorological parameters (temperature, humidity, pressure, wind speed, wind direction and rain) with the following numerical results: MSE=9.014, MAE=2.180, RMSE=3.002 and R2=0.918 are the best performing approach for predicting global solar radiation in Batna.

Key words : Solar Radiation Global , Prediction, Artificial Intelligence.

Resumé

Depuis la création de la terre, le soleil est une source d'énergie inépuisable. C'est pourquoi les travaux se concentrent sur l'exploitation de cet astre afin de maximiser son utilisation en prédisant le rayonnement solaire. Dans ce travail, l'objectif principal était d'améliorer la précision des prévisions du rayonnement solaire pour la ville de Batna, en Algérie, en exploitant les capacités avancées des techniques d'intelligence artificielle. Ces données couvrent une décennie (1996-2005) et proviennent de la base de données Helio-Clim1. Dans ce travail, plusieurs modèles d'intelligence artificielle sont présentés, divisés en deux catégories : les modèles classiques, tels que la régression, et les modèles intelligents, qui sont à leur tour divisés en deux sous-catégories, comprenant des modèles individuels (Fuzzy Logique, MLP, RNN, CNN, LSTM, DT, M5, GBDT, XGBoost, CatBoost, RF, SVR et KNN) ainsi que des modèles hybrides (La moyenne, La moyenne géométrique, La moyenne harmonique, Le vote majoritaire et La moyenne pondérée). Les résultats de nos analyses indiquent que le modèle de réseau neuronal multicouche (MLP), intégrant de multiples paramètres météorologiques (température, humidité, pression, vitesse du vent, direction du vent et pluie) avec les résultats numériques suivants : MSE=9.014, MAE=2.180, RMSE=3.002 et R2=0.918 est l'approche la plus performante pour prédire le rayonnement solaire global à Batna.

Mots clés : Rayonnement solaire global, prédiction, intelligence artificielle.

الملخص:

منذ خلق الأرض، كانت الشمس مصدراً لا ينضب للطاقة. ولهذا السبب يركز العمل على استغلال هذا النجم لتعظيم الاستفادة منه من خلال التنبؤ بالإشعاع الشمسي. كان الهدف الرئيسي في هذا العمل هو تحسين دقة توقعات الإشعاع الشمسي لمدينة باتنة بالجزائر، وذلك باستغلال القدرات المتقدمة لتقنيات الذكاء الاصطناعي. تغطي البيانات عقداً من الزمن (1996-2005) وهي مستمدة من قاعدة بيانات هيليو-كليم1. في هذا العمل، يتم عرض العديد من نماذج الذكاء الاصطناعي، مقسمة إلى فئتين: النماذج الكلاسيكية، مثل الانحدار، والنماذج الذكية، والتي تنقسم بدورها إلى فئتين فرعيتين، بما في ذلك النماذج الفردية (المنطق الضبابي، MLP، RNN، CNN، LSTM، DT، M5، GBDT، XGBDT، CatBoost، RF، SVR و KNN) بالإضافة إلى النماذج الهجينة (المتوسط، والمتوسط الهندسي، والمتوسط التوافقي، وتصويت الأغلبية، والمتوسط المرجح). تشير نتائج تحليلاتنا إلى أن نموذج الشبكة العصبية متعددة الطبقات (MLP)، الذي يدمج معاملات أرصاد جوية متعددة (درجة الحرارة والرطوبة والضغط وسرعة الرياح واتجاه الرياح وهطول الأمطار) مع النتائج العددية التالية: MSE=9.014 ، MAE=2.180 ، RMSE=3.002 و R2=0.918 هو أفضل النماذج أداءً للتنبؤ بالإشعاع الشمسي العالمي في باتنة.

الكلمات المفتاحية: الإشعاع الشمسي العالمي ، التنبؤ، الذكاء الاصطناعي.

Contents

List of Tables

List of Figures

GENERAL INTRODUCTION

Solar radiation constitutes a primary and crucial energy source, and a huge potential source of energy, of vital importance for a multitude of fundamental applications, including power generation, agriculture and tourism. Firstly, it powers electricity generation using photovoltaic and thermal technologies, offering a clean, renewable alternative to traditional energy sources. At the same time, the sun's impact is crucial in agriculture, influencing plant growth cycles, photosynthesis and the regulation of seasons, making it an essential pillar of global food production. The sun's rays also play an undeniable role in tourism, influencing climatic conditions and shaping attractive landscapes that attract travelers from all over the world to sunny destinations for leisure and relaxation. So the sun is much more than just a source of light; it is an essential pillar of our daily lives, supporting crucial sectors of our economy and well-being.

Algeria is the largest country in Africa and because of its privileged geographical location. It has one of the richest solar deposits in the world, with average annual insolation ranging from 2,000 to 3,900 kWh/m2 depending on the region. Most of Algeria receives more than 2,000 hours of sunshine a year, and up to 3,900 hours in the desert regions. The vast expanses of desert in the Sahara offer ideal conditions for the development of large-scale solar energy projects. Exploiting this abundant solar resource offers enormous potential for meeting the country's energy needs, reducing its dependence on fossil fuels and encouraging a transition to clean, renewable energy.

Predicting solar radiation is of vital importance in a number of areas. In environmental terms, it enables us to better understand and anticipate climate variations, changes in the ozone layer and their impact on human health. In terms of energy, accurate prediction of solar radiation is essential for maximizing the efficiency of photovoltaic and thermal installations, by planning their energy production according to solar availability. What's more, in the space sector, anticipating fluctuations in solar radiation is crucial for protecting satellites and astronauts from the harmful radiation emitted by the sun.

For agriculture, solar radiation forecasting is important for Optimizing crops by determining the best time to plant, harvest and waters their crops. For agriculture, solar radiation prediction is important for optimizing crops by determining the best time to plant, harvest and water crops.

Farmers use prediction to determine when and how much water to bring to their crops, and to combat the pests and diseases that affect their crops. Some pests and diseases are more active at certain times of the year, depending on the amount of sunlight at certain times of the year, depending on solar radiation.For the economy, solar radiation forecasts enable companies to plan their solar energy production more efficiently, adjusting their operations to maximize energy production during peak periods. This includes the ability to schedule maintenance during periods of low production, thus reducing repair and maintenance costs.

In short, the ability to accurately predict solar radiation has a significant impact on the environment, energy, space, and agriculture and economy exploration.

Despite extensive scientific advancements, humans continue to pursue technological improvements for daily tasks and quality of life. However, this progress often comes at the cost of increased electricity consumption. Thankfully, solar energy offers a renewable solution, and measuring its daily global radiation – a crucial climate factor – is essential. While pyranometers play a valuable role in this measurement, they have some limitations. Here are some key drawbacks of pyranometers:

•**Cost and Expertise:** They are expensive instruments requiring technical knowledge for proper installation and calibration.

•**Reflected Radiation:** They cannot measure radiation reflected from surfaces like water and buildings, leading to incomplete data.

•**Maintenance Needs:** Consistent upkeep is necessary to ensure accurate readings.

By acknowledging these limitations, we can explore alternative measurement techniques and refine pyranometer technology to achieve more comprehensive and effective solar radiation monitoring.

Despite its immense solar potential and vast surface area, Algeria has long faced a major challenge: the lack of data on solar radiation throughout the country.Also, in Algeria, a few stations for collecting solar radiation have been established to observe and quantify solar radiation.

- Center for the Development of Renewable Energies (CDER) - Algiers.
- Center of Research in Astronomy, Astrophysics, and Geophysics (CRAAG) - Bouzareah (Algiers).
- University of Science and Technology Houari Boumediene (USTHB) - Bab Ezzouar (Algiers).
- National Agency for the Promotion and Rationalization of Energy Use (APRUE) - Algiers (Algeria).

To remedy the problem of gaps in solar radiation data, it is crucial to turn to forecast these data. This approach would make up for the current shortcomings by estimating solar radiation information more accurately, thus offering more reliable prospects for various applications and fields of study. Traditional methods of forecasting solar radiation use physical models based on the laws of physics. Artificial intelligence (AI) techniques offer a promising approach to solar radiation forecasting. AIs are capable of learning from data and generalizing their knowledge to new cases. The aim of this thesis is to study the use of AI for forecasting daily solar radiation. The aim is to develop AI models capable of accurately predicting solar radiation. The specific objectives of the thesis are as follows:

- To study the different AI techniques that can be used for solar radiation forecasting.
- To develop an AI model capable of accurately predicting solar radiation.
- Compare the performance of different AI techniques.
- The thesis further aims to advance the field by exploring the fusion and synergy of various AI methodologies, culminating in the creation of hybrid models, a pivotal step towards achieving unprecedented accuracy and reliability in solar radiation prediction.

The thesis is divided into three chapters:

- The first chapter presents the solar resource solar potential in Algeria. It offers an in-depth exploration of the country's solar energy landscape, highlighting its geographical advantages and solar irradiance levels across different regions
- The second chapter is an extensive review of the research and developments in forecasting daily global solar radiation. It encompasses a detailed analysis of various forecasting models, methodologies, and techniques employed in predicting solar radiation.
- The third chapter is an in-depth experimental study of the models proposed and adopted for predicting solar radiation, highlighting the results obtained and the related discussions.

Finally, our conclusion focuses on the key takeaways from our research, their implications for ongoing scientific discourse, and promising areas for future research within this field.

Chapter I

SOLAR ENERGY IN ALGERIA

SOLAR ENERGY IN ALGERIA

I.1 Introduction

Solar energy, a generous gift from our Star, is a promising solution to today's energy challenges. By harnessing sunlight, this inexhaustible resource offers a clean, sustainable alternative to fossil fuels. From the discovery of the photovoltaic effect in the 19th century to today's large-scale solar power plants, the history of solar energy has been marked by major technological advances.

This chapter is devoted to the theoretical study of solar radiation. We undertake an in-depth exploration of the various crucial parameters and their interrelationships. Understanding these elements is of vital importance in fields as varied as solar energy, meteorology and ecology. First, we highlight the solar constant, the essential basis of our analysis, describing its significance and the associated measurement methods. Next, we look at solar inclination, examining its influence on the distribution of solar radiation at the Earth's surface and its role in seasonal phenomena. Solar declination, closely linked to the Sun's angle of elevation, is then detailed, highlighting its seasonal variations and its impact on the amount of radiation received at different latitudes. Incidence angle, the final key parameter, is explored in depth, demonstrating how it modifies the amount of solar energy reaching the Earth's surface as a function of latitude and time of day. We enrich our analysis by examining in detail the relationships between these parameters, clarifying the complex links that govern the behavior of solar radiation. These relationships are formalized using equations and illustrated graphically for a deeper understanding. Finally, we discuss the deposit in Algeria and in the city of Batna, and the prospects for exploiting this field.

I.2 Solar energy

The sun is indispensable to life on earth, acting as a gigantic nuclear reactor that radiates electromagnetic energy. Some of this energy reaches the Earth, making it a livable planet. Although solar energy has the disadvantage of being intermittent and diluted in space, it has the advantage of being free and inexhaustible on a human scale. As a result, solar energy is gradually replacing fuel energy, which is on the way out because of its many drawbacks, the most enormous of which is that it is polluting and harmful to nature. Solar energy can simply be collected using photovoltaic (PV) panels. The figure I.1 shows the solar system.

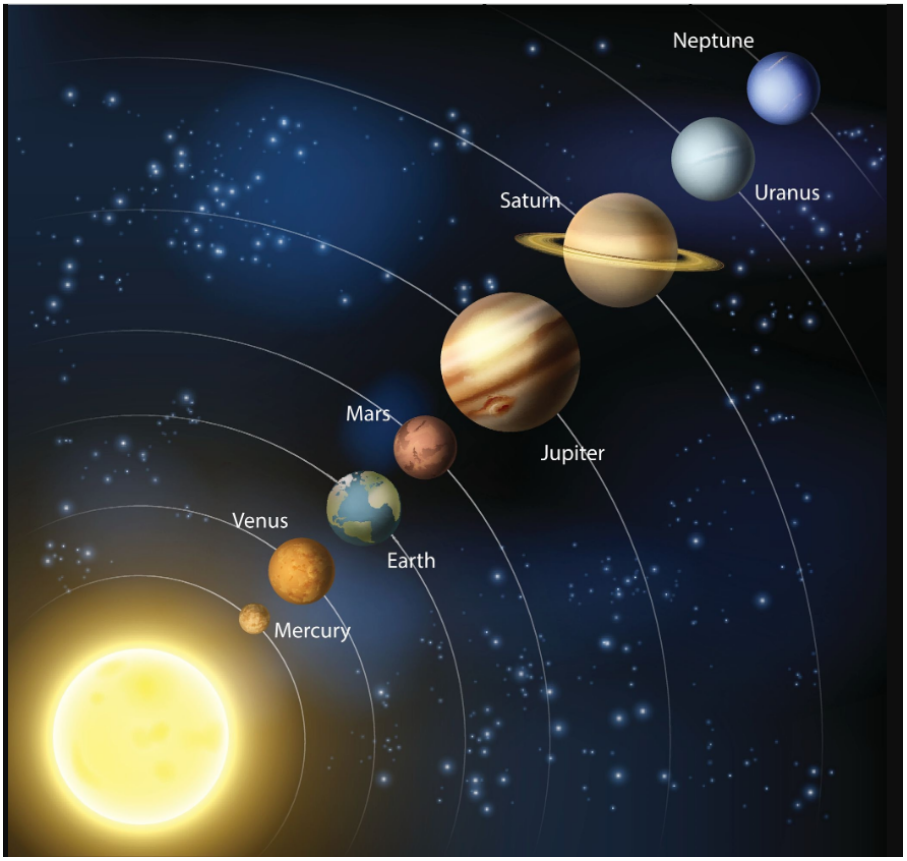

Figure I.1: The solar system [1]

Solar radiation is mainly composed of five different types of radiation:

- Infrared.
- Visible light.
- Ultraviolet.
- X-rays.
- Gamma rays.

They are differentiated by their wavelength and the amount of energy they carry. In figure I.2 represent the electromagnetic radiation spectrum.

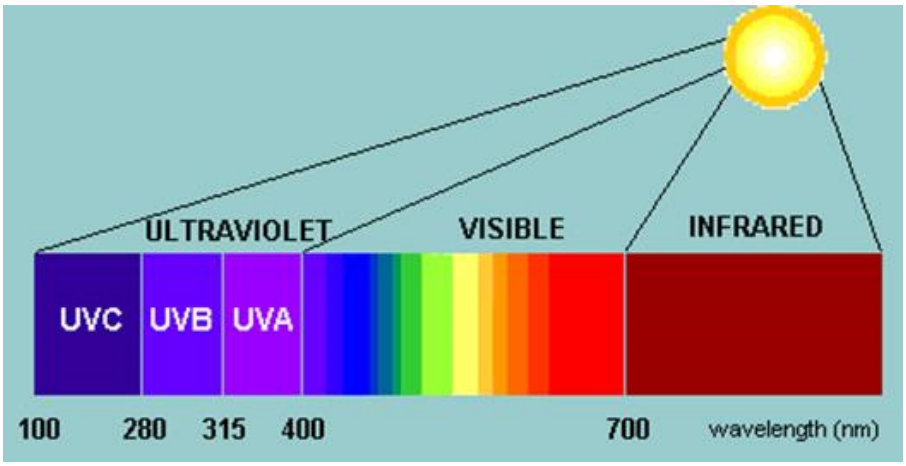

Figure I.2: Electromagnetic Radiation Spectrum[2].

I.2.1 Infrared (IR)

Infrared is a type of electromagnetic radiation with wavelengths between 0.7 and 300 micrometers. 44% of this radiation reaches the Earth's surface, with a wavelength of 800 to 1,400 nm. It carries the heat needed to maintain an average temperature of 17°C at the Earth's surface. If the temperature drops at night, it's because the Earth's surface is not exposed to infrared radiation.

I.2.2 Visible light

Visible light is a portion of the electromagnetic spectrum with wavelengths ranging from approximately 400 to 700 nanometers. It travels at the speed of light, which is about 299,792,458 meters per second. Around 50% of this radiation reaches the Earth's surface, giving our environment light and color (violet, indigo, blue, green, yellow, orange, red) and playing a role in plant photosynthesis.

I.2.3 Ultraviolet rays (UV) C, B,A

Ultraviolet rays are electromagnetic rays with a speed of 200-400 nm. Their wavelength lies between that of visible light and x-rays. Ultraviolet rays are invisible to the eye, and only 4% of them reach the Earth's surface. They are responsible for sunburn and tanning. These three types of ultraviolet radiation (C, B, A) are classified according to their biological properties and their ability to penetrate the skin. They do, however, help to synthesize vitamin D. Much of this radiation is blocked by the ozone layer.

I.3 Cosmic rays, gamma rays and X-rays

Cosmic rays influence the climate by forming clouds. These clouds, which are the source of rain, are part of the water cycle. Gamma rays and x-rays are similar in nature, but have different origins. X-rays are produced by electronic transitions, while gamma rays are produced by the radioactive decay of nucleir, atoms or other nuclear processes. As such, their wavelength is very short and extremely dangerous. But fortunately, they are stopped by the upper layer of the atmosphere.

We can conclude that these different rays play an important role on Earth, providing all the conditions required for Life (human, animal and plant). Part of the Sun's energy, on reaching Earth, heats up the water in the sea and oceans. The Sun transforms the water into steam, which falls as rain. The Sun provides the energy needed for plant photosynthesis, which combines with water from the soil (green plants) or the sea (algae) and carbon dioxide to give plants the ability to produce proteins. Following the principle that "nothing is lost, nothing is created, everything is transformed", a number of cycles use solar energy, its rays and its effects to function.

I.4 Elements of celestial mechanics and solar energy physics

I.4.1 Earth's distance from the sun

The earth is a solid geoid with an average diameter of 12742 kilometers, orbiting the sun in an elliptical orbit. The amount of solar radiation reaching the earth's surface is inversely proportional to the square of the earth's distance from the sun. It is therefore necessary to correctly estimate the Earth's distance from the Sun. This is around 150 million kilometers and is called an astronomical unit (1 AU). The minimum and maximum earth-sun distances are 0.983 AU and 1.017 AU respectively.

I.4.2 Sunshine duration (Insolation)

Sunshine duration corresponds to the time during which direct solar radiation received on a normal plane exceeds a threshold set by convention at 120. A point on the earth's surface is identified by these coordinates :$W.m^{-}2$. Without clouds, sunshine duration closely matches the theoretical daylight hours. It is defined by:

$$S_0 = \frac{2}{15} \times w_0 \tag{I.1}$$

With : w_0: Hourly angle at sunset (°).
S_0: Length of day (h).

I.4.3 Geographical coordinates

A point on the earth's surface is identified by these coordinates :

I.4.3.1 Latitude (λ)

Latitude gives the location of a point in relation to the equator, and varies between 0 and 90°, inversely toward the South Pole and in a positive manner toward the North Pole.

I.4.3.2 Longitude (L)

The longitude of a given place is the angle formed by the meridian of this place with the meridian of origin (Greenwich meridian). It is counted from 0° to 180°, positively towards the east and negatively towards the west.

I.4.3.3 Altitude(ϕ)

Altitude is the elevation of a place in relation to sea level, measured in meters (m).

I.4.3.4 Sun position

The apparent position of the sun at any time of the day and year is determined by two coordinate systems:

- **Time table coordinates**

Time coordinates are linked to the time of observation, and have no relation to the observer's position on the earth. Their reference plane is the equator. The figure I.3 displays the timetable coordinates.

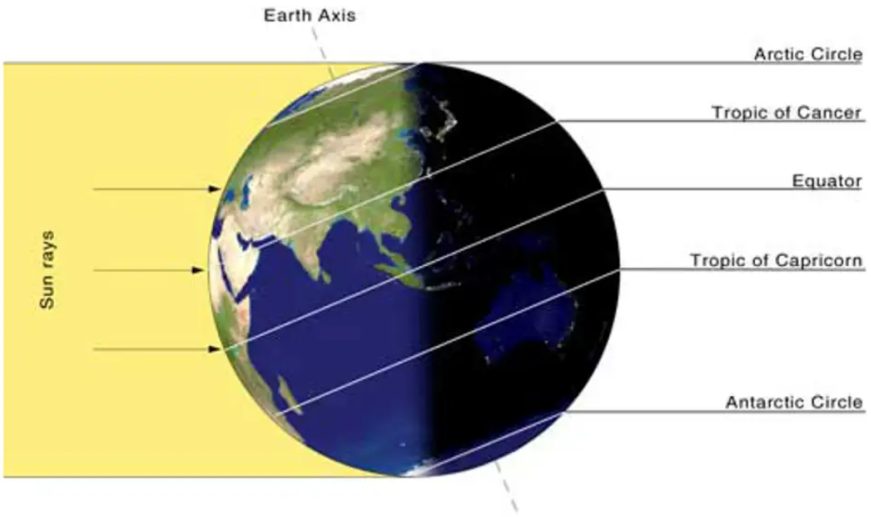

Figure I.3: Timetable coordinates [3]

- **Sun declination (δ, d)**

Declination is the angle between the direction in which the sun is observed and its projection on the equatorial plane. It is expressed in degrees (°), minutes (') and seconds (") of arc. It expresses the inclination of the equatorial plane in relation to the ecliptic plane. Taking declination δ as constant over a day, the Kopernic equation provides the relationship between these two quantities:

$$\delta = 23.45 \sin\left(\frac{360(284+n)}{365}\right) \tag{I.2}$$

n: is the number of the day of the year starting on January 1st.

Solar declination varies from -23°27' at the winter solstice to +23°27' at the summer solstice, and is zero at the equinoxes, and this variation leads to variations in the height of the sun for the same site.The figure I.4 shows Season in Hemisphere.

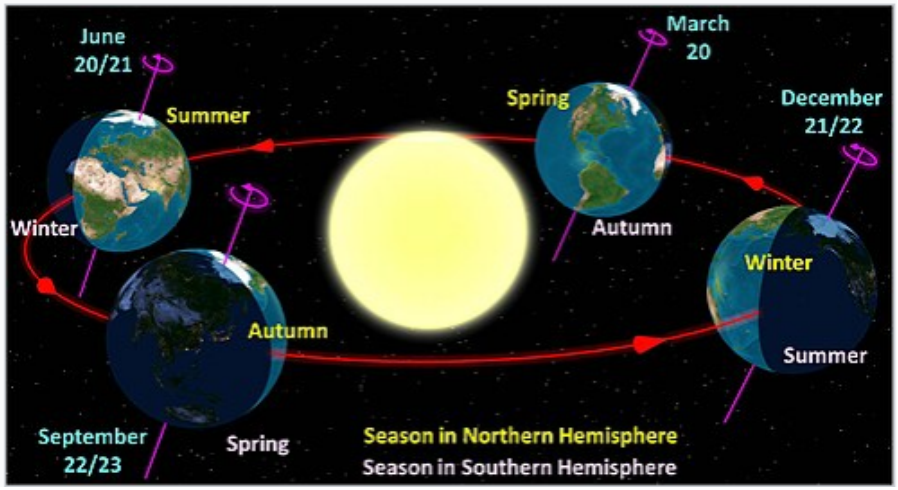

Figure I.4: Earth's revolution around the Sun [4]

In June, the northern hemisphere is closer to the sun; the sun is higher on the horizon for the same hour, and daylight hours are longer. Daily irradiance is thus automatically higher than at the winter solstice in December.

- **Hour angle of the sun (ω, Ah, h)**

The hour angle is the angle or arc counted on the equator in the retrograde direction from the vertical plane passing through the south to the meridian plane passing through the center of the sun. It measures the sun's path across the sky. The hour angle defines true solar time TSV, which is noon TSV if ω=0. Expressed in degrees of angle, its value is zero at solar noon, negative in the morning, positive in the afternoon and increases by 15° per hour (a 360° turn in 24 hours). The hourly angle ω (°) is given by the following formula:

$$\omega = 15(TSV - 12) \tag{I.3}$$

TSV : is the true solar time in hours, calculated by the following equation:

$$\text{TSV} = \text{TU} + \frac{L}{15} + E_T \tag{I.4}$$

$$E_T = 9.87\sin(2B) - 7.53\cos(B) - 1.5\sin(B) \tag{I.5}$$

$$B = \frac{2\pi(n-81)}{365} \tag{I.6}$$

TU : is Greenwich Mean Time (GMT). This formula is not valid for sunrise and sunset times. It is therefore necessary to determine the solar angle at sunset and sunrise, which depend on the declination and latitude of the location.

$$w_0 = \cos^{-1}(-\tan\lambda\tan\delta) \tag{I.7}$$

The sunset angle is simply the opposite of the sunrise angle.

I.4.3.5 Horizontal coordinates

Horizontal coordinates depend on the observation location. Their reference plane is the horizontal plane, perpendicular to the vertical of the location. An object is identified in this coordinate system by these components:

- **Sun height (γ, H)**

The angular height of the sun, commonly referred to as the sun's height or elevation, is the angle between the apparent direction of the sun and its projection on the horizontal plane of the location under consideration. Its value is zero at sunrise or sunset, and maximum when the sun is at its zenith. It varies throughout the day as a function of declination δ, hour angle ω, and latitude ϕ. Such that:

$$\sin\gamma = \cos\delta\cos(\omega\cos\phi + \sin\delta\sin\phi) \tag{I.8}$$

This is the fundamental formula for determining the height of the sun on the horizon, whatever the day, time or place. The maximum height of the sun (at solar noon) :

$$\gamma_{\max} = \frac{\pi}{2} - \phi + \delta \tag{I.9}$$

- **Azimuth of the sun (χ, A)**

This is the angle between the projection of the sun's direction on the horizontal plane and the south or north direction. It is measured starting from north or south, either east or west, across a 360° axis (the azimuth is between $-180° \leq \chi \leq 180°$). In the northern hemisphere, the azimuth origin corresponds to the southern direction. The azimuth angle is counted positively towards the west and negatively towards the east. In the Solar Atlas of

Algeria , the figure I.5 displays the azimuth of the sun. Capderou used the following formula to calculate the sun's azimuth:

$$\sin\chi = \cos\delta\cos(\omega\sin\phi - \sin\delta\cos\phi\cos\gamma) \tag{I.10}$$

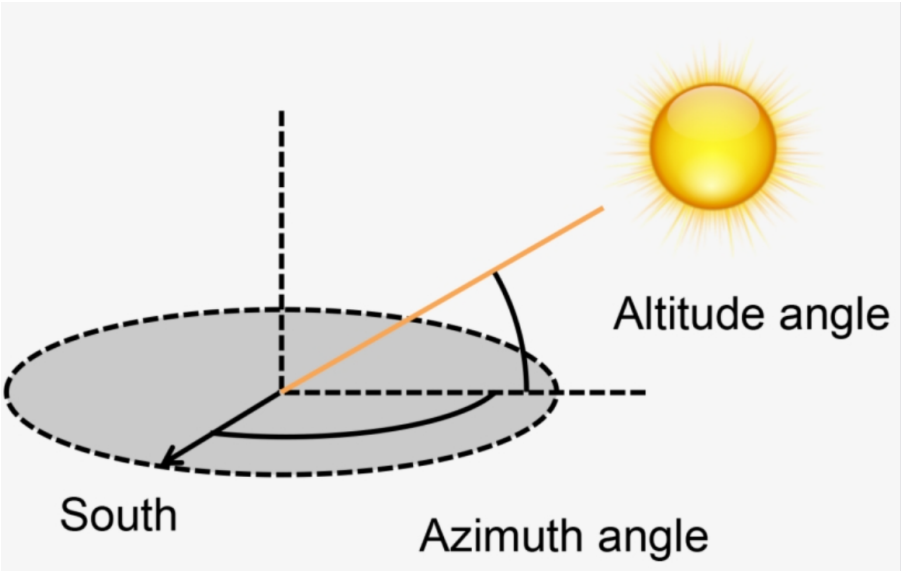

Figure I.5: Azimuth [5]

- **Zenith angle** (θ_z)

This is the angle between the local zenith and the line joining the observer and the sun. It varies from 0 to 90°. The figure I.6 shows azimuth and altitude for northern latitudes.

$$\cos\theta_z = \cos(\delta\cos(\omega\cos\phi) + \sin\delta\sin\phi) \tag{I.11}$$

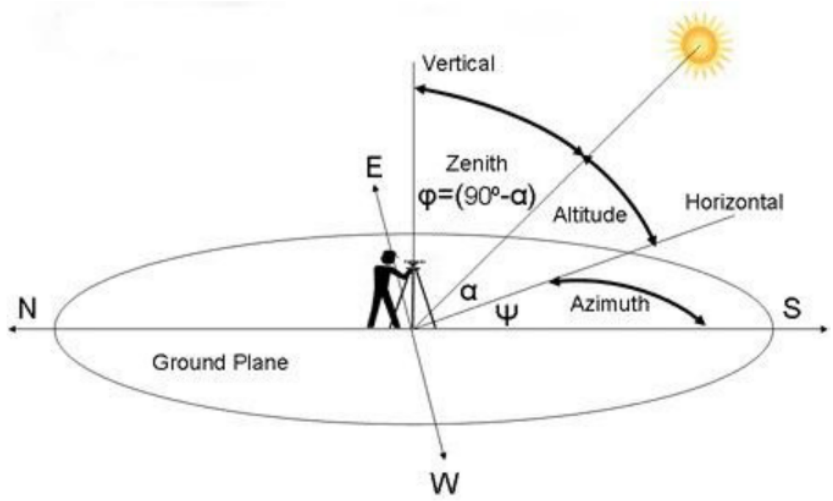

Figure I.6: Azimuth and altitude for northern latitudes [6].

I.5 Solar radiation

I.5.1 Basics and definitions

The sun is a hot gaseous sphere composed mainly of hydrogen (73.5%) and helium (24.9%). It has a diameter of 1.39 million kilometers, corresponding to a total surface area (Ss) equal to $6.08\times10^{1}8\mathrm{m}^2$, and lies at an average distance of 150 million kilometers from the Earth. This distance varies between 152 million kilometers (on July 1st) and 147 million kilometers (on January 1st). Seen from the Earth, the Sun has a solid angle of $6.8\times10^{-}5$ rad and an angular aperture of 0.53°. It emits radiation in wavelengths from 250 to 5000 nm.

I.5.2 Extraterrestrial radiation

Extraterrestrial solar radiation covers a very wide range of wavelengths. It does not depend on any meteorological parameters, but is a function of a few astronomical and geographical parameters such as: the latitude of the location (ϕ), the solar declination(δ), and the hour angle at sunset (ω_0). On a horizontal surface, and for day n, the extraterrestrial radiation G_0 (MJ.$m^{-}2.day^{-}1$) is obtained using the following equation:

$$G_0 = \frac{24}{\pi} \times I_0 \times \left(1 + 0.033\cos\left(\frac{360n}{365}\right)\right) \times \left(\cos\lambda\cos\delta\sin(\omega + \frac{2\pi}{360}) + \omega\sin\lambda\sin\delta\right) \quad \text{(I.12)}$$

I_0: is the solar constant = 0.0820 MJ $m^{-}2$ $\mathrm{min}^{-}1$, or 1367 Wh.$m^{-}2$.
n : is the number of the day from the first of January.
ω : The solar declination and hour angle at sunset.

I.5.2.1 The solar constant

The earth receives virtually all its energy from the sun, in the form of electromagnetic radiation. Its total heat content does not change significantly over time, generally indicating a balance between absorbed solar radiation and the diffuse radiation flux emitted by the planet. Outside the Earth's atmosphere, there is no diffuse component of solar radiation, only the direct component. For an average distance between the earth and the sun. The irradiation emitted by the sun to the earth results in an almost fixed intensity called the solar constant, which is $1360\mathrm{w}/m^2$.

The solar constant refers to the amount of solar energy received per unit time and per unit area of a surface that is perpendicular to the direction of solar radiation propagation. Various instruments have been employed to measure this constant, yielding diverse sets of data yielded a value of $1353\mathrm{w}/m^2$, estimated with an error of ±1.5%.

I.5.2.2 Solar radiation in the earth's atmosphere

The radiation received by the Earth's atmosphere occupies only a small portion of the solar electromagnetic spectrum. It is characterized by wavelengths between 0.2 and 2.5 µm, and includes the visible range (light waves from 0.4 to 0.8µm). Solar energy collectors, which correspond to solar cells, must therefore be compatible with these wavelengths to be able to trap photons and return them in the form of electrons.The figure I.7 shows the spectral distribution of solar radiation.

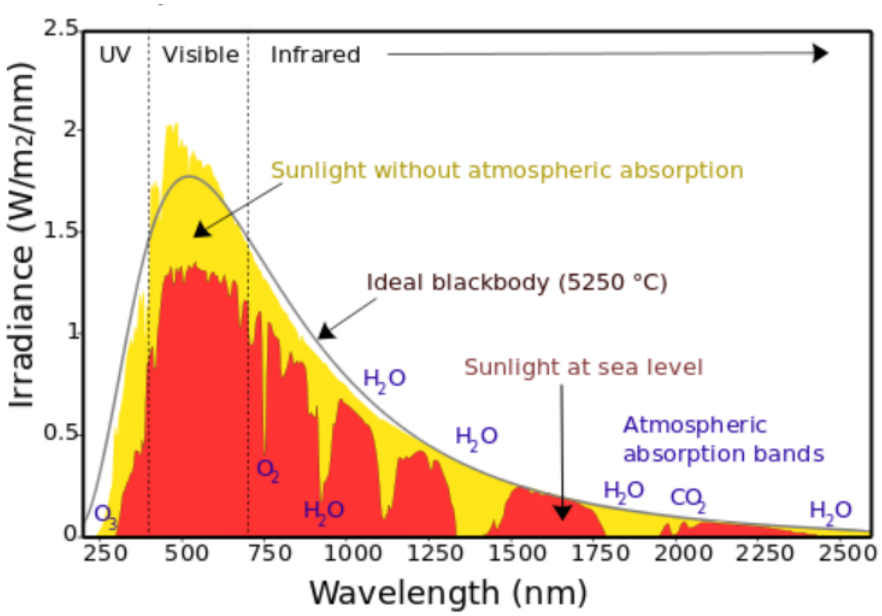

Figure I.7: Spectral distribution of solar radiation[7].

I.5.3 Incident solar irradiance

The angle at which the Sun's rays strike a surface determines the energy density received by that surface. Since solar radiation reaches the Earth in a parallel beam, a surface perpendicular to these rays intercepts the maximum energy density. And if the surface is tilted from this perpendicular position, its irradiance decreases.

Perhaps the best way to represent this phenomenon is to depict the Sun's parallel rays with a handful of pencils held in the hand above a sheet of paper, points down. The marks made by the points represent grains of energy. When the pencils are perpendicular to the sheet, the points are squeezed to the maximum: the density of energy per unit area is greatest. When all these parallel pencils are tilted together, the points spread out and cover increasingly elongated surfaces: the density of energy decreases as the marks spread out. The figure I.8 represents the solar radiation on inclined surface.

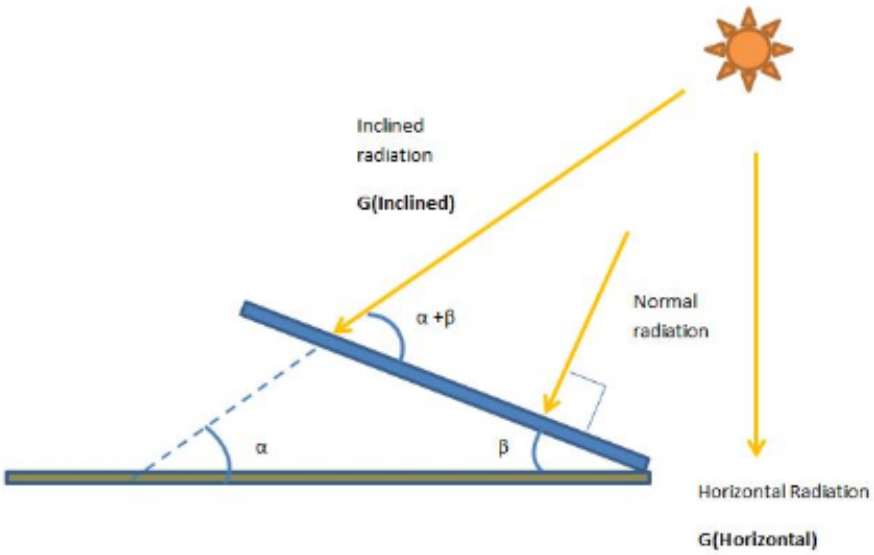

Figure I.8: Solar Radiation on Inclined Surface [8]

However, a surface that deviates 25% from this position perpendicular to the Sun still intercepts over 90% of the maximum direct radiation. The angle the Sun's rays make with the surface normal (angle of incidence) will determine the percentage of direct light intercepted by the surface.

In reality, the total radiation received by a surface, known as incident solar irradiance (or global irradiance), is defined by the sum of three components: Direct irradiance, coming directly from the Sun. This component is cancelled out if the Sun is hidden by clouds or obstacles. Diffuse irradiation, corresponding to radiation received from the sky, excluding direct radiation. This energy, diffused by the atmosphere and directed towards the Earth's surface, can account for up to 50% of the total radiation received when the Sun is low on the horizon, and 100% when the sky is completely overcast.
Reflected irradiance, corresponding to radiation reflected by the external environment, in particular the ground, whose reflection coefficient is called "albedo". In particular, hemispherical irradiance is also defined as the overall irradiance received on a horizontal surface (the component reflected by the ground is zero in this case).

Global irradiance is measured with a solarimeter at the desired inclination and orientation. Diffuse irradiance alone is measured by a shadow band solarimeter: this is the same instrument fitted with a semi-circular band which, when periodically adjusted, masks the direct sunlight from the measuring device. The amount of energy received depends not only on this power, but also on the duration of sunshine. Depending on weather conditions, the radiation will reach us in its diffuse and direct components in greater or lesser proportions.
Global solar radiation is considered here on a horizontal surface (on which the reflected component of the radiation is zero).In practice, meteorological conditions can be qualified by relative direct insolation: this is the ratio between effective insolation (S) and theoretical maximum

insolation (So). This determines the type of sky:

- A sky is considered serene when the relative direct insolation S/So is between 80 and 100%,
- A sky is considered medium when the relative direct insolation S/So is between 20 and 80%,
- A sky is considered overcast when the relative direct insolation S/So is between 0 and 20%.

I.5.4 Clarity index

The ratio of ground radiation to extraterrestrial radiation is called the clarity index. The clarity index, KT, is defined by :

$$K_T = \frac{G}{G_0} \tag{I.13}$$

Where: G is the solar irradiance received on a horizontal plane.

The monthly average of the KT clearness index varies according to location and season, and generally ranges from 0.3 (for rainy regions or seasons) to 0.8 (for dry, sunny seasons or climates).

I.5.5 Solar irradiance

Irradiance is the power of solar radiation per unit area. In the international system of units, it is measured in (Wh/m^2).The figure I.9 represents Different types of Solar Radiation .Solar irradiance measures the amount of energy per unit area of solar radiation incident on a surface. In other words, the power received over a period of time (J/m^2or Wh/m^2).

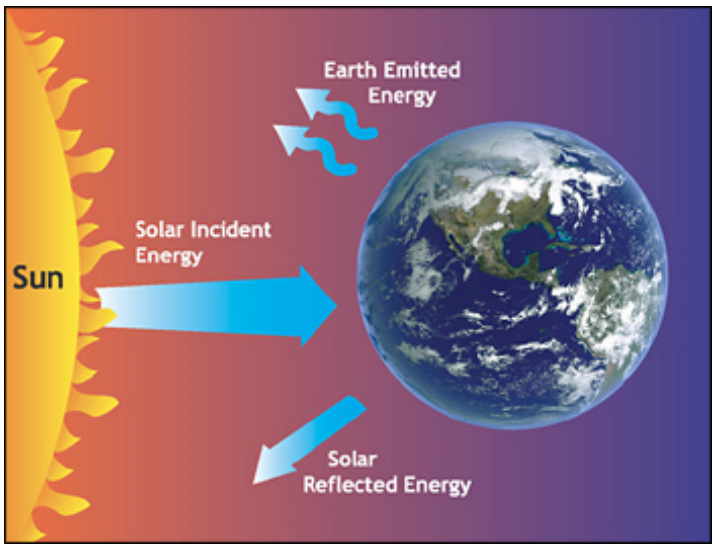

Figure I.9: Different types of Solar Radiation[9].

I.6 Solar potential

A deposit is an accumulation of raw material (oil, gas, coal, uranium, metal ore, useful substance,... etc.) located at varying depths underground. Algeria has got some major potential when it comes to renewable power, especially solar. Of all the countries along the Mediterranean and in Africa, I'd say Algeria is sitting the prettiest in this department. They've got sun for days and wide open spaces perfect for solar farms. Now solar ain't the only renewable Algeria could tap into, there some options with wind, hydro geothermal ...etc. But solar feels like the biggest slam dunk and it's just everywhere across the landscape, plus the technology keeps getting better and cheaper.

Algeria is endowed with one of the world's largest solar energy deposits. The term "insolation" refers to the amount of solar radiation received on a given surface during a specific time period. In the case of Algeria, it experiences an insolation period ranging from 2,000 to 3,900 hours per year. This substantial duration of sunlight makes it an ideal location for harnessing solar power. The daily irradiation in Algeria is impressive, with values ranging from 3,000 to 6,000 Wh/m^2. This level of solar irradiation is approximately ten times the global average consumption. The figure I.10 shows daily global solar radiation in Algeria.

This abundance of sunlight provides a significant opportunity for Algeria to tap into solar energy as a sustainable and renewable resource. With such favorable conditions, Algeria has the potential to become a major player in the field of solar energy. The country can leverage this vast solar resource to generate clean and sustainable electricity, contributing not only to its own energy needs but also potentially exporting solar power to neighboring regions. Investing in solar energy infrastructure and technology could not only address Algeria's energy demands but also position the country as a leader in renewable energy on the global stage. It offers the opportunity for sustainable development, reducing reliance on non-renewable energy sources and mitigating the environmental impact associated with conventional energy production.

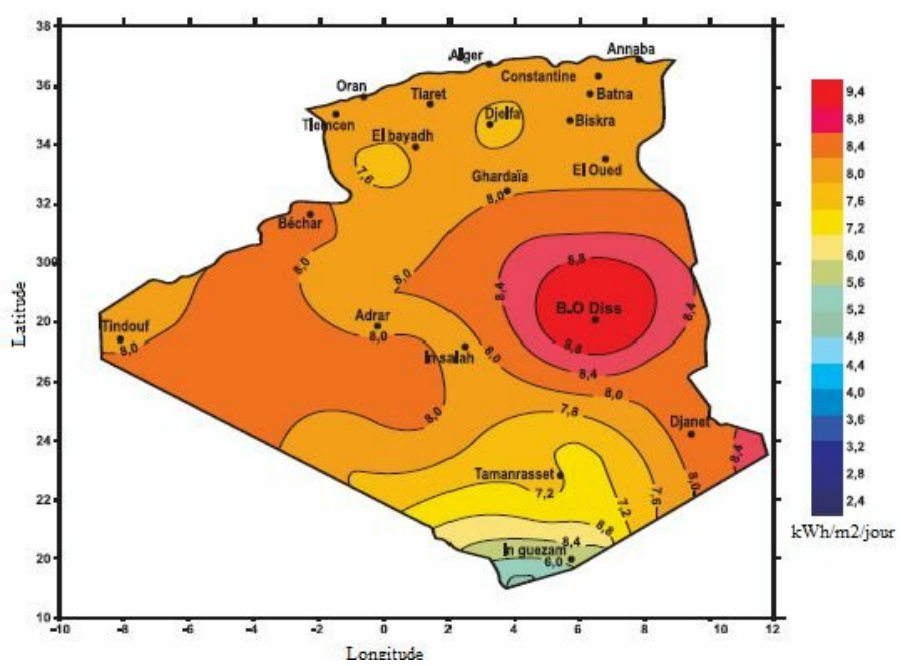

Figure I.10: Daily global irradiation received on a horizontal plane over the Algerian territory [10].

Batna, a city located in Algeria's northeast region, benefits from significant year-round exposure to the sun's rays. This region, characterized by a semi-arid climate, is ideally positioned to take advantage of the abundant solar energy. Incident solar radiation, measured in kilowatt-hours per square meter per day (kWh/m^2/d), is relatively high in this area, making it an ideal location for solar energy development.

Batna's solar potential offers considerable opportunities for the exploitation of photovoltaic and thermal energy. Solar panels can be deployed to generate electricity from sunlight, while solar thermal systems can be used to heat water for domestic and industrial needs. This abundance of solar resources offers the city of Batna the opportunity to diversify its energy supply, reducing its dependence on conventional energy sources and contributing to the transition to cleaner, more sustainable energy.

In addition, harnessing solar radiation in Batna can have significant environmental benefits by reducing greenhouse gas emissions and mitigating the negative impacts associated with non-renewable energy sources. Raising awareness of the importance of solar radiation and its potential as part of a sustainable energy strategy can stimulate the development of local solar projects and encourage the adoption of solar technologies in various sectors of the city.

I.7 Conclusion

In conclusion, this chapter has delved into a comprehensive examination of the fundamental parameters governing solar radiation, showcasing their intricate interplay. The significance of understanding these elements transcends disciplinary boundaries, encompassing

domains such as solar energy, meteorology and ecology.

Beginning with a focus on the solar constant, the cornerstone of our investigation, we elucidated its meaning and the methodologies employed for its measurement. Subsequently, our exploration extended to solar inclination, unveiling its impact on the spatial distribution of solar radiation and its role in seasonal variations. Solar declination, intricately linked to the Sun's angle of elevation, was meticulously elucidated, emphasizing its seasonal flux and consequential effects on radiation reception at varying latitudes.

The examination reached its apex with an in-depth analysis of the incidence angle, delineating its nuanced role in shaping the amount of solar energy reaching the Earth's surface across diverse latitudes and times of the day. By elucidating the relationships between these parameters, we sought to unravel the intricate web that governs the behavior of solar radiation, encapsulating these dynamics through equations and visual representations. Lastly, we turned our attention to the specific context of solar deposition in Algeria and the city of Batna, exploring potential prospects for harnessing this valuable resource.

This chapter, therefore, not only serves as a theoretical guide to solar radiation but also lays the groundwork for practical applications and future considerations in the context of specific geographical locales.

Chapter II

THE STATE OF THE ART IN GLOBAL SOLAR RADIATION PREDICTION

THE STATE OF THE ART IN GLOBAL SOLAR RADIATION PREDICTION

II.1 Introduction

The state of art is an essential step in scientific research, providing a general idea of the subject. The state of art has many uses, including: contextualizing research, identification of gaps, developing a methodology, validation of results, exploration of theoretical perspectives, identification of sources of inspiration, communicating knowledge, avoiding duplication, justification of methodological choice, establishing credibility .

The prediction of solar radiation is crucial for several applications and sectors such as: meteorology, agriculture and the environment ... etc. It also contributes to a more efficient use of solar energy and a better management of natural resources.

The chapter offers an interesting exploration of the solar radiation prediction of using meteorological parameters as a basis. It begins with an introduction that highlights the importance of solar radiation prediction in various fields and presents the objectives of the chapter. Then, a dive into the history of solar radiation prediction is undertaken, retracing the historical developments and technological advances that have shaped this discipline over time. Then a section is devoted to the main theories, models and approaches used to make precise solar radiation predictions based on meteorological data. The next section presents an overview of the most recent developments in the field of solar irradiance forecasting. Recent research has exploited various AI techniques, including deep neural networks and machine learning methods, to improve the quality of solar predictions. The state of the art should therefore reflect this remarkable convergence towards AI for solar radiation prediction. It covers a wide range of cutting-edge research and advances in solar irradiance forecasting.

Finally, the chapter concludes by summarizing the essential points, highlighting the lessons learned from history and discussing future prospects in the field of solar radiation prediction, thus offering a comprehensive and enlightening overview.

II.2 Definition of solar radiation prediction

Solar radiation prediction refers to the modeling and anticipated estimation of solar energy received on the earth's surface at specific times. This discipline relies on various methodologies, such as the use of atmospheric models, historical data and meteorological observations. The main objective is to provide accurate forecasts of solar irradiance, taking into account seasonal variations, changing weather conditions and specific geographical properties. These predictions are essential for various sectors, including solar photovoltaics, agriculture, meteo-

rology and energy planning. By optimizing the accuracy of solar radiation forecasts, users can more effectively plan the use of solar resources, improve the management of solar installations and contribute to the transition to renewable energy sources. Solar radiation prediction thus plays a crucial role in sustainable development and maximizing the efficiency of solar technologies.

II.3 History of Solar radiation prediction

Solar radiation prediction, also known as sunshine prediction, involves forecasting the amount of solar radiation that will reach a specific location at a given time in the future. This prediction is crucial for a variety of applications, especially solar energy planning, power grid management, agriculture, meteorology, and other fields where the availability of sunlight is a key factor.

- At the beginning of the 20th century, early attempts to predict solar radiation were rudimentary and based on local meteorological observations. However, these predictions were often inaccurate due to a lack of appropriate data and models [11-13].
- With advances in meteorology, more advanced weather stations were set up in the 1950s-1960s, enabling more solar data to be collected. However, solar radiation prediction was still limited by the lack of accurate mathematical models.
- In the 1970s-1980s, the first solar radiation prediction models were developed, notably those based on solar geometry and meteorological data. These models improved the accuracy of solar radiation forecasts.
- The advent of computers in the 1990-2000s and numerical modeling techniques enabled the development of more sophisticated solar radiation prediction models. These models have integrated a wider range of meteorological and astronomical data to improve forecast accuracy.[14-16]
- Advances in solar technologies have increased the importance of solar radiation prediction in the years 2010-2020 for the efficient integration of solar energy into power grids. This has led to the development of real-time solar radiation forecasting systems using satellite data, advanced atmospheric models and machine learning techniques.[16-18]
- Beyond 2020, research is continuing to improve the accuracy of solar radiation forecasts, notably by integrating high-resolution data, climate models and short-term forecasts. Advances in artificial intelligence and machine learning continue to be applied to improve solar radiation prediction.

II.4 Solar radiation prediction approaches

Solar radiation prediction approaches are varied and essential for solar installations, meteorology and energy management. The importance of the classification of solar radiation prediction methods lies in the fact that it provides a better understanding of the factors that influence solar radiation and enables the most suitable prediction method to be chosen for the application concerned. It has attracted researchers to classify it according to various factors (methodology, spatial resolution and model type) and the duration of the prediction (horizon). The figure II.1 shows the classification of solar radiation prediction.

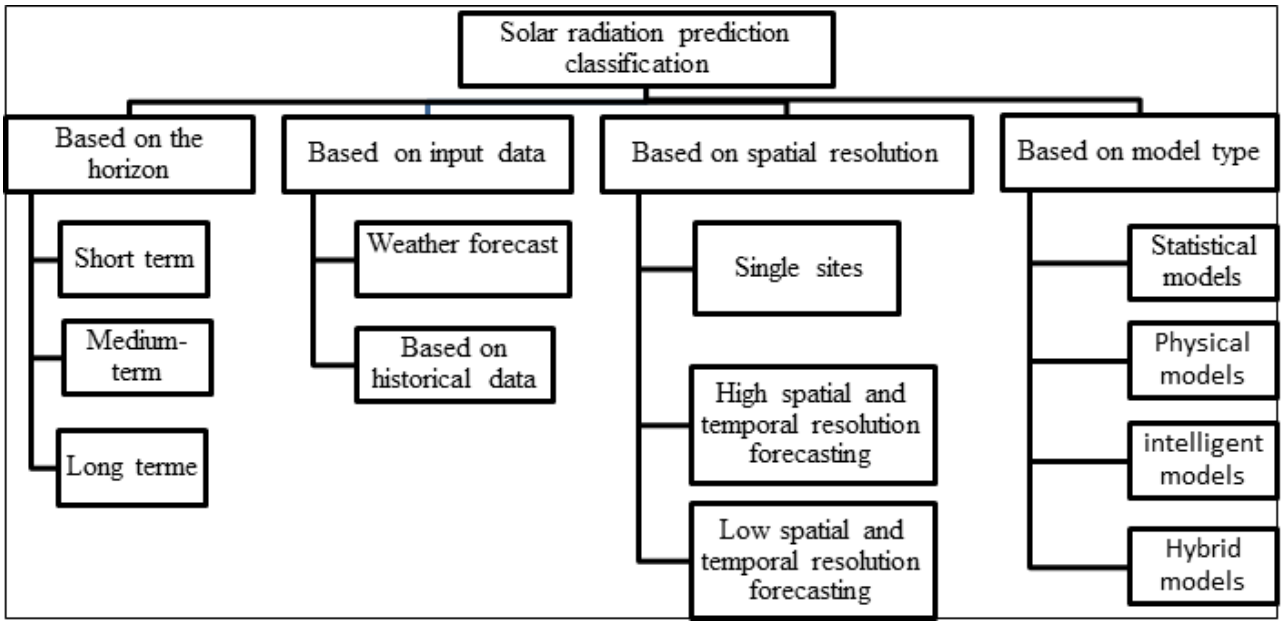

Figure II.1: Solar radiation prediction classification

II.4.1 Classification based on horizon

Solar radiation prediction can be divided into three categories depending on the forecasting horizon: short-term forecasting, medium-term forecasting and long-term forecasting.

- **Short-term forecast**

This category concerns the prediction of solar radiation for the coming minutes, hours or days. It is essential for the integration of solar energies into the electricity network.

- **Medium-term forecast**

It concerns the prediction of solar radiation for the next few days based on longer-term meteorological data.

- **Long-term forecasting**

Prediction over a broader period of time, such as weeks, months or years, often used for planning long-term solar energy projects.

II.4.2 Classification based on input data

Depending on parameters used for solar radiation prediction may be classified into two categories: weather predictions and historically based forecasts.

- **Weather forecasts**

These forecasts use weather models to estimate global solar radiation. Weather data, such as cloud cover, temperature, wind speed and humidity are used to predict solar energy production.

- **Historically based forecasts**

These forecasts use past data of global solar radiation in a given region to estimate future radiation. Statistical methods and regression techniques are commonly used.

II.4.3 Classification based on spatial and temporal resolution

Solar radiation prediction may be divided into three categories depending on the spatial and temporal resolution used: single sites, forecasting with high geographical and temporal resolution and forecasting with low spatial and temporal resolution.

- **Single sites**

These are forecasts made for a specific site, based on ground measurements or extrapolation of nearby measurement. The forecast is representative of the measurements point only.

- **High spatial and temporal resolution forecasting**

These forecasts aim to predict global solar radiation at a fine scale in time (minutes to hours) and space (meters to kilometers). They are often used for real-time management of solar installations.

- **Low spatial and temporal resolution forecasting**

These forecasts are less detailed and aim to predict global solar radiation on longer time scales (hours to days) and broader spatial scales (entire regions).

II.4.4 Classification based on the model type

Solar radiation prediction can be classified into four categories based on the model type used: statistical models, physical model, machine learning model and hybrid models.

- **Statistical models**

These models utilize historical data to predict future solar radiation using statistical methods and regression techniques.

- **Physical models**

These models are based on the physical principles that determine the amount of solar radiation reaching the earth's surface, taking into account parameters such as the angle of the sun, atmospheric refraction, weather conditions... etc.

- **Intelligent models**

Artificial intelligence (AI) models for solar radiation prediction rely on advanced machine learning and data analysis approaches to improve forecast accuracy.

- **Hybrids models**

By combining models, hybrid models take advantage of the benefits of each approach, resulting in more accurate and robust solar radiation forecasts. This combination offers a more satisfying solution to the needs of solar energy applications, enhancing the efficient use of this renewable energy source.

II.4.5 State of the art of application of approaches for solar radiation prediction

A state of the art is an important step in many activities in scientific research, designating a detailed and critical synthesis of academic work, methods, technologies and results relating to the prediction of solar radiation. The review articles on solar radiation prediction provide a detailed overview of the most recent approaches, models and advances in this field, exploring innovative predictive methods for accurately anticipating the availability of solar radiation in various geographical contexts.

In the beginning section, a number of reviews on solar radiation prediction are explored. These critical studies provide an essential overview of the advances, methodologies and challenges encountered in this crucial area of research. Next, we compile a selection of recent and relevant works. They are divided into five categories as follows: empirical, fuzzy logic, deep learning, tree based and hydrid.

The article of Samuel Chukwujindu Nwokolo and Julie C. Ogbulezie [19] provide a comprehensive review and classification of empirical models for predicting global solar radiation (GSR) in West Africa. They have identified 356 empirical models and 68 functional forms that were developed for estimating Global Solar Radiation (GSR) in West Africa. This review writing by Javier Almorox et al [20] emphasize the importance of considering TSI and its variations and Solar Constant (SC) values when applying empirical models for solar radiation estimation for 29 stations Spain. L. Suganthi et al [21] give an overview of research on solar radiation modeling utilizing fuzzy logic, neural networks, and genetic algorithms. M.Sridharan [22] used a technical analysis from the literature to create fuzzy logic for solar irradiance prediction. D. Shah et al [23] offered a summary of numerous research studies that used ANN and fuzzy logic to estimate solar radiation. And for a review of Daxal Patel et al [24], which include

research employing ANN, Fuzzy, GNN (Graph neural network) and ANFIs models for solar radiation prediction. The review article, written by Nourdine Kabouche et al [25], deal with the assessment of solar radiation in Algeria, highlighting the importance of solar radiation data, particularly in the Saharan region of Algeria. It deal mainly with empirical and satellite models for solar radiation assessment. In another review the authors [26] examine in detail the evaluation and forecasting of solar radiation in Algeria, focusing specifically on Stochastic models, Artificial neural networks, Fuzzy logic, Combined Models, Support vector machines, Wavelet networks and Wavelet-Gaussian process regression model. The review of Cyril Voyant et al [27] analyze the potential of machine learning (ML) methods for forecasting solar radiation, highlighting their strengths and limitations compared to traditional approaches. The paper covers a broad range of ML techniques utilized for solar forecasting including: Regression models, Artificial neural networks, Support vector machines, and Ensemble methods. The article of Shubham Gupta et al [28]review various techniques(empirical, satellite-based and machine learning) for estimating solar radiation received at a different locations, taking into account the losses that occur as sunlight interacts with the Earth's atmosphere and reaches the surface. Pratima Kumari and Durga Toshniwal [29] linked a review on deep learning models (CNN, LSTM, GRU, RNN, and DNN) and a hybrid CNN-LSTM model for solar radiation prediction. The paper provides an overview of deep learning techniques that can be used to improve the prediction and planning of solar photovoltaic power plants. The authors Faisal Nawab et al [30] summarize the different empirical techniques commonly used. These methods use historical radiation data and meteorological variables to train statistical prediction models. They then describe convolutional neural network (CNN) methods, support vector machines (SVM) and deep learning. These techniques make it possible to better capture non-linear relationships in the data. The paper written by Abbas Mohammed Assaf et al [31] provide a detailed overview of neural network-based models for short-term solar irradiance forecasting, highlighting their applications, challenges and prospects for improvement in this crucial area of renewable energy. The study by Meenu Ajith et al [32] compare in detail the performance and architecture of the models, the datasets used and the evaluation methods in recent literature such as: time series-based models, image-based models and hybrid models.

The tables presented in this study highlight the importance of the quality and diversity of the data used to drive solar radiation forecasting models. In fact, model performance is highly dependent on the climatic characteristics of the study site, the period considered and the input variables selected. By comparing results obtained in different contexts, we can better understand the impact of these factors on forecast accuracy and identify the models best suited to each situation.

Work	Country	Climat	Kind of forcast	Period of used data	Models	Best model	Inputs	Performances metrics
Victor H. Quej et al[33]2016	Mexico	Tropical	Daily	2000 to 2014	13 model of regression	$H = H_0((\mathrm{T_{max}} - \mathrm{T_{min}})^a + b(1 + c\mathrm{RH}) + d\mathrm{RT}_j$	maximum and minimum Temperature, transformed rainfall and average relative humidity	RMSE= 2.604, MBE= 0.014, MPE=3.175, MAPE= 12.327, MABE= 1.981 and R2= 0.706
Victor H. Quej et al[34] 2017	Mexico	Tropical	Daily	2000 to 2014	Bulut and Büyükalaca,Kaplanis and Kaplani, Al-Salaymeh,Li et al,Gaussian DYB	Gaussian DYB	maximum and minimum Temperature, transformed rainfall and average relative humidity	RMSE= 1.122, MBE=0,00, MPE= 0.308, MAPE= 4.345, MABE= 0.877 and R2= 0.884.
Muhammed A. Hassan et al[35] 2018	Egypt	Desert	Daily	Oct 2012 to Dec 2016	12 independent models,3rd polynomial sunshine,linear Temperature-based,non-linear meteo parameters-based ,multivariate linear meteo parameters-based and non-linear meteo parameters-based	non-linear meteo parameters-based	Day number ,sunshine duration, extra-terrestrial , inclinaison	MPE = 0.006, MBE=0.021, RMSE=1.322, NDRMSE = 4.452 and R2=0.955

Work	Country	Climat	Kind of prediction	Period of used data	Models	Best model	Inputs	Performances metrics
Yu Feng Wu et al[36] 2019	China	Arid and humid	Daily	1997–2016	Hargreaves-Samani model, Bristow-Campbell model, Jahani model, and Fan model),ML optimisé	Bristow Campbell model	maximum and minimum Temperature, transformed rainfall and average relative humidity	RMSE= 1.122, MBE=0,00 , MPE= 0.308, MAPE= 4.345, MABE= 0.877 and R2= 0.884.
Cyril Voyant et al[37] 2020	France	Mediterranean	time series	1998 to 2008	persistence (P), smart persistence (SP), classical PAR model (using TMY stationary process) and PAR model coupling BIC and BC	PAR-BC	/	nRMSE= 0.3438
Sandeep Dhakal et al[38] 2020	Nepal	subtropical	Daily	2006 to 2015	6 Temperature-based empirical models,ANN ,5 ML	Fan et al	Extra-terrestrial solar radiation (Ra) and Temperature	RMSE=2.5810, R2= 0.6435 and R2adj=0.6373
Rishal Asri et al[39] 2021	Indonesia	Tropical	10min	365 days	Linear model	/	Sun radiation, air Temperature, humidity, wind direction and speed.	R2=0.727

Work	Country	Climat	Kind of prediction	Period of used data	Models	Best model	Inputs	Performances metrics
Bishwa B. Acharya et al[40] 2021	Nepal	subtropical	Daily	2015	Falayi ,Garcia ,Chen and Li, Falayi	Falayi	Extra-terrestrial solar radiation (Ra) Sunshine Hours and Temperature (Tmax,Tmin)	MBE=14.1%, R2adj= 0.61 and RMSE=22.6%
Zineb Bounoua et al[41] 2021	Morroco	Continental	Daily		22 empirical models (ANN) and tree-based (Boosting,Bagging and RF)	RF	(Tmean), (Tmin), (Tmax), (RHmean), (RHmin), (RHmax), (Ws), (Wd), (DOY), and (H0)	R: 87.53–96.20%; nMAE: 5.84–11.81%; nRMSE: 7.85–15.33%
Olanrewaju M. Oyewola[42] 2022	Island	Temperate oceanic	Monthly	1984-2018	20 empiricals models	/	(TMAX), (TMN), (TMIN), (S), (RH), (CLD), and (GSR)	R2= 0.988
Qi Li et al[43] 2023	Island	Temperate oceanic	Daily	2007 to 2016	multiple linear regression (MLR), principal component regression (PCR), stepwise regression (SR), and partial least squares regression (PLSR)	principal component regression (PCR)	Season	MAE= 7.97 . 102 , MSE= 9.24. 105and RMSE= 9.61 . 102

Table II.1: Comparative Analysis of Regression Models for Solar Radiation Prediction in Diverse Climatic Regions.

Work	Country	Climat	Kind of prediction	Period of used data	Models	Best model	Inputs	Performances metrics
Zeynab Ramedani et al[44] 2014	Iran	Arid	Daily	1994-2000	SVR_rbf, SVR_poly and FLR	SVR_rbf	Extra-terrestrial solar radiation, Daylight hours, number of days, min and max Temp, the actual duration of sunshine and clear-sky solar radiation	RMSE= 3.3 and R2= 0.889
M. Rizwan et al[45] 2014	India	Subtropical Humid	Monthly	1986-2000	Fuzzy and ANN	Fuzzy	mean duration sunshine, temperature, latitude, longitude, altitude and months	/
R. Boata and N. Pop[46] 2015	five European cities	/	Monthly	1997-2000	Takagi-Sugeno fuzzy algorithm	Δt=tmax-tmin,j :julian day, Δtm5j = tmj- t5j, where tmj = (tmax,j +tmin,j)/2 and t5j = (tmj-2 + tmj-1 + tmj+1 + tmj+2)/5	Rmse=0.037... 0.260 and mbe=–0.22... 0.091	
R. Boata and N. Pop[47] 2018	Romania	Continental	Daily	1998 - 2001	Takagi-Sugeno fuzzy	/	kt-1 and kt-2	RMSE = 1.178, MBE = 0.005

Work	Country	Climat	Kind of prediction	Period of used data	Models	Best model	Inputs	Performances metrics
Jwan Abdulkhaliq Mohammed and Berivan-Hadi Mahdi[48] 2018	Iraq	Temperate Mediterranean	Daily	2016	Four fuzzy systems	/	Temperature, humidity, wind speed and solar radiation	MAPE=1.523,APE=15.22.
Sahil Mehta and Prasenjit Basak[49] 2019	India	Subtropical Humid	10min	/	15 multi-linear regression model,Fuzzy	Fuzzy	time of day, Temperature, wind speed, humidity, and atmospheric pressure	MBE= -1.395 , MAPE= 0.01703 , RMSE= 10.011.
Idris A. Masoud Abdulhamid et al[50] 2019	Turkey	Mediterranean and continental	Daily	2005–2010	12 Fuzzy	/	The daily values of ambient Temperature and relative pressuredurations	MAE=0.547, RMSE=0.830 , and R2= 0.8920

Work	**Country**	**Climat**	**Kind of prediction**	**Period of used data**	**Models**	**Best model**	**Inputs**	**Performances metrics**
Khalid Bahani et al[51] 2020	Morroco	Tropical	Hourly	2000 samples	MLP, SVR and Fuzzy	Fuzzy	Solar radiation, Temperature, Humidity and Pressure	RMSE = 139.62 and MAE = 110.96
Shahad M. Alkaissi et al[52] 2020	Iraq	Mediterranean	Daily	2018-2019	Fuzzy	/	Temperature and cloud cover	MAPE =4%
M.Sridharan[53] 2021	India	Subtropical Humid	Monthly	/	GRNN, MLP and Fuzzy	GRNN	Month of the year, altitude, longitude, latitude, T/T0 and S/S0	MARE= 3,5%

Table II.2: Comparative Analysis of Fuzzy Logic Models for Solar Radiation Prediction in Diverse Climatic Regions.

Work	Country	Climat	Kind of prediction	Period of used data	Models	Best model	Inputs	Performances metrics
Ahmad Alzahrani[54] 2017	Saudi Arabia	Desert	Monthly	2014 and mid-2016.	ARMA and FFNN-based PSO ,AM-ELM	AM-ELM	Temperature, humidity, solar radiation	MAE = 0.2444, MSE = 0.1727, and RMSE = 0.3012
Maurício Bruno Pradoda Silva et al[55] 2017	Brazil	Tropical	Daily	1996-2011	MLP		Extra-terrestrial, fractional daily sunshine duration, maximum air Temperature, minimum air Temperature, Precipitation and relative humidity	rMBE=13.20–8.10, MBE=2.30–1.38, rRMSE= 15.60–16.60 RMSE=2.68–2.89, r=0.95–0.96, R2= 0.90–0.92
Sivaneasan B et al[56] 2017	Singapore	Equatorial	5 min	January to March 2017	MLP , ANN with fuzzy pre-processing, improved ANN with error correction factor and fuzzy logic pre-processing	improved ANN with error correction factor and fuzzy logic pre-processing	Temperature, dew point,wind speed,wind deriction, gust speed,irradiance , error, humidity, rainfull,time	MAPE=29.6%
Giorgio Guariso et al[57] 2020	Italy	Mediterranean	Hourly	2014 - 2019	Multi-Model (MM) , Multi-Output (MO) ,FF-Recursive, FF-Multi-Output, FF-Multi-Model and LSTM	FF-Multi-Model and LSTM	t-1,t-2	Bias=0.17,MAE=39.26,RMSE=82 and S=0.44

Work	Country	Climat	Kind of prediction	Period of used data	Models	Best model	Inputs	Performances metrics
Zhihong Pang et al[58] 2020	USA	Continental subarctic	10 min	May 22 - May 29 2016	ANN, ANN_Moving window RNN, RNN_Moving window	RNN_Moving window	Global solar radiation, outdoor air-dry bulb Temperature, relative humidity, dew-point Temperature, wind speed, and wind direction.	NMBE= 0.2 %, CV(RMSE)= 5.2% , RMSE= 28.9 and R2= 0.998 .
Syed Altan Haider et al[59] 2022	Pakistan	Desert	monthly	from 2015 to 2019	CNN	/	Horizontal Irradiance, Direct Normal Irradiance, Wind Speed, Ambient Temperature, Wind Direction and Deviation of WD	MSE= 2309.05, RMSE= 48.05, MAE= 28.42, R2= 0.977
Xuan Liao et al[60] 2022	China and Austalia	Arid and humid	hourly	from 2015 to 2020	GBM, RF, SVR, and MLP	GBM	The maximum Temperature, minimum Temperature, average humidity, average wind speed, and average atmosphere pressure	Australia (nMBE= 0,01, nRMSE= 0,8 and R2= 0,99) china (nMBE= 0,01, nRMSE=1,6 and R2= 0,98

Work	Country	Climat	Kind of prediction	Period of used data	Models	Best model	Inputs	Performances metrics
Yuan Gao et al[61] 2022	Japan	Humid subtropical	Hourly	1/1/2019 – 31/12/2021	LSTM, generative model, bidirectional-LSTM	LSTM	solar irradiation (MJ/m2), penetration (mm); Temperature (C); dew Temperature (C); humidity; and radiation time per hour	MAE= 20.9% and RMSE= 14.3%
Salwan Tajjour et al[62] 2023	India	Subtropical	Daily	2010/05/01 to 2021/05/01	MLP,LSTM and GRU	MLP	Wind speed and direction, Temperature, clear-sky index, Humidity, Pressure, Precipitation, dew/FrostPoint	RMSE= 11.8
Gulizar Gizem Tolun1 And Yusuf Alper Kaplan[63] 2023	Turkey	Mediterranean	Monthly	2014-2017	MLP	/	Temperature, relative humidity, sunshine duration and precipitation	R2= 0.9019

Table II.3: Comparative Analysis of Deep Learning Models for Solar Radiation Prediction in Diverse Climatic Regions.

Work	Country	Climat	Kind of forecast	Period of used data	Models	Best model	Inputs	Performances metrics
L. Benali et al[64] 2018	France	Metropolitan	Hourly	. 2001-2004	smart persistence (naïve model), artificial neural network and random forest	RF	Clear sky, the monthly mean values of aerosol optical depth, and water vapor column.	MAE= 61.49, RMSE = 88.62, nRMSE = 19.65% nMAE = 13.64%
J Liu et al[65] 2019	China	Continental humid	Monthly	2004–2014	MV,IRF,RF and SVM	RF	sunshine, mean atmospheric pressure, mean wind speed, mean air Temperature, angle of elevation of the sun, and mean humidity	R2= 0.9665, RSME =19.6085
Rachit Srivastava et al[66] 2019	India	Subtropical	Hourly	2017	MARS, CART, M5, and random forest	Random Forest	min Temperature, max Temperature, average Temperature, wind speed, rainfall, dew point, global solar radiation, atmospheric pressure, and solar azimuth	/
Lifeng Wu et al[67] 2019	China	Continental humid	Monthly	2001–2015	M5Tree ,RF CatBoost, MLP, MARS ,KNEA	KNEA	H0 ,n/N ,Tmax, Tmin, Hr, P	RMSE =1.846, R2=0.919, nRMSE=0.113 and MAE=1.398

Work	Country	Climat	Kind of prediction	Period of used data	Models	Best model	Inputs	Performances metrics
Junliang Fan et al[68] 2019	China	Four different climates zones	Daily	1966–2015	Linear, Quadratic, Cubic, Logarithmic, Linear logarithmic, Exponential 1, Exponential 2, Linear exponential, Power 1, Power 2, Rational 1 and Rational 2, MLP, RBF, GRNN, ELM, SVM, LSSVM, M5Tree, RF, GBDT, XGBoost, ANFIS, MARS	MARS	sunshine duration	MBE =-0.664, RMSE =1.807, NRMSE=0.122, R2 =0.960,t-statistic= 27.122 and U95=4.838
Meysam Alizamir et al[69] 2020	Turkey and USA	Mediterranean and	Monthly		GBT, MLPNN, ANFIS-FCM, ANFIS-SC, MARS, and CART	GBT	Wind speed, maximum air Temperature, minimum air Temperature, and relative humidity	RMSE =4%, R =1.37%, MAE= 0.24% and NS 4.12%,

Work	Country	Climat	Kind of prediction	Period of used data	Models	Best model	Inputs	Performances metrics
Isha Arora et al[70] 2020	India	Subtropical	Daily	2017 to 2018	Fine Tree, Medium Tree, Coarse Tree, and Optimisable Tree Bagging, Boosting, and Optimisable Ensemble	the ensemble models DT	average Temperature, min Temperature, max Temperature, relative humidity, precipitation, sunshine hours, clearness index, surface pressure, wind speed, and calendar variables	RMSE=0.125, MSE=0.015, MAE=0.088, and R2=0.99.
Elysia Jumin et al[71] 2021	Malaysia	Equatorial	Hourly	2008-2010	BDTR, linear regression, neural network	BDTR	/	R2=0.90183=, MAE= 0.06625 ,RMSE=0.08551, RAE =0.27746 and RSE=0.09817
Hakan Kor[72] 2021	Honolulu	Tropical	Monthly	September-December 2016	Bagging, RF, AdaBoost, gradient tree boosting, and histogram-based gradient algorithms	RF	variables of time, radiation value, Temperature, pressure, humidity, wind direction; speed, sunrise time, and sunset time	R=0,93

Work	Country	Climat	Kind of prediction	Period of used data	Models	Best model	Inputs	Performances metrics
Rahul et al[73] 2021	China	Arid and humid	Daily and Monthly	1980-2016	multiple linear regression , RBF, KNN , DT , MLP , ELM, SVM, GPR, Adaboost, XGBoost ,RF and stacking	stacking and XGBoost	the visibility (VIS), the mean relative humidity (RHU-mean), the minimum relative humidity (RHU-min), the mean wind speed (WIN-mean),the mean precipitation (PRE-mean), the mean pressure (PRS mean),the maximum pressure (PRS-max), the minimum pressure (PRS-min), the sunshine duration (SSD), the mean Temperature (TEM-mean), the maximum Temperature(TEM-max), the minimum Temperature (TEM-min), the mean ground Temperature (GST-mean), and the total solar radiation (RAD).	MAPE=0,77

Work	Country	Climat	Kind of prediction	Period of used data	Models	Best model	Inputs	Performances metrics
Wei Wu et al[74] 2021	China	Arid and humid	Daily	1980-2010	BART	/	daily global solar radiation (H), horizontal diffuse solar radiation (Hd), sunshine duration (N), mean Temperature (Tmean), maximum Temperature (Tmax), minimum Temperature (Tmin), relative humidity (RH), and rainfall (Rain)	R=0.965, RMSE=1.536, NSE=0.903 ,RRMSE=0.129and MAE=1.203,RIR=1.90 ,RIRMSE=21.23
Modeste Kameni Nematchoua et al[75] 2022	27 European	/	Daily	1960–1990 and 2000–2019	LM, DT, SVM, DL, RF, and GBT	DL, LM, GB, RF, and DT	daily air Temperature (Ta), wind speed (Va), relative humidity (RH), and solar radiation.	/
Neha Sehrawat et al[76] 2023	India	Subtropical	/	2018 to 2022	8 STR-CV, RF,XGB ,DT, GBoosting, XGB RF , LR, Catboost , Light GBM	8 STR-CV	time of day ,Temperature, cloudiness index, relative humidity, and day of the week	RMSE = 13.54 and R2= 0.9780

Table II.4: Comparative Analysis of Tree Based Models for Solar Radiation Prediction in Diverse Climatic Regions.

Work	Country	Climat	Kind of forecast	Period of used data	Models	Best model	Inputs	Performances metrics
Ahmad Alzahrani et al[77] 2017	Canada	humid continental	Hourly	March 24, February 8, October 8, and August 12	SVR, FNN and LSTM	LSTM	/	RMSE=0.086 and MBE= 0.004
Muhammed A. Hassan et al[78] 2017	Egypt	Desert	daily	October 2012 - December 2013	MLP,ANFIS, SVM, decision tree, and regression models (linear, multi-linear, and non-linear	MLP		
A. Khosravi et al[79] 2018	United Arab Emirates (UAE)	Hot desert	Hourly	/	(MLFFNN), (RBFNN), (SVR), (FIS), and (ANFIS)	SVR and MLFFNN	local time, Temperature, pressure, wind speed, and relative humidity	with R = 0.9999 and 0.9795
Junliang Fan et al[80] 2018	China	Arid and humid	Daily	1966 to 2015	four empirical Temperature-based models ,SVM and XGBoost	SVM and XGBoost	Daily solar radiation H, air Temperatures (Tmax and Tmin), and extra−terrestrial solar radiation (H0)	R2 = 0.753, RMSE = 3.326, MAE = 2.493 and MBE =0.093

Work	Country	Climat	Kind of prediction	Period of used data	Models	Best model	Inputs	Performances metrics
Abeera Javed et al[81]2019	Pakistan		10 min	2015 to 2017	Linear Regression, Elastic Net, Lasso Regression, Ridge Regression, SVM with Linear Kernel, and RBF kernel) and Regression Trees	SVM- RBF	Temperature, wind speed, atmospheric pressure, and humidity	R2=0.94
Juan Antonio Bellido Jiménez[82] 2021	Spain and USA	Mediterranean and Continental	Monthly	2000 to 2018	MLP, ELM, RF, SVM, XG Boost, and GRNN	SVM	Max and Min Daily Air Temperature (Tx and Tn), (Tx prev and Tn prev), (Tn next), (Tx difference Tn), (HourminTx), (HourminTn), the integral of the half-hourly Temperature values during each day (EnergyT)	MBE = 0.005, RMSE = 0.209, NSE = 0.917, R2 = 0.920, GPI = 0.264
Dongyu Jia et al[83] 2022	China	Arid and humid		2015-2020	SVM GLMNET and RF	SVM		nRMSE=17.02, nMAE=13,54, nMBE=10,02, and R =0,97

Work	Country	Climat	Kind of prediction	Period of used data	Models	Best model	Inputs	Performances metrics
Modeste Kameni Nematchoua et al[84] 2022	27 cities European	/	Daily	1960-1990 and 2000-2019	Linear model (LM), Decision Tree (DT), Support Vector Machine (SVM), Deep Learning (DL), Random Forest (RF) and Gradient Boosted Trees (GBT)	DL	Daily solar radiation, air Temperature, wind speed, and relative humidity	R2= 0.989, RMSE= 1.119, AAE= 0.157 and ARE= 8.07
Vahdettin Demir and Hatice Citakoglu[85] 2023	Turkey	Arid and semi-arid	Monthly	1967–2020	SVMR, LSTM, GPR, ELM and KNN.	LSTM	Monthly solar radiation (SR, MJ/m2), (Tmax, C), (Tavg), (Tmin, C), (WSavg, m/s), elevation (m), year, longitude (), month, latitude (), (RHmax, %) and (RHmin, %)	MARE=15.17 and 28.31, MAE = 1.759 and 3.358, RMSE = 2.297 and 4.422 and mean NSE = 0.875

Table II.5: Comparative Analysis of Based Kernel Models for Solar Radiation Prediction in Diverse Climatic Regions.

Work	Country	Climat	Kind of forcast	Period of used data	Models	Best model	Inputs	Performances metrics
Chao-Rong Chen and Unit Three Kartini[86] 2017	Taiwan	Subtropical	Hourly	8 June 2012	KNN, KNN-ANN	KNN-ANN	Solar radiation, Temperature, humidity, wind speed and direction	MABE=42 W/m2 and RMSE= 242 W/m2.
A. Khosravi et al[87] 2018	U.A.E	Desert	Monthly	2016	GMDH, MLFFNN, ANFIS models, optimized with PSO, GA, and ACO algorithms	GMDH	Month day, top of atmosphere insolation ,air pressure ,average air Temp, max Temp,min air Temp, relative humidity, wind speed, latitude and longitude	R2=0.9886,RMSE=0.2456 and MSE=0.0608
Yixuan Zhang et al[88] 2019	China	Four different zones	Daily	1997 - 2016	Ångström-Prescott, Bristow-Campbell, Swartman-Ogunlade, Sebaii, Chen and Abdalla), BP and PSO-BP	PSO-BP	Sunshine duration, maximum Temperature, minimum Temperature and extraterrestrial solar radiation.	R2 = 0.92 and 0.97.

Work	Country	Climat	Kind of prediction	Period of used data	Models	Best model	Inputs	Performances metrics
Chigbogu Godwin Ozoegwu[89] 2019	Nigeria	Tropical humid	Daily	February 2004 to April 2018	Non-linear autoregressive hybrid time series methods, ANN	hybrid time series methods	Hj-1,Hj-2,.....Hj-d , Nj	R2= 0.96 - 0.98

Work	**Country**	**Climat**	**Kind of prediction**	**Period of used data**	**Models**	**Best model**	**Inputs**	**Performances metrics**
Shaban G. Gouda et al[90] 2019	China	Arid and humid	Daily	1961 to 2010	Al-Salaymeh model 1, Al-Salaymeh model 2, Al-Salaymeh model 3, Al-Salaymeh model 4, Bulut and Büyükalaca model, Kaplanis and Kaplani model, Li model, Zang model and Quej model	D7,D8,D3 and D4	/	(RMSE= 0.780, MABE= 0.586, R2= 0.984,r= 0.976 and U95= 2.062)D7 , (RMSE= 0.783, MABE= 0.622, R2= 0.991,r= 0.992 and U95= 2.160)D8 , (RMSE= 1.042, MABE= 0.835, R2= 0.980,r= 0.983 and U95= 2.743)D3 and (RMSE= 1.309, MABE= 1.030, R2= 0.912,r= 0.944 and U95= 3.557)D4

Work	Country	Climat	Kind of prediction	Period of used data	Models	Best model	Inputs	Performances metrics
Haixiang Zang et al[91] 2019	China	Arid and humid	Daily	1994 to 2015	GPR,SVR,empirical models (EMs) and machine learning (ML)		the day of the year	RMSE=1.203, MAPE=2, 4.516%, MABE= 0.879 and R=0.983
Foster Lubbe et al[92] 2020	Southern African	Subtropical	Hourly	1 February 2015 to 8 February 2015	Periodic Kernel(Per), RBF Kernel, Rational Quadratic Kernel(RQ)	Per × RQ	GHI, DNI, DHI, DHI_shadowband, UVA, UVB, air_Temp, RH, WS, WD, WD_SD and BP	RMSE= 94.1
Banalaxmi Brahma and Rajesh Wadhvani[93] 2020	India	Subtropical	Daily	1983–2019	LSTM, GRU, bidirectional LSTM, CNN-LSTM	Bidirectional LSTM	Times series	MSE= 7.610, RMSE= 8.724 and R2= 73.34

Work	Country	Climat	Kind of prediction	Period of used data	Models	Best model	Inputs	Performances metrics
Jose Manuel Soares de Araujo 2020	Timor oriental	Arid and humid	Hourly	1st January to 31st March 2015	WRF-LSTM	/	wind speed, wind direction, Temperature and solar radiation	MBE=0.006, RMSE=161 W/m2, nMBE=0.65% and nRMSE=16.18%
Amit Rai te al[94] 2020	Timor oriental	Arid and humid	Hourly	1/1/2014-31/12/2015	LSTM,GRU , CNN-LSTM, CNN-GRU and CNN-Bi-LSTM	CNN-Bi-LSTM	Latitude, Longitude, Elevation, Optimum Slope, Azimuth, Max. Solar radiation (W/m2) and Temperature	MSE=0.0034, MAE=0.0347, r2= 0.94236097 and Sk=0.945182421 and Kurtosis=-0.694346292

Work	Country	Climat	Kind of prediction	Period of used data	Models	Best model	Inputs	Performances metrics
Haixiang Zang et al[95] 2020	USA	continental subarctic	Hourly	01/01/2006 - 31/12/ 2012.	Persistence, SVM, ANN, CNN, LSTM, and hybrid models :CNN-ANN,ANN-LSTM and CNN-LSTM	CNN-LSTM	latitude, longitude and the statistical mean value (m) of the GHI Hourly GHI, dew point Temperature (DPT), solar zenith angle (SZA), wind speed (WS), wind direction (WD), precipitable water (PW), relative humidity (RH) and Temperature(T)	MAE=30.50, nMAE=5.76, RMSE=50.95, nRMSE=9.62 and R=0.9854
Yanfeng Liu et al[96] 2020	China	Arid and humid	Daily	1981-2000 and 2001-2010	ten empirical models, five copula-base non-linear quantile regression (CNQR), five SVM models and support vector machine-firefly algorithm (SVM-FFA)	SVM-FFA	Solar radiation measured , Extra-terrestrial ,clearness index (Kt); sunshine ratio (S); Kt and S; Kt, S and average Temperature (Ta) and average relative humidity	MABE= 0.67% and R2=0.67%

Work	Country	Climat	Kind of prediction	Period of used data	Models	Best model	Inputs	Performances metrics
YHamza Ali-Ou-Salah et al[97] 2021	Portugal	Subtropical	Daily	12012 to 2016	RF, GB, SVM ,ANN and (SVR-RF)	SVR-RF	/	/
Shuting Zhao et al[98] 2022	China	Arid and humid	Daily	2011 to 2015	Gradient boosting decision tree (GBDT), Random forest (RF), Support vector machine (SVM), Extreme gradient boosting (XGBoost),	SVM	Extra-terrestrial radiation (H0), sunshine hours (n), maximum possible sunshine duration (N), maximum Temperature (Tmax), minimum Temperature (Tmin), and relative humidity (RH).	RMSE= 1.732and R2 = 0.939

Work	Country	Climat	Kind of prediction	Period of used data	Models	Best model	Inputs	Performances metrics
Sujan Ghimire et al[99] 2022	Australia	Equatorial	Daily		LSTM, DBN, RBF, BRF, MARS, WKNNR, GPML, M5TREE and hybrid CNN-SVR	CNN-SVR	Cloud Area Fraction, Surface Upward Sensible Heat Flux, Relative Humidity, Near Surface Specific Humidity, Precipitation, Convective Precipitation, Solid Precipitation ,Sea Level Pressure, Near Surface Relative Humidity, Surface Daily Max Relative Humidity, Surface Daily Min Relative Humidity, Wind Wind Speed, Wind max Daily Maximum Near-Surface Wind Speed, Air Temperature, Near Surface Air Temperature, Daily Max Near Surface Air Temperature, Daily Min Near Surface Air Temperature, Eastward Wind ,Eastern Near-Surface Wind, Northward Wind, Northern Near-Surface	RMSE=2.172-3.305 and MAE:1.624-2.370

Work	Country	Climat	Kind of prediction	Period of used data	Models	Best model	Inputs	Performances metrics
Sujan Ghimire et al[100] 2022	Australia	Arid	Daily		CNN,LSTM,CNN with Multilayer-Perceptron output (SCLC algorithm hereafter), Artificial Neural-Network, Random-Forest, Self-Adaptive Differential-Evolutionary Extreme-Learning-Machines	SCLC	/	RMSE=2.314,r=0.933, Willmott's Index (WI)=0.928,NSE=0.865, McCabes index (LM)= 0.525 and explained variance score (Evar)= 0.757
Neha Sehrawat et al[101] 2023	India	Subtropical	Hourly	2018 to 2022	Random Forest, XGB, Decision Tree, Gradient Boosting, XGB Random Forest, Linear Regression, Catboost, Light GBM and 8 STR-CV	8 STR-CV	time of day, Temperature, cloudiness index, relative humidity and day of the week	R2= 0.9895, RMSE=9.32

Work	Country	Climat	Kind of prediction	Period of used data	Models	Best model	Inputs	Performances metrics
Jingxuan Liu et al[102] 2023	China	Subtropical	Daily	January 1, 1994 to December 31, 2015	TimeGAN-based, DBN	Time GAN-based	daily maximum Temperature (Tmax), daily minimum Temperature (Tmin), daily average Temperature (Tmean), daily shine radiation (S), daily average humidity (Hmean)	MAE=1.706, RMSE=2,2.352 and R^2 =0.955
Kashif Irshad et al[103] 2023	Saudi Arabia	Desert	/	/	MLR, KNN, FFNN, SVR, and DBN models and AOHDL-SRP	AOHDL-SRP	Radiation, Temp, Pressure, Humidity, Wind direction, Wind speed, Time Sunrise, Time sunset	R2=100%, MSE=0.18, RMSE=0.43 and MAE= 0.32.

Work	Country	Climat	Kind of prediction	Period of used data	Models	Best model	Inputs	Performances metrics
Mehdi Neshat et al[104] 2023	USA	Continental	Monthly	January 2014 to June 2022	FFNN, ANFIS ,LSTM, BiLSTM, GRU, S-LSTM, S-BiLSTM, S-GRU, GRU-LSTM, LSTM-GRU ,GRU-BiLSTM and 2GRU-LSTM, 5CNN_3LSTM 5CNN_3GRU 5CNN_3BiLSTM, 5CNN_GRU-2LSTM 5CNN_2GRU-LSTM 4CNN_GRU-2LSTM, 3CNN_GRU-2LSTM 2CNN_GRU-2LSTM CNN_GRU-2LSTM, Xception_LSTM Resnet50_LSTM Resnet50_GRU_2LSTM	ADCMAResNet50-GRU-2LSTM	wind speed, direction, temperature and SRAD	MSE= 0.0137, RMSE=0.1150 R-value=0.7837, MAE 0.0782 and SMAPE=0.1228

Work	Country	Climat	Kind of prediction	Period of used data	Models	Best model	Inputs	Performances metrics
Mohammed Abdallah et al[105] 2023	Sweden	Temperate	Daily	2008 to 2021	(VMD), (MFRFNN) (QRF) and (VMD-MFRFNN-QRF)	VMD-MFRFNN-QRFV	average daily GSR, air temperature (Tmin, Tmax, T), wind speed (WS), RH, and SSH	RMSE=23.3, MAE=17.4 , MAPE=38.4 and NSE=0.946
Neha Sehrawat et al[106] 2023	India	Subtropical	Hourly	2018 to 2022	Random Forest ,XGB ,Decision Tree, Gradient Boosting, XGB Random Forest , Linear Regression,Catboost ,Light GBM and 8 STR-CV	8 STR-CV	time of day ,Temperature, cloudiness index, relative humidity, and day of the week	R2 = 0.9895, RMSE= 9.32
Meysam Alizamir et al[107] 2023	USA	Continental subarctic	Daily	1/0 1/2019 to 5/03/2021	WMLPANN, LSTM, MLPANN and MARS	WLSTM	maxi and min relative humidity, potential evapotranspiration, max and min temperature, precipitation, and wind speed	RMSE =6-14%

Work	**Country**	**Climat**	**Kind of prediction**	**Period of used data**	**Models**	**Best model**	**Inputs**	**Performances metrics**
Liwen Xing et al[108] 2023	China	Subtropical	Daily	1994 to 2016	MEA ,DBN , LSTM and MEA-DBN-LSTM	MEA-DBN-LSTM	daily measurements of Rs temperature, humidity, sunshine duration, precipitation, wind speed	R^2 = 0.999 and NSE=0.954
Yunbo Lu et al[109] 2023	China	Subtropical		2009 to 2017	RTM-LightGBM, RTM-XGBoost, RTM-RF, RTM-DNN, RTM-MLP, and RTM-MARS	RTM-RF	optical properties of aerosols, water vapour, ozone and the albedo of the Earth's surface	R^2 = 0.98, MAE=15.57

Table II.6: Comparative Analysis of Hybrid Models for Solar Radiation Prediction in Diverse Climatic Regions.

Work	Country	Climat	Kind of forecast	Period of used data	Models	Best model	Inputs	Performances metrics
K. Ouali et al[110] 2014	Bejaia	Mediterranean	Monthly	2010 to 2013	Angstrom-Prescott, Bahel, Newland Abdalla and multiple linear regression	multiple linear regression	sunshine hours, Temperature, pressure, humidity and rainfall	MBE=0. 1722 RMSE=2. 0317, MPE =2. 1198 and R2= 0.9644
Mohamed Salah Mecibah et al[111] 2014	Algiers, Oran, Batna, Ghardaia, Bechar and Tamanrasset	Mediterranean, semi- arid ,Arid and Desert	Monthly	/	linear, quadratic, cubic, logarithmic, exponential, exponent, Allen (1), Chen (1), Chen (2).and Allen (2)	cubic and quadratic models	mean sunshine and air Temperature	R2=0.9516, MPE=3.4149, MAPE=5.7009, MBE=0.0173, MABE=0.0313, and RMSE=0.0359
S. Belaid et al[112] 2016	Ghardaia	Semi-arid	Daily and monthly	2012-2014	SVM and MLP	MLP	Tmax; Tmin; Tmean and Tdif), max extra-terrestrial sunshine duration, and extra-terrestrial solar radiation	NRMSE=13.163%, MAPE=10.403% , and R=0.894 for the DGSR prediction. For the monthly NRMSE=7.442%, MAPE = 8.940%, and R=0.986.

Work	Country	Climat	Kind of prediction	Period of used data	Models	Best model	Inputs	Performances metrics
L. Achour et al[113] 2017	Tamenrasset	Desert	Monthly	2000-2004	Linear,Quadratic, Cubic,Logarithmic, Exponential,Exponent,Linear, latitude related,Linear ,known constants,Fourier series,Weibull model, Sin equations,Power series,Rational model,Gaussian series, SHBM	SHBM	Extra-terrestrial solar irradiance (G0), duration sunshine (S) and daylight hours (S0)	pRMSE=4.6246, pRAE= 0.0935, pMAE=3.3294 and R2= 0.9770
K. Smaili et al[114] 2018	Ghardaia , Bouzerah	Semi-arid and Mediterranean	Daily	/	Yaiche, Garg, Hussain, Swartman, Sabbagh, Sayigh, Sivkov and Coppolino	Yaiche	Ambient Temperature, relative humidity, duration of insolation, , the declination of the sun, and extra-terrestrial irradiation.	RMSE= 0.99
Y. Marif et al[115] 2018	Illizi	Desert	Monthly	2007-2018	Linear,Quadratic, Cubic	Cubic	Extra-terrestrial solar irradiance (H0), duration sunshine (S) and daylight hours (S0)	RMSE = 0.51822, MBE= 0.21197, MABE= 0.369839 ,MPE=0.64767 and R2=0.99399

Work	Country	Climat	Kind of prediction	Period of used data	Models	Best model	Inputs	Performances metrics
Abdelaziz Rabehiet al[116] 2018	Ghardaïa	Semi- arid	5 min	2014-2016	MLP, BDTand LR-MLP,LR-BDT	MLP	Extra-terrestrial solar radiation, daily minimum and maximum and mean Temperatures, and sunshine duration ratio	nRMSE=0.033, R2 =97.7%
Mawloud Guermoui et al[117] 2018	Ghardaïa	Semi- arid	Daily	2013-2015	WGPR-PFA and WGPR-CFA	WGPR-PFA	Number of Day (D), Air Temperature (Tmin, Tmax, Tmean), Relative Humidity (RHmin, RHmax, RHmean), Pressure (Pmin, Pmax, Pmean), Sushine Duration (S), Maxumum Elevation (ME), Declination angle (Da), Day Duration (Dd) and Sunshine Ratio (SS).	RMSE = 3.18 (MJ/m2) and R2 = 85.85 (%)daily global horizontal radiation, and RMSE = 5.23 (MJ/ m2) and R2 = 56.21(%) for daily direct horizontal radiation.

Work	Country	Climat	Kind of prediction	Period of used data	Models	Best model	Inputs	Performances metrics
D.Benatiallah et al[118] 2018	Adrar	Arid	Monthly	2014	R.sun model	/	height of the sun, azimuth, solar incidence angle, and altitude, relative optical air mass and the Linke turbidity factor	MAPE= 9.44 %,.,MBE= -7.94 %, RMSE= 12.31 % and R= 0.9984
D.Benatiallah et al[119] 2019	Adrar	Arid	Daily	2016	Campbell model	/	duration of sunshine, daily solar radiation	MAPE=6.13%, MBE=13.95 Wh/m2, RMSE=36.55 Wh/m2, R=0.9969
Khalil Benmouiza[120] 2022	Ghardaia,	Semi- arid	Hourly	01/012020 - 31/12/2020	(BP), (SVM), (LTSM), BP-MLP, RNN-MLP, LSTM-MLP hybrid (WPD), (CNN) ,LSTM-MLP, ANFIS and LGC-GMDH	LGC- GMDH	solar irradiation; air Temperature, humidity, wind speed, atmospheric pressure	RMSE= 35.96,MAE= 22.26,R2= 0.982 and FS= 48.12%

Work	Country	Climat	Kind of prediction	Period of used data	Models	Best model	Inputs	Performances metrics
Senouci Ahlam et al[121] 2023	Adrar, Tindouf and Tamanrasset	Arid	Daily	2016 to 2017	ANN,ANN_GA,ANN-PSO,ANFIS,ANFIS-GA,ANFIS-PSO	ANN-PSO	day of the year, year, Temperature, relative humidity, pressure, wind speed, and the measured global solar radiation	MPE = 0.0013, RMSE = 2.2587 and R = 0.9999
Mostefaoui Mohamed Dhiaeddine et al[122] 2023	Lagouat	Arid	Hourly	/	FFNN, FCNN and FNN	FCNN	clear sky, Temperature, sun height, wind speed and the top of atmosphere solar irradiation.	NMSE=0.0507, RMSE=65.6802, NRMSE=0.2252, R=0.9774 and R2=0.9554
Halima Djeldjli et al[123] 2023	Adrar, Eloued, Ouargla, Tamanrasset, Timimoun and Bechar	Arid	Daily	01/01/2010-31/12/2021	ANN, SVM and FFA-ANN	FFA-ANN	Extra-terrestrial solar irradiation (H0), declination and average Temperature (Tavg) with relative humidity (RH)	R = 0.9321, rRMSE = 9.35% and MAPE = 6.29%

Work	Country	Climat	Kind of prediction	Period of used data	Models	Best model	Inputs	Performances metrics
S.Yahiaoui and O.Assas[124] 2023	Batna	Semi-arid	Daily	1996-2005	Multi-Linear regression,Fuzzy logic and MLP	MLP	G0 (extraterrestrial), temperature (T), humidity (Hu), pressure (Pr), wind speed (Ws), and rainfall (R)	RMSE=7.701, MAE=14.989, MSE=59.315and $R^2 = 0.999$
S.Yahiaoui and O.Assas[125] 2023	Batna	Semi-arid	Daily	1996-2005	Fuzzy-T,Fuzzy-Hu,Fuzzy-Ws,Fuzzy-R,Fuzzy-Pr, Fuzzy-ALL	Fuzzy-Ws-Gauss	G0 (extraterrestrial), temperature (T), humidity (Hu), pressure (Pr), wind speed (Ws), and rainfall (R)	MSE=18,009, MAE=3,397, RMSE=4,244 and $R^2 = 0,824$
S.Yahiaoui and O.Assas[126] 2023	Batna	Semi-arid	Daily	1996-2005	MLP,RNN,CNN and LSTM	LSTM	G0 (extraterrestrial), temperature (T), humidity (Hu), pressure (Pr), wind speed (Ws), and rainfall (R)	MSE=7.742, MAE=2.043, RMSE=2.782 and$R^2 = 0.860$

Table II.7: Comparative Analysis of Differents Models for Solar Radiation Prediction in Diverse Climatic Regions of Algeria.

II.5 Conclusion

In conclusion, this chapter provides a captivating exploration into the prediction of solar radiation using meteorological parameters as a foundational framework. The chapter begins with an insightful introduction, emphasizing the significance of solar radiation prediction across diverse fields and outlining the chapter's objectives. A historical retrospective is then embarked upon, tracing the evolution of solar radiation prediction through key milestones and technological breakthroughs that have shaped its trajectory. The subsequent section delves into the core theories, models, and approaches employed to achieve precise solar radiation predictions grounded in meteorological data. A comprehensive overview of recent developments follows, highlighting the integration of cutting-edge AI techniques, including deep neural networks and machine learning methods, to enhance the accuracy of solar predictions. The culmination of these advancements underscores the contemporary reliance on AI in the realm of solar radiation prediction.

This chapter encapsulates a broad spectrum of research and progress in the field of solar irradiance forecasting. In its final strides, the chapter consolidates its insights by summarizing essential points, extracting valuable lessons from historical perspectives, and engaging in a forward-looking discussion on the future prospects of solar radiation prediction. In doing so, it offers a thorough and enlightening overview, paving the way for continued advancements and innovation in this dynamic field.

Chapter III

EXPERIMENTAL STUDY OF THE MODELS ADOPTED, RESULTS AND DISCUSSION

EXPERIMENTAL STUDY OF THE MODELS ADOPTED, RESULTS AND DISCUSSION

III.1 Introduction

Predicting global solar radiation over a horizontal surface is essential for assessing the availability of solar energy in a given region. It allows the determination of the amount of solar energy that can be measured by the pyranometer. The prediction of global solar radiation depends on mathematical models that take into account data such as geographical position, time of day, season, cloud cover and local weather conditions. Meteorological data is often collected from weathers stations or weather satellites, and mathematical models are used to extrapolate this data over a wider area.

One of the most widely used and successful methods over the last decade in the scientific field is artificial intelligence. AI plays a key role in predicting solar radiation because of its ability to accurately model the relationships between meteorological variables and solar radiation. Its use is helping to promote a more efficient and sustainable use of solar energy.

This chapter provides an in-depth analysis of the different models based on AI adopted and proposed for the prediction of global solar radiation on a horizontal surface for the city of Batna, evaluating their performance, limitations and then a comparison of the different models with each other and with others works is done. The second section describes the study site then the collection of meteorological data used to train and test the models designed is provided in the third one. Fourth and fifth section outlines the methodology of approaches used and finally discusses the results.

III.2 Site of study

The city is known for its rich history and culture, with Roman remains dating back to Numidian times. Batna is also an important economic and educational center in the region, home to a variety of industries such as agri-food, textiles and construction. As a crossroads between different regions, Batna plays a key role in Algeria's socio-economic development. Its strategic location also makes it a hub for trade and tourism activities. Batna (Figure III.1) is located in the High Plateau region of Algeria, around 430 kilometers south-east of Algiers. It lies at an altitude of almost 1,050 meters, giving it a semi-arid climate with four distinct seasons. In fact, in winter it is quite cold, in summer it can be very hot and rainfall is quite rare. The rains are not abundant because Batna is situated in the south of Tellian Atlas, the

mountain range parallel to the coast that receives most of the rainfall, finally to conclude.

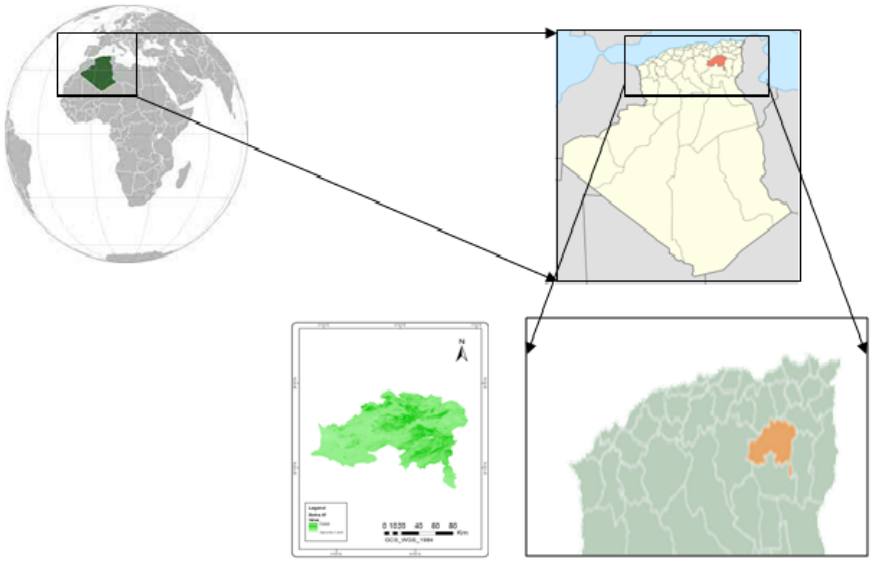

Figure III.1: Geographical map of Batna Study Site

III.3 Data

These databases provide historical meteorological and solar information recorded over extended periods. The size, the richer, more complete and diversified the data of database contributes to the prediction, which can improve the accuracy of predictions. The databases are used in two stages: data collection, Pre-processing and organization of collected data.

III.3.1 Data collection

Collecting meteorological data is of vital importance for predicting solar radiation; these data are collected from weather stations, satellites, solar sensors and other sources to cover a wide geographical area. The data used in this work have been extracted from the Helio Clim-1 website [127]. Helio Clim-1 is a meteorological data collection platform specializing in solar radiation. This site gathers information from various sources such as weather satellites and ground weather stations. This data includes measurements of direct, diffuse and global solar radiation, as well as meteorological variables such as temperature, humidity, pressure, wind speed, direction wind and rain. Using this data, researchers and solar energy professionals can develop accurate predictive models to estimate solar radiation at a given location at different times of the day and year.

These forecasts are essential for planning and optimizing solar systems, contributing to the expansion of solar energy as a clean, renewable energy source. The continuous collection of solar radiation data by Helio Clim-1 helps to improve prediction models, refine strategies for using solar energy and promote a sustainable energy transition.

The data are collected from the Helio Clim1 site for the city of Batna and incorporated into an Excel file (see Figure III.2). The data cover a ten-year period (1996-2005).The climatic features utilized in this study include air temperature (T), relative humidity (Hu), wind speed (Ws), air pressure(Pr), Wind direction(Wd) and rain(R). Climatic data were downloaded from the SoDa-MERRA2 site[128].

The Excel file downloaded from the site has a CSV extension and a header which contains information on the geological parameters of the site, the start and end data, some information on solar radiation (unit, number of data, extraterrestrial radiation, clear sky,... etc.) and expressed as a percentage, it is the ratio of the number of hours used for computation to the length of the day in hours, given by the figure III.2.

R284

	A	B	C	D	E	F	G	H	I	J	K	L	M	N	O	P
32	nb de jour	# Date	Time	Global Ho	Clear-Sky	Top of Atr	Nb slots	Temperati	Relative H	Pressure	Wind spee	Wind dire	Rainfall	Snowfall	Snow depth	
33	1	01/02/2004	24:00:00	4341	4452	5718	75	281.33	59.50	916.77	1.10	295.36	0.000003	0.000000	0.000000	
34	2	02/02/2004	24:00:00	4321	4429	5768	77	281.86	57.14	917.87	0.41	291.03	0.000012	0.000000	0.000000	
35	3	03/02/2004	24:00:00	4333	4420	5820	77	282.79	69.11	918.44	1.35	39.78	0.006032	0.000000	0.000000	
36	4	04/02/2004	24:00:00	4475	4585	5872	79	282.14	63.58	919.95	1.31	79.31	0.023019	0.000000	0.000000	
37	5	05/02/2004	24:00:00	4495	4628	5926	79	282.74	47.33	920.42	0.69	95.72	0.000000	0.000000	0.000000	
38	6	06/02/2004	24:00:00	4487	4660	5980	81	282.45	51.38	918.52	0.75	187.79	0.000000	0.000000	0.000000	
277	245	02/10/2004	24:00:00	5767	6073	7901	84	293.39	39.54	912.22	0.51	135.84	0.000000	0.000000	0.000000	
278	246	03/10/2004	24:00:00	5739	5901	7840	84	293.07	47.10	912.68	0.80	235.45	0.000028	0.000000	0.000000	
279	247	04/10/2004	24:00:00	-999	5799	7779	0	293.30	49.33	911.74	1.32	198.68	0.004896	0.000000	0.000000	
280	248	05/10/2004	24:00:00	-999	5883	7718	0	292.98	48.15	911.31	1.33	227.54	0.004445	0.000000	0.000000	
281	249	06/10/2004	24:00:00	-999	5839	7656	0	293.31	40.10	910.44	1.82	217.42	0.000194	0.000000	0.000000	
282	250	07/10/2004	24:00:00	5556	5580	7595	52	293.86	37.88	909.81	2.05	250.08	0.001094	0.000000	0.000000	
283	251	08/10/2004	24:00:00	5600	5729	7534	83	292.89	35.69	909.18	2.92	195.47	0.000000	0.000000	0.000000	
284	252	09/10/2004	24:00:00	5447	5569	7472	81	293.82	30.88	909.20	2.95	185.22	0.000000	0.000000	0.000000	
285	253	10/10/2004	24:00:00	2061	5434	7411	77	291.88	45.72	908.33	1.60	206.40	1.182852	0.000000	0.000000	
286	254	11/10/2004	24:00:00	1468	5226	7350	77	289.04	72.69	908.16	1.29	232.69	11.443302	0.000000	0.000000	
287	255	12/10/2004	24:00:00	5283	5482	7288	80	289.15	58.70	907.38	0.73	290.65	9.100613	0.000000	0.000000	
288	256	13/10/2004	24:00:00	5172	5311	7227	69	288.43	67.05	906.31	1.63	293.01	5.513065	0.000000	0.000000	
289	257	14/10/2004	24:00:00	3336	5437	7166	83	287.16	57.90	904.94	1.15	217.04	0.010049	0.000000	0.000000	
290	258	15/10/2004	24:00:00	5073	5417	7105	81	288.78	48.88	903.93	2.28	235.57	0.000038	0.000000	0.000000	
291	259	16/10/2004	24:00:00	5134	5434	7045	81	287.49	47.55	903.49	2.17	281.73	0.000079	0.000000	0.000000	
292	260	17/10/2004	24:00:00	5098	5328	6984	81	289.97	42.44	905.42	1.85	233.20	0.000000	0.000000	0.000000	

Figure III.2: Excel File Format Provided by Helio-Clim1.

III.3.2 Pre-processing and organization of data

As shown in the previous figure, missing data are indicated by the number -999, a pre-processing is applied on these data which consists in eliminating the missing measurements and replacing them by the calculation of the average of the neighboring measurements. The data are then divided into two categories (see Figure III.3), one was for the three-year test period (2003-2005), while the other was for the seven-year learning period (1996-2002).

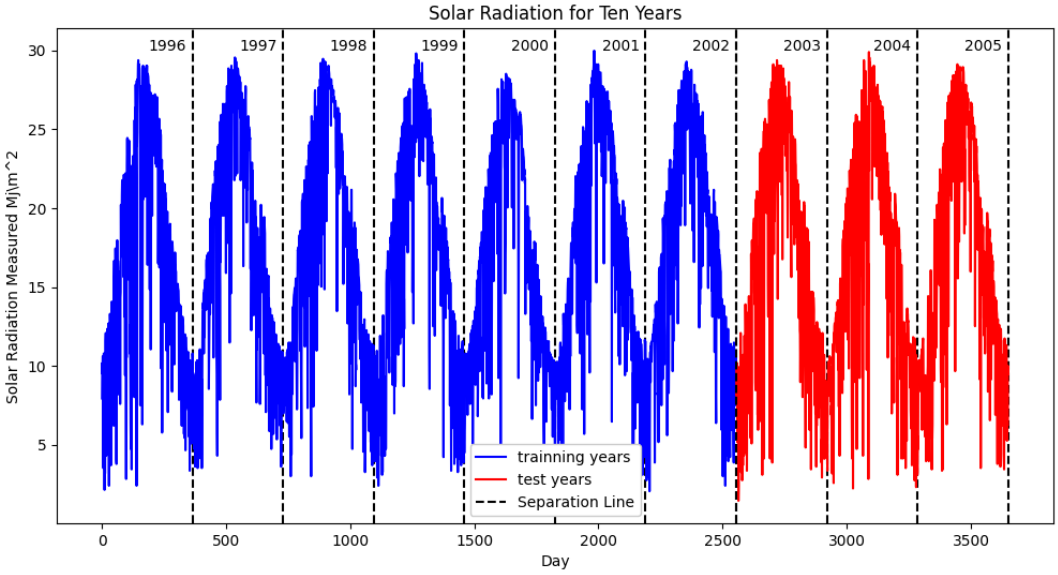

Figure III.3: The Solar Radiation of the City of Batna for the Period 1996-2005.

III.4 Methodology

Prediction modeling is a powerful approach to anticipating and estimating the future values of a variable based on historical data. It is a process that involves the creation of a mathematical, statistical or smart model capable of capturing the relationships present in the data. Different modeling techniques can be used, such as regression models, neural networks, machine learning methods and many others.

In this work, the adopted and proposed models for the prediction are divided into two groups: classical and intelligent models (see Figure III.4).

The classical group contains different regression models. They are essential and basic tools for predicting continuous numerical values as a function of input characteristics. Among the different types of regression models a few that have been used are: linear regression (also known as Angstrom-Prescott, which is based on the linear relationship between the features and the target), logarithmic, exponential, exponent models and polynomial regression, which capture more complex relationships using polynomial terms. Regularized regression techniques, such as Ridge and Lasso regressions offer mechanisms for managing over-fitting and selecting the most relevant features.

For the second intelligent group contains two categories: individual and hybrid.

Individual models where the latter consists of four of models: fuzzy logic, tree-based, Kernel-based and ANN-based.

Hybrid models combine different ML techniques or approaches to create a more powerful or efficient model. This involves taking features or components from different models and combining them synergistically.

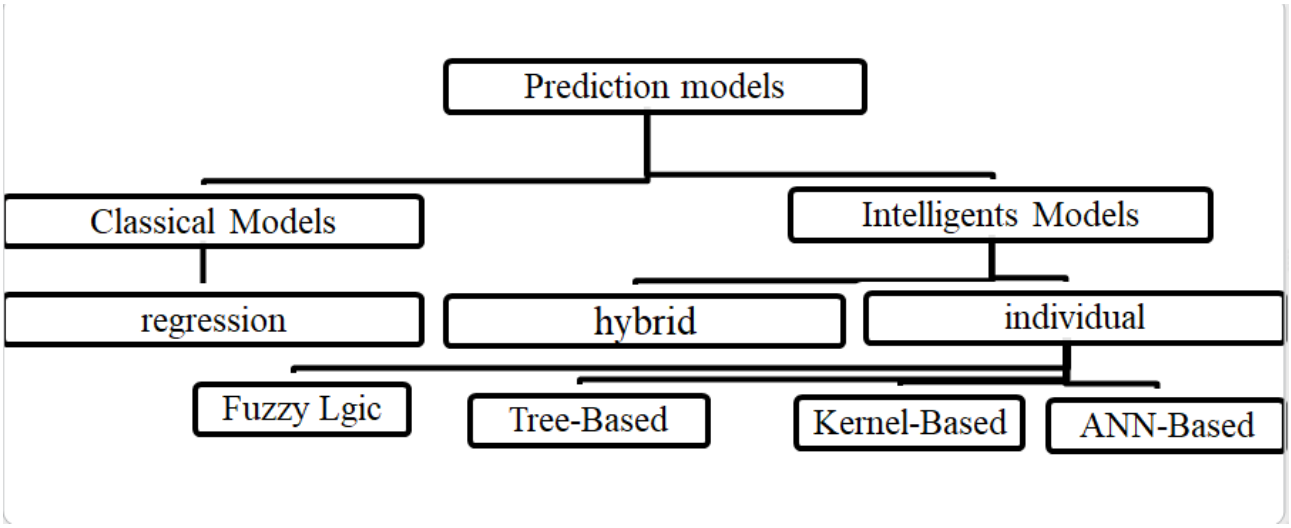

Figure III.4: The Models Adopted .

III.4.1 Classical models

In the solar energy literature, several studies have been carried out to predict solar radiation using regression models. These techniques seek to establish a relationship between a dependent variable and one or more independent variables, in order to predict the value of dependent variable. In this work, several regression models were developed, which are classified into three groups represented in the table 1: basic regression, polynomial regression (first-order (linear) and second-order (quadratic)) and regularized regression.

III.4.1.1 Basic regression

The aim is to create a model that can be used to make predictions or estimates. The percentage ratio is calculated by determining the proportion of the dependent variable based on the values of the independent variables. In this work we have adopted four models(linear, logarithmic, exponent and exponential):

- **Linear model**

This is one of the simplest and most commonly used regression models for prediction. It assumes a linear relationship between the dependent variable and the independent variables. The model seeks to fit a straight line that minimizes the difference between the predicted and actual values. The general equation of the linear model is of the form:

$$y = \beta_0 + \beta_1 \times x_1 + \epsilon \tag{III.1}$$

Where: y :represents the dependent variable.
x_1 : the independent variables.
β_0, β_1 :are the coefficients of the model. ϵ :quantifies the differences between the values actually observed and the values predicted by the model.

- **Logarithmic model**

This model assumes a logarithmic relationship between the dependent variable and the independent variables. It is useful for data showing exponential growth, which can be linearized by taking the logarithm of the values. The equation for the logarithmic model is usually of the form:

$$y = \beta_0 + \beta_1 \times \log(x_1) \tag{III.2}$$

- **Exponential model**

Is used when the dependent variable grows or decreases exponentially with respect to the independent variables ,the equation of exponential model is usually of the form:

$$y = \beta_0 + \exp \beta_1 \times x_1 \tag{III.3}$$

- **Exponent model**

This is a transformation of the logarithmic model, and to make the exponential model linear, we can take the logarithm of the values of the dependent variable. This transforms the exponential relationship into a linear relationship and makes it possible to use linear regression techniques. The equation for the exponential model with log transformation is usually of the form:

$$y = \beta_0 + x_1^{\beta 1} \tag{III.4}$$

III.4.1.2 Polynomial regression

Is an extension of linear models, where the relationships between dependent variable and the independent variables are modeled in the form of polynomial. They can be of different degrees, depending on the maximum power of the independent variables used in the model.In this work we have adopted the first and second degrees.

- **Degree 1 polynomial model (linear)**

This is the simplest model and equivalent to the classical linear model. It takes the form:

$$y = \beta_0 + \beta_1 \times x_1 + \beta_2 \times x_2 \tag{III.5}$$

Where:
y : the dependent variable.
x : the independent variable.
β_0,β_1 and β_2 : the coefficients of model.
r : the number of independent variables.

- **Degree 2 polynomial(quadratic) model**

This model includes terms of degree 2 (x^2) in addition to the linear terms. The equation of model is:

$$y = \beta_0 + \beta_1 \times x + \beta_2 \times x^2 \tag{III.6}$$

This model can be used to model non-linear relationships that form a parabola. Note: In our work the dependent variable is: G/G0 and for the independent variable is S/S0.

III.4.1.3 Regularized regression

Also known as penalized regression is an extension of classical linear regression models where it adds penalty terms to the cost or loss function used to fit the model. The aim of this regression is to prevent over-fitting by imposing a constraint on the model coefficients. In this work, we adopted the four models described as follows:

- **Ridge regression**

Ridge regression, also known as Tikhonov regularization, tackles a key challenge in linear regression: multi-collinearity. It builds upon the familiar Ordinary Least Squares (OLS) method, but with a twist. While OLS minimizes the sum of squared residuals, ridge regression adds a penalty term. This penalty "shrinks" the coefficients towards zero, reducing their magnitude and ultimately preventing over-fitting when features are highly correlated. Think of it as adding a gentle nudge to keep the coefficients in check, leading to a more robust and generalizable model.

- **Lasso(Least Absolute Shrinkage and Selection Operator)**

This is a combination of two methods: variable selection and regularization. It selects the relevant subset of variables in a linear regression model then regularizes these variables to avoid over-fitting the model.

- **Elastic Net**

This is an extension of Lasso regression. It solves a minimization process that aims to determine regression coefficients that reduce Both the prediction error and the weighted combination involve assessing the model's performance by considering the sum of the absolute values of the coefficients (L1 regularization) and the sum of the squares of the coefficients (L2 regularization).

- **Logistic Regression**

Logistic regression is a statistical technique used to predict the probability of an event occurring as a function of independent variables. It is a type of regression used when the target variable to be predicted is categorical or qualitative, unlike linear regression, where the target variable is quantitative. In practical terms, logistic regression models the probability of the

quantity of solar radiation of a specific day. The general form of the logistic model is:

$$P(Y = 1|x) = \frac{1}{1 + e^{\beta_0 + \beta_1 \times x_1 + ... + \beta_r \times x_r}} \quad \text{(III.7)}$$

P(Y=1|x) is the probability that the dependent variable Y is equal to 1 given a set of values for the independent variables x.

$\beta_0, \beta_1, ..., \beta_r$ are the regression coefficients to be estimated.

x_1,..., x_r are the values of the independent variables.

The parameters β are then estimated by maximum likelihood to best fit the predicted probabilities to the observations.

Sixteen models were developed, including four models: Angstrom-Prescott, logarithmic, exponential and exponent and five first-order empirical non-linear models. The majority of these non-linear solar radiation estimation models are described as Angstrom expression changes. These include first-order non-linear models combining measurements of the following six meteorological parameters: mean temperature T, relative humidity Hu, pressure, precipitation, wind speed and fraction of sunshine duration S/S0. For second-order quadratic models, three models are designed with fraction of sunshine duration S/S0, temperature T and humidity Hu. Finally, four regularized regression models corresponding to the adopted models cited above. In this work, the mathematical equations employed for the models are presented in the following table 1:

Table III.1: The mathematical equations of the regression models.

Model	Mathematical equation
Basic regression	
Angstrom-Prescott	$G/G_0 = a \times S/S_0 + b$
Exponential	$G/G_0 = a \times e^{b \times (S/S_0)}$
Exponent	$G/G_0 = a \times (S/S_0)^b$
Logarithmic	$G/G_0 = a + b \times \log(S/S_0)$
First-order Polynomial regression	
Model with T	$G/G_0 = a \times S/S_0 + b \times T + c$
Model with Hu	$G/G_0 = a \times S/S_0 + b \times Hu + c$
Model with Pr	$\frac{G}{G_0} = a \times \frac{S}{S_0} + b \times Pr + c$
Model with R	$\frac{G}{G_0} = a \times \frac{S}{S_0} + b \times R + c$
Model with W	$\frac{G}{G_0} = a \times \frac{S}{S_0} + b \times W + c$
Second-order polynomial regression	
Quadratic_ SS0	$\frac{G}{G_0} = \beta_0 + \beta_1 \times \frac{S}{S_0} + \beta_2 \times (\frac{S}{S_0})^2$
Quadratic_T	$\frac{G}{G_0} = \beta_0 + \beta_1 \times T + \beta_2 \times (T)^2$
Quadratic_Hu	$\frac{G}{G_0} = \beta_0 + \beta_1 \times Hu + \beta_2 \times (Hu)^2$
Regularized regression	
Ridge	$L_2(\beta) = \frac{1}{n}\sum_{i=1}^{n}(y_i - \hat{y}_i)^2 + \lambda \sum_{i=1}^{n} \beta_i^2$
Lasso	$L_1(\beta) = \frac{1}{n}\sum_{i=1}^{n}\lvert y_i - \hat{y}_i\rvert + \lambda \sum_{i=1}^{n} \lvert\beta_i\rvert$
Elastic Net	$L(\beta) = \frac{1}{n}\sum_{i=1}^{n}(y_i - \hat{y}_i)^2 + \lambda_1 \sum_{i=1}^{n} \lvert\beta_i\rvert + \lambda_2 \sum_{i=1}^{n} \beta_i^2$
Logistic Regression	$p(y=1\lvert x) = \frac{1}{1+\exp(-z)} = \frac{1}{1+\exp -(\beta_0+\beta_1\times x_1+\beta_2\times x_2+.....+\beta_r\times x_r)}$

The calculation of the coefficients a, b and c using the method of least squares is an approach commonly used in data analysis and mathematical modeling. The aim of this method is to find the values of the coefficients that minimize the sum of the squares of the differences between the observed values and the values predicted by the model. On the other hand, to calculate the parameters β and $\lambda$for the regularized regression, we first need to define the cost function with the appropriate regularization term, and then use an optimization method to adjust the β coefficients while choosing the optimal value for λ. The optimization methods used to calculate the parameters (Gradient Descent, Stochastic Gradient Descent (SGD), Coordinate Descent...etc. In this work the method used is Gradient Descent.

III.4.2 Intelligent Models

Intelligent models have the ability to learn from data to generalize and perform tasks on unknown data. They are highly adaptable and have become essential in many fields. Intelligent models are divided into two categories: Individual models and hybrid models.

III.4.2.1 Individual models

Among the artificial intelligence models, the approaches adopted to design predictors of daily global solar radiation on a horizontal surface are : fuzzy logic, tree-based, Kernel-based and ANN-based. Each approach is used to elaborate several individual models.

III.4.2.2 Hybrid models

Hybrid models combine the advantages of different approaches for improved performance,the hybrid models designed to predict daily global solar radiation in this work are : average, geometric average, harmonic average and weighted average.

III.4.3 Individual models

III.4.3.1 Fuzzy logic models

Fuzzy logic is a powerful tool for improving the accuracy of global solar radiation forecasts and facilitating decision-making in areas. The fuzzy logic tool is used to develop fuzzy predictors of the daily solar radiation of the city of Batna, which are divided into four groups. These predictors are presented in the table 2:

Table III.2: Representation of Fuzzy Models

Model	**Inputs**
Fuzzy_SS0_Season	S/S0, Season
Fuzzy_SS0_T	S/S0, one of weather parameter
Fuzzy_Season_T	Season, one of weather parameter
Fuzzy_SS0_Season_T	S/S0, Season, one of weather parameter

In the fuzzy models, there are three distinct entries:

- The first input of the proposed fuzzy system is the isolation fraction S/S0 (ratio between the measured isolation time and the day length).
- The second is Season which has five linguistic variables (because the functions of membership begin on the first of January): winter1(1 Janury-20 March), spring(21 March-21 June), summer (22 June-23 September),autumn (24 September-22 December)and winter2(23 December-31 December). It is important to note that the exact dates of the seasons may vary slightly from year to year due to the complex nature of the Earth's orbital motion.
- The last input is one weather parameter: temperature (T), humidity (Hu), Pressure (Pr), Wind speed (Ws) and Rain-fall (R).

The single and unique output is the Ratio between the global solar irradiation and extraterrestrial irradiation G /G0. The overall description of the proposed fuzzy systems (Figure III.5)

for predicting daily solar irradiation is outlined as follows:

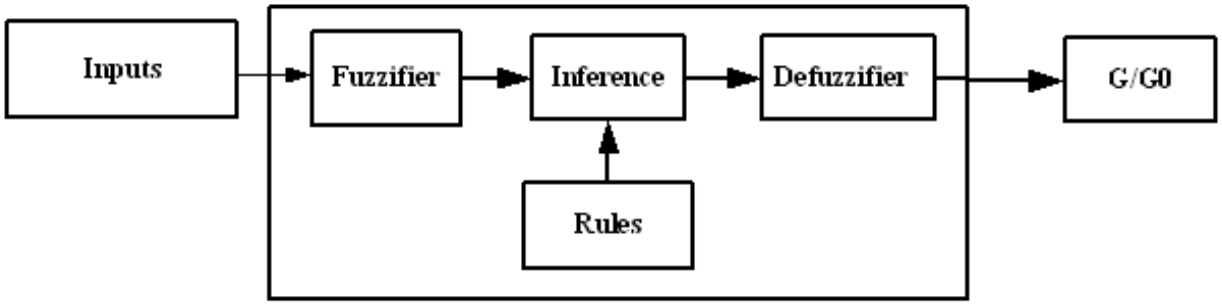

Figure III.5: Structure of a Fuzzy System

According to the general structure of the fuzzy system (Figure III.5) there are three distinct blocks:

- **Fuzzification**

The aim of fuzzification is to convert input values (which can be numerical or linguistic data) into degrees of membership of fuzzy sets. For all groups of fuzzy models an increase in the number of membership functions from three to seven and a change in the type of membership functions from Trapeze, Gaussian and Triangular to have two subgroups. All the models generated are Mamdani [129] systems.

◇ **Models of first group**

This first group consists of fuzzy models with two inputs: S/S0 and the season. The type of membership function is then changed between: Trapeze, Gaussian and Triangular. The figure (Figure III.6) highlights the entries in the first group, the number of linguistics variables is three for the first and the output which are: small, medium and large.

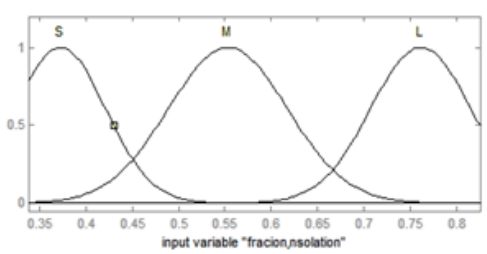

(a) Input variable S/S0

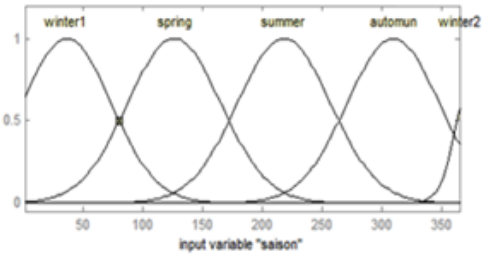

(b) Input variable Season

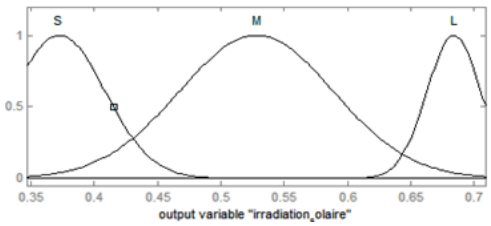

(c) Output variable G

Figure III.6: Linguistic variables of the three fuzzy systems.

We keep the same entries but this time we increase the number of membership functions to seven with the following linguistic variables: very small, small, medium small, medium, medium large, large and very large. The figure (Figure III.7) below highlights these latters.

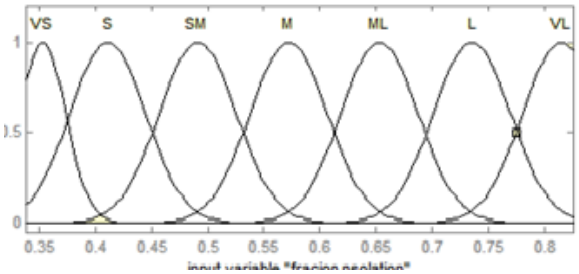

(a) Input variable S/S0

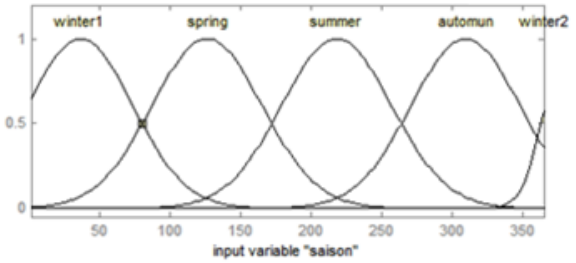

(b) Input variable Season

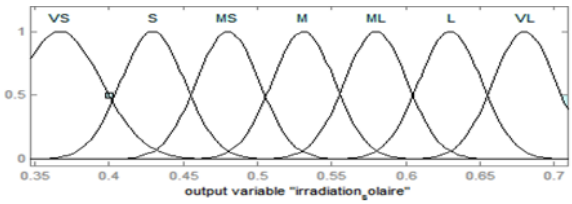

(c) Output variable G

Figure III.7: Linguistic variables of the seven of fuzzy system.

◇ Models of second group

The models in the second group have two inputs: S/S0 and a single meteorological parameter (temperature, humidity, pressure, wind speed and rainfall). We then followed the same procedure as for the first group of models, i.e. we changed the type and number of membership functions. However, for the second input, which concerns one of the climatic parameters, for example temperature, the responses are: too cold, cold, not very hot, hot, too hot, hot and too hot. The figure (Figure III.8) shows the inputs and the output and their membership functions.

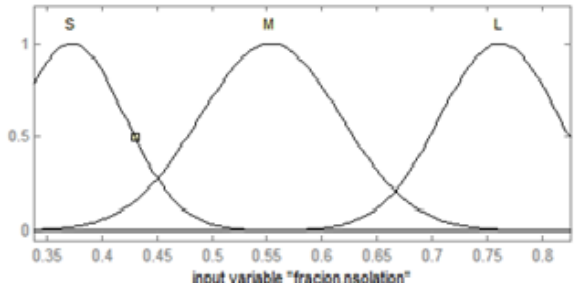

(a) Input variable S/S0

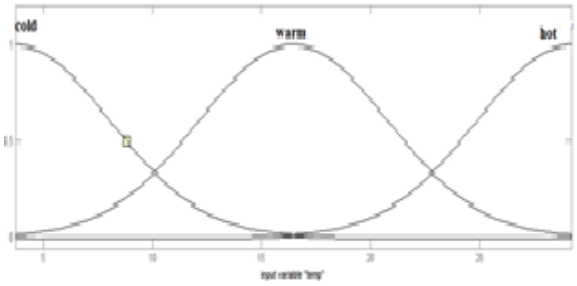

(b) Input variable Temperature

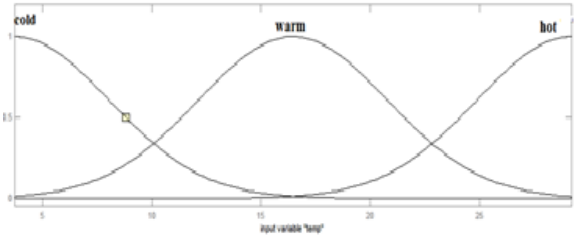

(c) Output variable G

Figure III.8: Linguistic variables of the three of fuzzy system.

◇ Models of third group

The fuzzy proposed models in this group have two inputs: the season and a meteorological parameter. For this group of models, the same procedure for changing types and number of memberships is used. The figures (Figure III.9 and Figure III.10) show membership functions with three and seven linguistic variables respectively.

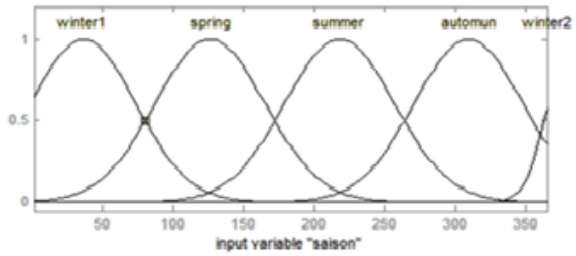

(a) Input variable S/S0

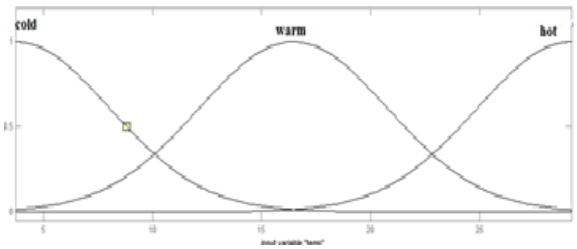

(b) Input variable Temperature

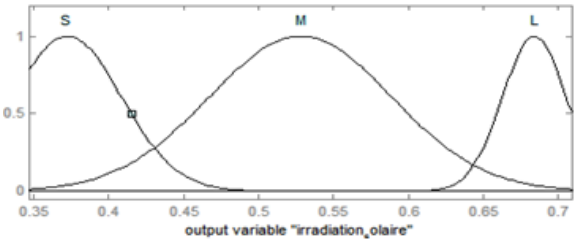

(c) Output variable G

Figure III.9: Linguistic variables of the three of fuzzy system.

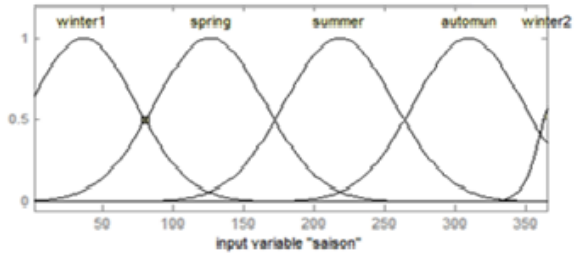

(a) Input variable S/S0

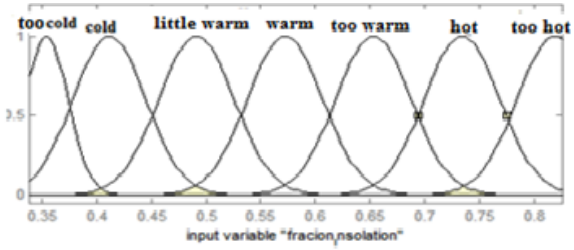

(b) Input variable Temperature

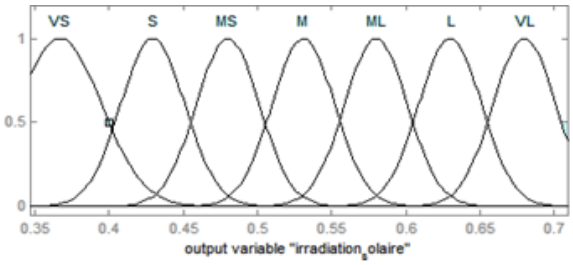

(c) Output variable G

Figure III.10: Linguistic variables of the seven of fuzzy system.

◇ **Models of four group**

Another group of fuzzy systems are developed in which a meteorological parameter is taken as the third input. For the five fuzzy models presented in the table 3, the output variable being modeled is global solar radiation. The input variables used to predict solar radiation are: insolation fraction, temperature, humidity, atmospheric pressure, wind speed and precipitation. Each input variable is assigned qualitative linguistic terms based on degrees of imprecision. For the three-term fuzzy logic models the linguistic classifications are:

- **Solar radiation:** Low, Medium and High.
- **Insolation fraction:** Small, Medium and Large
- **Season:** Winter, Spring, Summer and Autumn
- **Temperature:** Low, Medium and High
- **Wind speed:** Low, Medium and High
- **Humidity:** Dry, Medium and Wet.
- **Pressure:** Low, Medium and High
- **Precipitation:** Light, Medium and Heavy

Table III.3: Inputs of Fuzzy Models

Model	Inputs
Fuzzy_T	S/S0, Season and T
Fuzzy_Hu	S/S0, Season and Hu
Fuzzy_Pr	S/S0, Season and Pr
Fuzzy_Ws	S/S0, Season and Ws
Fuzzy_R	S/S0, Season and R

For models with seven membership functions, we kept the same linguistic variables and added four linguistic variables: very small, moderately small, moderately large and very large. We then modified the membership functions successively (triangular, trapezoidal and Gaussian) for the fuzzy systems developed.

- **Inference**

One of the crucial elements for the whole process considered in this section is the fuzzy inference block. The links between the required output and the input parameters are found in the rules base. The rules base is the intelligent part used to predict global solar radiation. A fuzzy inference engine manipulates continuous values in a range between 0 and 1, allowing vague and uncertain concepts to be processed. It is based on fuzzy rules, which are conditional statements of the type "IF (premise) THEN (conclusion)", where premises and conclusions can be expressed in linguistic rather than numerical form. Fuzzy rules are obtained by associating input and output sets using fuzzy logic operators such as union and intersection. The rules base for each group is presented as follows:

◇ **Models of first group**

The rules of the fuzzy system describe the relationships between the input variables and the output variable, i.e. the predicted solar radiation. The inference engine of the three memberships proposed models is described by the following five rules:

If $\left(\frac{S}{S_0} \text{ is } \boldsymbol{S}\right)$ **or** (season is winter) **then** $\left(\frac{G}{G_0} \text{ is } \boldsymbol{S}\right)$

If $\left(\frac{S}{S_0} \text{ is } \boldsymbol{L}\right)$ **or** (season is summer) **then** $\left(\frac{G}{G_0} \text{ is } \boldsymbol{L}\right)$

If $\left(\frac{S}{S_0} \text{ is } \boldsymbol{M}\right)$ **or** (season is autumn) **then** $\left(\frac{G}{G_0} \text{ is } \boldsymbol{M}\right)$

If $\left(\frac{S}{S_0} \text{ is } \boldsymbol{M}\right)$ **or** (season is spring) **then** $\left(\frac{G}{G_0} \text{ is } \boldsymbol{M}\right)$

If $\left(\frac{S}{S_0} \text{ is } \boldsymbol{S}\right)$ **or** (season is winter) **then** $\left(\frac{G}{G_0} \text{ is } \boldsymbol{S}\right)$

The inference engine of the seven memberships proposed models is described by the following eight rules:

If $\left(\dfrac{\boldsymbol{S}}{\boldsymbol{S_0}} \text{ is L}\right)$ **or** (Season is summer) **then** $\left(\dfrac{\boldsymbol{G}}{\boldsymbol{G_0}} \text{ is VL}\right)$

If $\left(\dfrac{\boldsymbol{S}}{\boldsymbol{S_0}} \text{ is M}\right)$ **or** (Season is autumn) **then** $\left(\dfrac{\boldsymbol{G}}{\boldsymbol{G_0}} \text{ is M}\right)$

If $\left(\dfrac{\boldsymbol{S}}{\boldsymbol{S_0}} \text{ is M}\right)$ **or** (Season is spring) **then** $\left(\dfrac{\boldsymbol{G}}{\boldsymbol{G_0}} \text{ is M}\right)$

If $\left(\dfrac{\boldsymbol{S}}{\boldsymbol{S_0}} \text{ is MS}\right)$ **and** (Season is autumn) **then** $\left(\dfrac{\boldsymbol{G}}{\boldsymbol{G_0}} \text{ is MS}\right)$

If $\left(\dfrac{\boldsymbol{S}}{\boldsymbol{S_0}} \text{ is VS}\right)$ **or** (Season is winter) **then** $\left(\dfrac{\boldsymbol{G}}{\boldsymbol{G_0}} \text{ is VS}\right)$

If $\left(\dfrac{\boldsymbol{S}}{\boldsymbol{S_0}} \text{ is ML}\right)$ **or** (Season is spring) **then** $\left(\dfrac{\boldsymbol{G}}{\boldsymbol{G_0}} \text{ is ML}\right)$

If $\left(\dfrac{\boldsymbol{S}}{\boldsymbol{S_0}} \text{ is ML}\right)$ **or** (Season is summer) **then** $\left(\dfrac{\boldsymbol{G}}{\boldsymbol{G_0}} \text{ is ML}\right)$.

◇ **Models of second group**

The following five rules form the inference engine of the proposed for three memberships:

If $\left(\frac{S}{S_0}\text{ is S}\right)$ **or** (Temp is cold) **then** $\left(\frac{G}{G_0}\text{ is S}\right)$.
If $\left(\frac{S}{S_0}\text{ is L}\right)$ **or** (Temp is hot) **then** $\left(\frac{G}{G_0}\text{ is L}\right)$
If $\left(\frac{S}{S_0}\text{ is M}\right)$ **or** (Temp is warm) **then** $\left(\frac{G}{G_0}\text{ is M}\right)$
If $\left(\frac{S}{S_0}\text{ is M}\right)$ **or** (Temp is hot) **then** $\left(\frac{G}{G_0}\text{ is M}\right)$
If $\left(\frac{S}{S_0}\text{ is L}\right)$ **or** (Temp is cold) **then** $\left(\frac{G}{G_0}\text{ is S}\right)$.

The following eight rules form the inference engine of the proposed for seven memberships:

If $\left(\frac{S}{S_0}\text{ is VS}\right)$ **or** (Temp is cold) **then** $\left(\frac{G}{G_0}\text{ is VS}\right)$
If $\left(\frac{S}{S_0}\text{ is L}\right)$ **or** (Temp is too cold) **then** $\left(\frac{G}{G_0}\text{ is VL}\right)$
If $\left(\frac{S}{S_0}\text{ is M}\right)$ **or** (Temp is warm) **then** $\left(\frac{G}{G_0}\text{ is M}\right)$
If $\left(\frac{S}{S_0}\text{ is M}\right)$ **or** (Temp is too warm) **then** $\left(\frac{G}{G_0}\text{ is M}\right)$
If $\left(\frac{S}{S_0}\text{ is M}\right)$ **or** (Temp is little warm) **then** $\left(\frac{G}{G_0}\text{ is M}\right)$
If $\left(\frac{S}{S_0}\text{ is VS}\right)$ **or** (Temp is cold) **then** $\left(\frac{G}{G_0}\text{ is VS}\right)$
If $\left(\frac{S}{S_0}\text{ is ML}\right)$ **or** (Temp is too warm) **then** $\left(\frac{G}{G_0}\text{ is ML}\right)$
If $\left(\frac{S}{S_0}\text{ is ML}\right)$ **or** (Temp is too warm) **then** $\left(\frac{G}{G_0}\text{ is ML}\right)$

◇ **Models of third group**

The following five rules form the inference engine of the three memberships fuzzy proposed models :

If (season is winter2) **or** (Temp is cold) **then** $\left(\frac{G}{G_0}\text{ is S}\right)$
If (season is summer) **or** (Temp is hot) **then** $\left(\frac{G}{G_0}\text{ is L}\right)$
If (season is autumn) **or** (Temp is warm) **then** $\left(\frac{G}{G_0}\text{ is M}\right)$
If (season is spring) **or** (Temp is warm) **then** $\left(\frac{G}{G_0}\text{ is M}\right)$
If (season is winter1) **or** (Temp is cold) **then** $\left(\frac{G}{G_0}\text{ is S}\right)$

The following eight rules form the inference engine the seven memberships fuzzy proposed models:

If (Season is winter2) **or** (Temp is cold) **then** $\left(\frac{G}{G_0} \text{ is VS}\right)$

If (Season is summer) **or** (Temp is too hot) **then** $\left(\frac{G}{G_0} \text{ is VL}\right)$

If (Season is autumn) **or** (Temp is warm) **then** $\left(\frac{G}{G_0} \text{ is M}\right)$

If (Season is autumn) **or** (Temp is too warm) **then** $\left(\frac{G}{G_0} \text{ is M}\right)$

If (Season is spring) **or** (Temp is little warm) **then** $\left(\frac{G}{G_0} \text{ is M}\right)$

If (Season is winter1) **or** (Temp is cold) **then** $\left(\frac{G}{G_0} \text{ is VS}\right)$

If (Season is spring) **or** (Temp is too warm) **then** $\left(\frac{G}{G_0} \text{ is ML}\right)$

If (Season is summer) **or** (Temp is too warm) **then** $\left(\frac{G}{G_0} \text{ is ML}\right)$

◇ **Models of four group**

For the four group of models, the rules are, in general, as follows:

If A is B **or** C is D **Then** E is F.

• F is value of the estimated solar radiation.

• A and D are the two input variables to the fuzzy system.

• B and C are the qualitative linguistic terms assigned to inputs A and D respectively based on their membership functions.

• E represents the output variable, which is the estimated global solar radiation.

• F is the final numeric value predicted by the fuzzy system for the global solar radiation (E), given the linguistic values of the inputs A and D.

- **De−fuzzfication**

The fuzzy inference engine aggregates the outcomes from all the membership functions to produce a set of fuzzy output values. These fuzzy outputs must then be converted into a single crisp numeric prediction through a process called *de-fuzzification*. There are several possible *de-fuzzification* techniques. The most commonly used approach is the centroid method, which calculates the center of area under the aggregated membership function curve. This centroid method is utilized in all the fuzzy logic models discussed here to generate a final numeric estimate for the solar radiation value based on defuzzifying the fuzzy output sets. By applying *de-fuzzification*, the models can provide a definitive quantitative prediction from the qualitative fuzzy reasoning process. The centroid technique was chosen as it is widely adopted to convert fuzzy output sets into clear, usable numeric solar radiation estimates.

III.4.3.2 ANN-Based models

Artificial neural networks (ANNs) have become a popular approach in the field of machine learning and artificial intelligence because of their ability to solve complex classification and regression problems. ANN-based models are a powerful and versatile class of machine learning algorithms. Inspired by the way the human brain works, these models are capable of learning from unstructured data to perform complex tasks such as classification, regression, anomaly detection and even content generation. The adopted models in this category are MLP, RNN, CNN and LSTM. The system designed follows (see figure III.11)the steps prescribed in the following diagram:

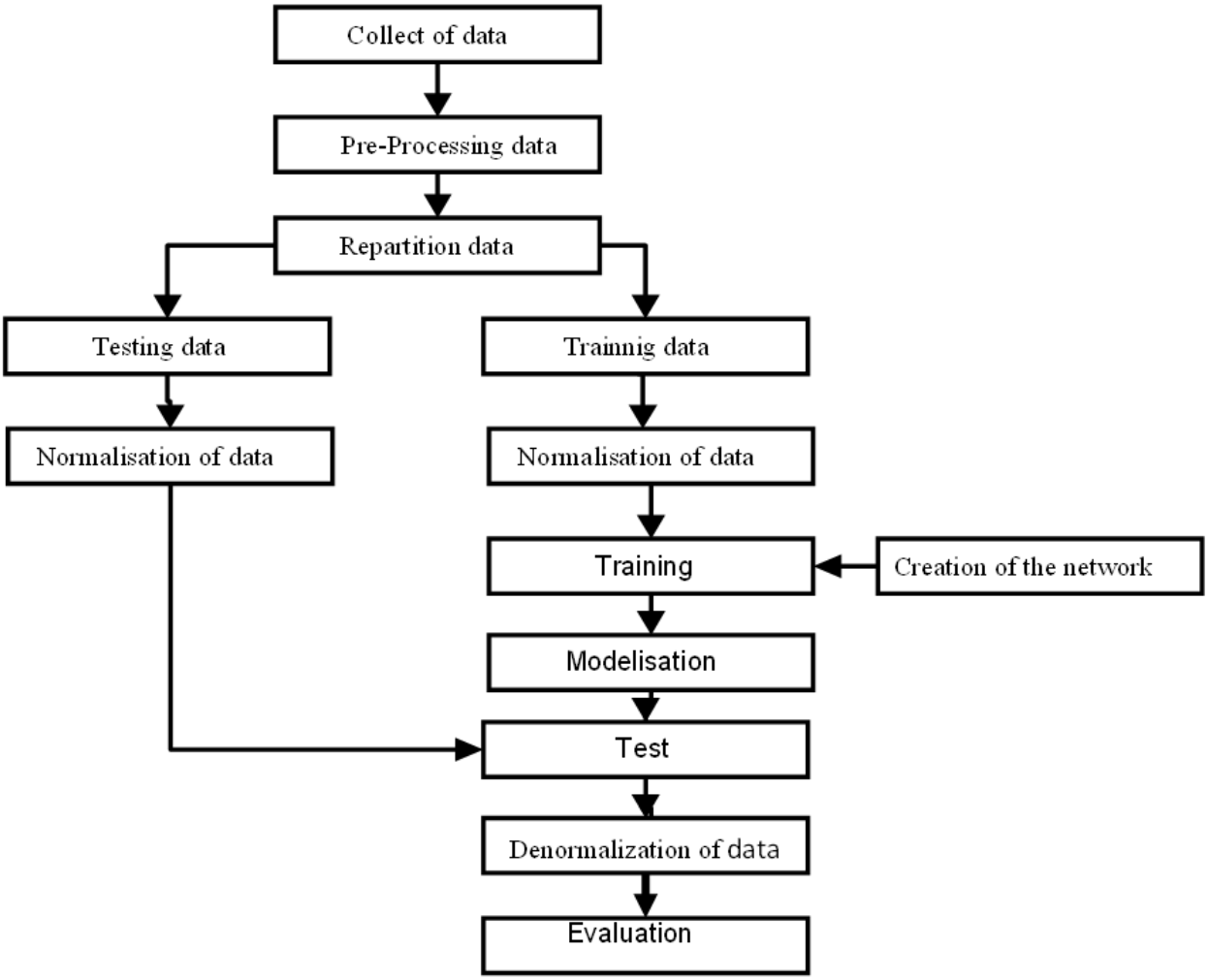

Figure III.11: Designing Artificial Neural Network Model

All artificial neural network (ANN) models follow the same fundamental workflow determining the model architecture, training the model parameters, and validating model performance.

Architecture model

The key difference between ANN models lies in their underlying structure. While

training approach and validation steps stay consistent across ANNs, architectural details vary between models. These architectural differences include: number of layers (input, hidden, output), nodes per layer, activation functions for each layer,weight initialization strategies, connectivity patterns between nodes and additional specialized layers/units (if used).

The fundamental structure is relatively simple: Input Layer where raw data is fed into the network, Hidden Layers are intermediate between the input layer and the output layer and transform the input data, Output Layer produces the final results of the model. These layers are connected to each other with a weight.

The basic architecture of machine learning models based on artificial neural networks (ANNs) generally comprises the following elements:

-Neurons organized into layers:input layer(receives raw data),hidden layers(one or more layers that process and extract complex features from the data) and output layer(provides the final prediction of the model.)

- Connections between neurons with associated weights, which are adjusted during training.

- An activation function in each neuron and each layer, usually non-linear, such as sigmoid or ReLU. This determines whether or not the neuron should be activated.

-An optimization algorithm (gradient descent, Adam, etc.) that iteratively adjusts the network weights to minimize the loss (error between predictions and true values).

-A loss function (mean square error, cross-entropy, etc.) that evaluates performance at each batch or epoch.

- Unidirectional data flow, from inputs to outputs through hidden layers.

The basic architecture of each ANN model is different, and will be described individually for each model. The common steps are: Training and Validation.

Training

During this phase the Artificial Neural Network is trained in order to create a behavioral model while minimizing a cost function that uses the errors between measured and estimated values. The back-propagation technique is used to modify network weights over time, improving predictions.

Validation

Following the training of ANN model, it must be validated before being used on real-world tasks. Evaluation guarantees that the model generalizes adequately to new, previously unseen data and does not merely remember learning samples.

- **Multi-Layer Perceptron (MLP)**

Every neuron in each layer is linked to every neuron in its neighbor, resulting in a completely connected network. Information flows in a direct direction across an MLP network, from the input layer to the output layer. Nonlinear adjustments to the input data are applied to the neurons in the hidden layers, while the neurons in the output layer provide the final predictions. The artificial intelligence is used specifically the MLP methodology, to predict global solar radiation over the horizontal surface. For model training, we employ the Levenberg-Marquardt

method. This latter is the most commonly employed for predicting solar radiation. A neuronal system has multiple activation functions. The transfer functions in the hidden layer and output layer were the hyperbolic tangent sigmoid function (HTSF) and Purelin function (PF), respectively.As each modeling approach has its own steps to be followed for its application the same for neural networks the following phases are adopted for all ANN models:
After data collection, three pre-processing procedures are performed for sorting, organizing the data, learning and testing the adopted models in an efficient way:

- Solving the problem of missing data:

The missing data are replaced by the average of neighboring values.

- Normalizing the data:

The normalization procedure before presenting the input data to the network a normalization of these data is carried out. Their values will be between one and zero.

- Randomizing the data:

It is a mixture of variables of large and small amplitude.

The inputs used across the 26 ANN-based models for predicting daily global solar radiation (G) on a horizontal surface are: insolation duration (S0), sunshine duration (S), extraterrestrial irradiation (G0), temperature, relative humidity, atmospheric pressure, wind speed, wind direction and rainfall. The output variable is the estimated daily global solar radiation (G).
The models were generated by varying:Number of inputs,input combinations and transfer functions in the hidden layer.

The common architecture has hyperbolic tangent sigmoid activations (HTSF) in the hidden layer(s) and pure linear functions (PF) in the output layer.All models were trained using the Levenberg-Marquardt algorithm, one of the most utilized methods for solar radiation prediction problems. This algorithm outperforms basic gradient descent and converges faster.All the MLP models designed have the following architecture (Figure III.12):

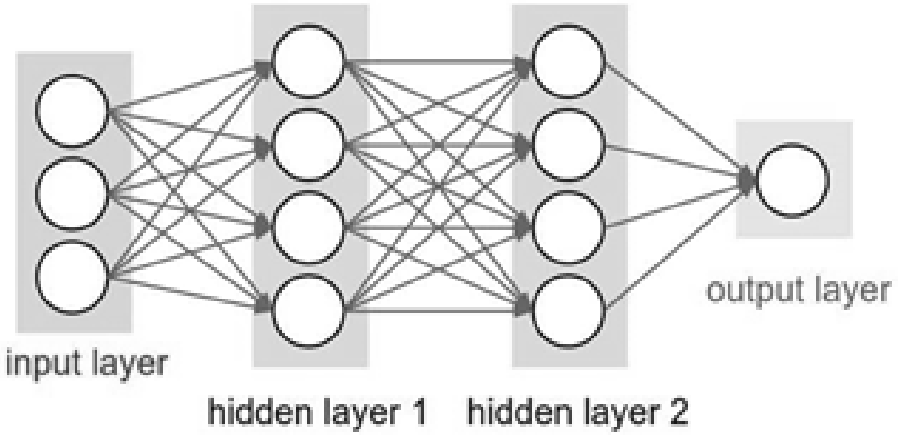

Figure III.12: Architecture of MLP Neural Network[130].

-The input layer contains a number of neurons that depends on the number of input parameters used for each model. Four parameters are taken into account in all models: the number of days, S0, S and G0. Then, for each new model one or more weather parameters are added. All these models are displayed in the table 4.
-Two hidden layers are integrated, and in each layer, 25 neurons are added.
-The output layer contains just one neuron, as the solar radiation estimate is the only output.

Table III.4: Model Input Parameters.

Model	Inputs parameters
MLP	Day, S0, S, G0
MLP_T	T
MLP_Hu	Hu
MLP_Pr	Pr
MLP_Ws	Ws
MLP_Wd	Wd
MLP_R	R
MLP_T_Hu	T, Hu
MLP_T_Pr	T, Pr
MLP_T_Ws	T, Ws
MLP_T_Wd	T, Wd
MLP_T_R	T, R
MLP_Hu_Pr	Hu, Pr
MLP_Hu_Ws	Hu, Ws
MLP_Hu_Wd	Hu, Wd
MLP_Hu_R	Hu, R
MLP_Pr_Ws	Pr, Ws
MLP_Pr_R	Pr, R
MLP_Ws_Wd	Ws, Wd
MLP_Ws_R	Ws, R
MLP_Wd_R	Wd, R
MLP_T_Hu_Pr	T, Hu, Pr
MLP_T_Hu_Pr_Ws	T, Hu, Pr, Ws
MLP_T_Hu_Pr_Ws_Wd_R	T, Hu, Pr, Ws, Wd, R

- **Recurrent Neural Network (RNN)**

The model based RNN is developed to take into consideration the relationship between subsequent items in data, as opposed to traditional neural networks, which process each input independently of the others. RNN is distinguished by its capacity to have an internal memory that can be modified with each incoming input. RNN remember earlier stages of the sequence's processing and utilize that knowledge to impact future predictions or calculations by this memory (hidden state). The following is the architecture basis step for designing an RNN model:

Fundamental structure

The Recurrent Neural Networks (Figure III.13) is formed up of recurrent cells that are repeated

at each epoch of the sequence. To modify prediction the network use the cell which contain intern memory that saves data from past phases. **Forward propagation**

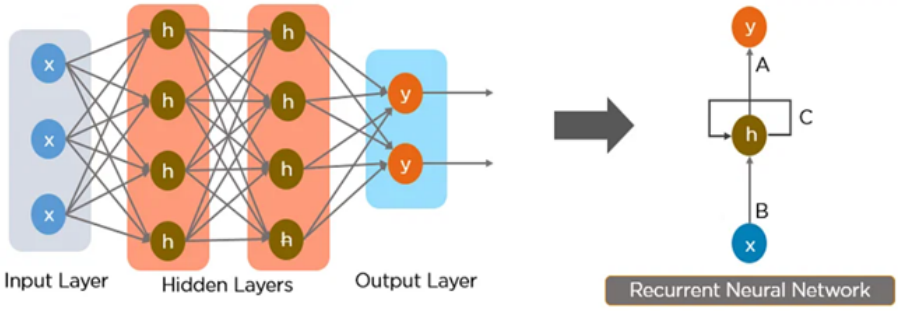

Figure III.13: Simple Reccurent Neural Network[131].

At every iteration the output for the current step is generating by combining the data from previous step (the memory) and from the current step. **Internal state update**
First the network calculate the output for this actual step, then each recurrent cell is modified with the new data so, the recording of long-term relationships in the data can be made by the network.

Data pre-processing

The data must be pre-processed into a network-friendly format before training an RNN model. This entails standardizing the entry data.

The RNN model used in this work is a typical RNN architecture with the following parameters: Count of layers equal to one, Sequence size equal to one hundred, Count of neurons per layer equal to ten, Activation function=hyperbolic tangent, Weight initialization=none, Optimizer kind is Adam, Deep learning equal to one, Iterations equal to hundred, Batch_size=42 and Test rate is 25% .

Remarks: In the design of all models, some values of parameters are the same: Data preparation=normalization of data between 0 and 1. Costs function is MSE, Optimizer=Adam.

- **Convolutional Neural Network (CNN)**

This type of networks by the use of convolution layers which extract significant features from the input data, is the major feature. Convolution layers filter sequence by employing a set of filters to find certain estimation models. The structure of RNN model must begin with the following steps:

Fundamental structure

The CNN model's basic architecture is as follows: A CNN is made up of layers such as inputs layers, pooling layers, convolution layers, and output layers. The following sequence: Convolution, ReLU, Pooling, Repetition (optional) and Output layers is the base layer sequencing in CNN model (Figure III.14).

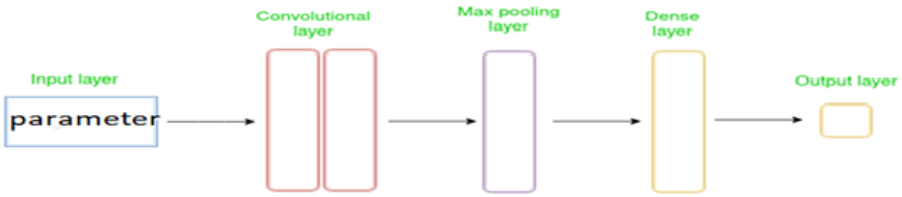

Figure III.14: Architecture of CNN Unit[132]

Convolution

The CNN's heart is the convolution layer. It detects local features by applying convolution filters (or kernels) to the incoming data. An activation map is created by each filter which accumulates the results and carries out the local multiplications.

Activation

To inject non-linearity in the model an activation function is apply to activation map element by element.

Pooling

By capturing sub-samples, using the most frequent pooling method named max pooling. This method consist to recovers the greatest value from each sub-sampling zone. So pooling layers reduce the resolution of activation map in other words this decreases data size while keeping critical information.

Layer repetition

In order to capture increasingly complicated and abstract data features, the repetition of three following steps :convolution, activation and pooling is done.

Fully connected layers

The output layers collect data and transform it into relevant outputs. After extracting spatial characteristics, output layers are applied to create final predictions.

The parameters selected for the CNN model are provided in the following: Count of layers equal to three, Convolution filter scale is 3×3, Count of filters equal to sixty four, Activation functions is Relu, Pooling approach is MaxPooling2D with a pool_size of (1,1), Output layer=1, Regularization= Dropout with a rate of 20% and Batch_size=42.

- **Long Short-Term Memory (LSTM)**

Because of the structure of internal memory cells, they have the ability to store knowledge for lengthy periods of time. To store previous data and to update it as new data arrives in the sequence we use the internal memory. This enables LSTMs to keep long-term temporal dependencies and capture complicated interactions between sequence parts. The LSTM model has the same basic design as any other ANN model:

Fundamental structure

An LSTM model is formed of LSTM cells, which are that, are repeated at each step in the sequence. Gates command the flux of information and liaisons between layers in each

LSTM cell (Figure III.15).

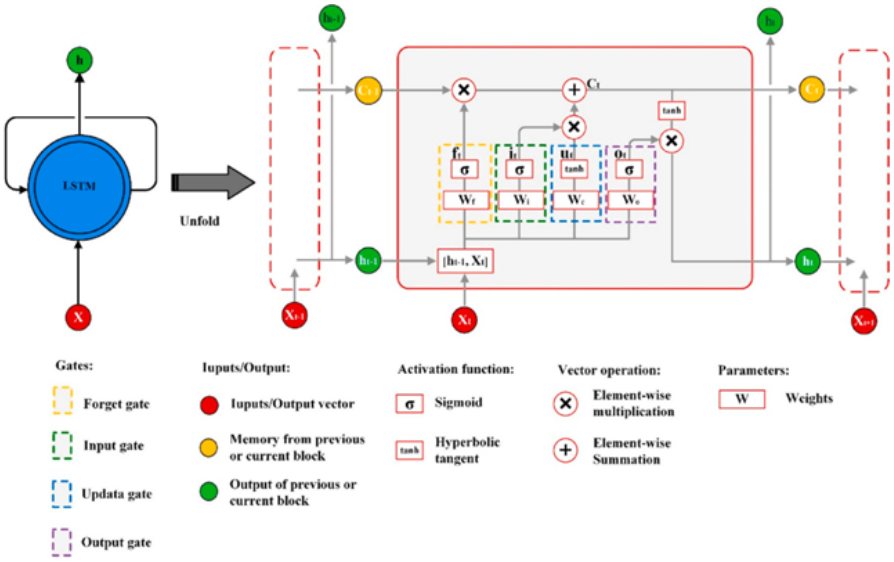

Figure III.15: Architecture of LSTM Unit[133]

LSTM gates

Forget gate, input gate and output gate are three kinds of gates in LSTM cells. These gates govern whether the anterior hidden state's elements should be retained, forgotten or used to change the actual state.

Forward propagation

At each time step a new hidden states is generated by LSTM gates which compute the way how the new data will be combined with the old internal state.

Long-term dependency management

The ability of LSTMs to administer long-term relationships in sequences is one of their primary features. This is accomplished through the use of forget gates, these latter enable the network to select which operation will be done: forget or preserve information over lengthy of time.

Layer stacking

As with other neural network architectures, LSTM uses multi-layer stacking to capture hierarchical abstractions and more complex features.

Bi-directionality

If required, bidirectional LSTMs can be used to take into account both past and future information in a sequence. In this configuration, one LSTM cell analyses the sequence in both directions.

The parameters selected for the LSTM model are provided in the following:Count of layers equal to one, Count of LSTM units equal to sixty, Activation function is hyperbolic tangent (tanh), Bidirectional recurrence=none, Batch size=none, Iterations equal to hundred, Dropout equal to zero, Weight initialization is none, Time window equal to one, Output acti-

vation function is linear function and Hyper-parameters is equal to learning rates 80%.

III.4.3.3 Tree-Based models

These models are based automatic learning methods that use tree structures to make decisions and predictions. These models are mainly used for classification and regression and are known for their ability to capture complex relationships between variables. For predicting solar radiation seven models were developed, which are: Decision Tree (DT), Models 5 trees (M5), Gradient Boosting Decision Tree (GBDT), Extreme Gradient Boosting (XGBoost), Category Boosting (Cat-Boost) , Random Forest (RF) and Extremely Randomized Trees(Extra Tree). Like all ML models, tree-based specimens also have steps to follow which are described in the Figure III. 16:

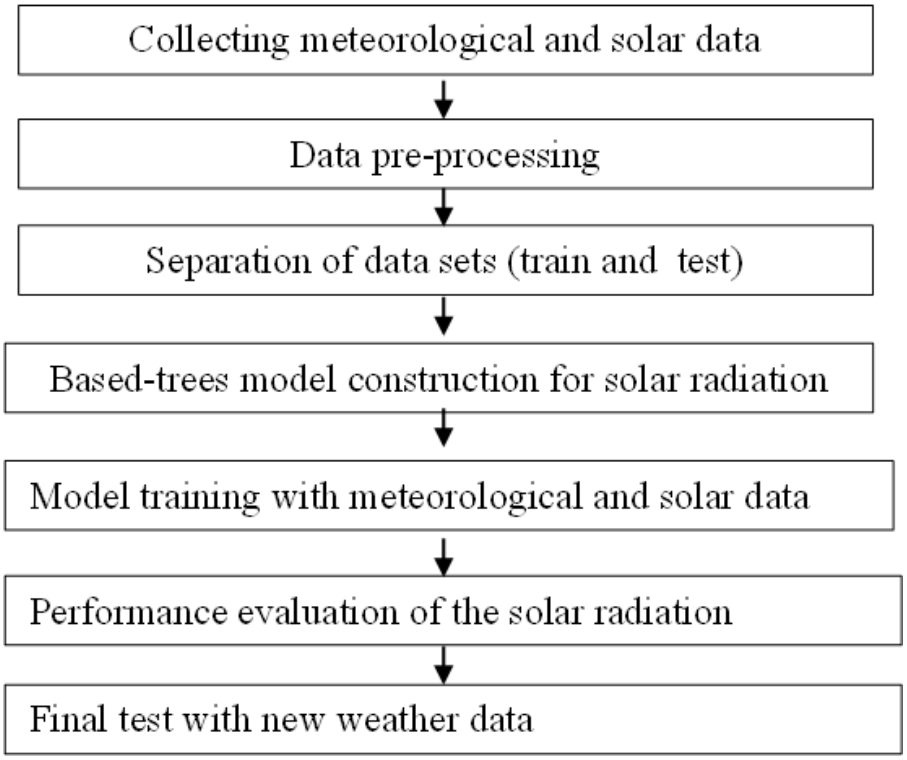

Figure III.16: Tree-based model step-by-step diagram.

- **Decision Tree (DT)**

It is used to create a tree model of decisions and their possible consequences. The tree is created by recursively dividing the data into subsets based on the most significant characteristic. The final output of these results is a tree whose leaf nodes are the predictions made by the model. The figure III.17 represents principle diagram of the algorithm Decision tree.

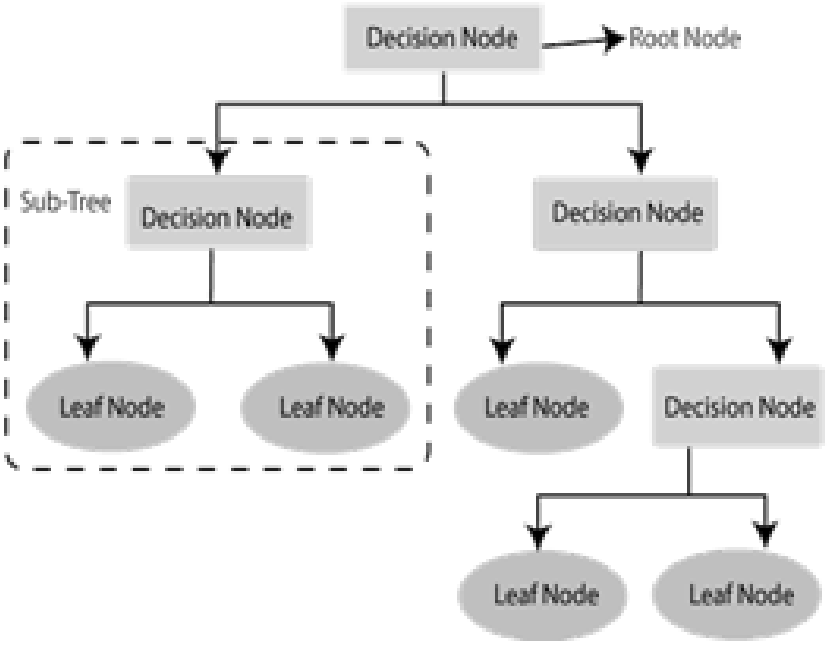

Figure III.17: Principle diagram of the algorithm Decision tree[134] .

The table 5 shows the specific parameters of the DT model and their explanations.

Table III.5: Specific parameters of the DT model.

Name parameter	**Explain**	**Value in the model adopted**
criterion	The criterion used to measure the quality of a split	squared_error
splitter	The strategy used to choose the split at each node.	Best
max_depth	The maximum depth of the tree.	20
min_samples_split	The minimum number of samples required to split an internal node.	2
min_samples_leaf	The minimum number of samples required to form a leaf (terminal node).	40
max_features	The maximum number of features to consider when searching for the best division.	0
random_state	The seed used by the random number generator for initialization.	0
min_impurity_decrease	The minimum threshold for a division to have sufficient impurity reduction.	0
presort	Indicates whether the data should be sorted before searching for the best division.	False

- **Models 5 trees (M5)**

  They are also known as "function trees". M5 trees differ from standard decision trees

in the linear combinations of features at each node of the tree, rather than selecting only one feature. As a result, they are more adaptable and able to model non-linear interactions between features and the objective variable. The specific M5 model parameters are displayed in the table 6 along with an explanation of each one.

Table III.6: Specific parameters of the M5 model.

Name parameter	**Explain**	**Value in the model adopted**
Maximum tree depth (Max Depth)	This is the maximum number of levels the tree can have. This limits the complexity of the tree and can help prevent over-fitting.	10
Splitting Criterion	This determines how the algorithm chooses the best way to split the nodes. Common criteria include variance reduction (for regression) and impurity reduction (for classification).	Mse
Stopping Criteria	This indicates when the algorithm should stop splitting nodes. This could be based on the minimum number of observations per node, a certain maximum depth, etc.	Best
Minimum fraction of observations per node (Min Node Size)	This defines the minimum number of observations that must be in a node for it to be considered divisible.	none
Min Leaf Size	This defines the minimum number of observations that must be in a leaf (terminal node).	0
Regression/Classif	regression or classification	regression
Other model-specific hyperparameters	Depending on the model implementation, there may be other specific parameters to set.	

- **Gradient Boosting Decision Tree (GBDT)**

Boosting is an ensemble approach that builds several sequential models with error corrections (bias and variance errors, outliers and over-learning errors) from the previous model (DT). In the case of the GBDT model designed, here are its characteristics presented in the table (see Table 7):

Table III.7: Specific parameters of the GBDT model.

Name parameter	**Explain**	**Value in the model adopted**
n_estimators	The number of decision trees to be trained in the algorithm. This is the number of iterations of the boosting algorithm.	200
learning_rate	The learning rate controls the contribution of each tree to the overall model.	80%
max_depth	The maximum depth of each decision tree. This controls the complexity of the trees.	3
min_samples_split	The minimum number of samples required to split an internal node of the tree.	2
min_samples_leaf	The minimum number of samples required in a leaf of the tree.	1
Subsample	The proportion of samples to be used for training each tree.	1
Loss	The loss function used to optimize the model.	squared_error
random_state	A random seed for reproducibility of results.	0

- **Extreme Gradient Boosting (XGBoost)**

These implements the GBDT algorithm, with improvements (sampling techniques, model sets, hyper-parameters and data processing) aimed at increasing prediction accuracy and learning speed. In the case of the Extreme Gradient Boosting (XGBoost) model designed here, its parameters encompass a range of advanced capabilities that contribute to its remarkable performance. These functionalities include (Table 8):

Table III.8: Specific parameters of the XGBoost model.

Name parameter	**Explain**	**Value in the model adopted**
n_estimators	The number of decision trees to be trained in the algorithm.	1000
learning_rate	The learning rate which controls the contribution of each tree to the overall model.	80%
max_depth	The maximum depth of each decision tree.	7
min_child_weight	The minimum weight required to create a new partition in a node of the tree.	0
Subsample colsample_bytree (or colsample_bylevel, colsample_bynode)	The proportion of samples to be used for training each tree. The proportion of features to be used for the construction of each tree.	0.7 0.8
gamma	A regularization parameter which controls the minimum reduction in the loss function required to perform a division.	0
lambda (or reg_lambda)	An L2 regularization parameter to control the complexity of the model.	1
alpha (or reg_alpha)	An L1 regularization parameter to control the complexity of the model.	0
Objective	The loss function to be optimized during training, which depends on the type of problem (regression, classification, etc.).	Reg:Squared-error
eval_metric	The metric used to evaluate the performance of the model during training.	rmse
early_stopping_rounds	If specified, training will be stopped if the validation metric does not improve over a certain number of consecutive iterations.	10
random_state	A random seed for reproducibility of results.	0
Booster	The type of booster to use (gbtree for decision trees or gblinear for linear regression).	gbtree

- **Category Boosting (Cat-Boost)**

Cat-Boost is one of a number of gradient-enhanced decision tree algorithms that use a new technique to deal with categorical variables by encoding them in numerical form, thus avoiding the over-fitting problems often associated with traditional encoding techniques. The table 9 lists the specific Cat-Boost model parameters along with an explanation of each one.

Table III.9: Specific parameters of the Cat-Boost model.

Name parameter	**Explain**	**Value in the model adopted**
iterations	The number of iterations (trees) to be trained.	100
learning_rate	The learning rate that controls the contribution of each tree to the overall model.	0.1
Depth	Maximum tree depth.	7
l2_leaf_reg	L2 regularization parameter.	0
border_count	Number of possible cutting points for categorical features.	0
bagging_Temperature	Temperature parameter for bag sampling.	none
random_strength	The random strength parameter for samples.	none
colsample_bylevel, colsample_bynode, colsample_bytree	Subsampling parameters for columns.	1
auto_class_weights	Enables CatBoost to automatically calculate class weights for unbalanced classification problems.	1
class_weights	Allows you to manually specify class weights for unbalanced classification problems.	none
scale_pos_weight	The weight of positive examples in unbalanced binary classification problems.	1
loss_function	The loss function to be optimized (default is "Logloss" for binary classification).	RMSE
eval_metric	The metric used to evaluate model performance during training.	RMSE
early_stopping_rounds	The number of consecutive iterations without improvement on the validation metric to stop training prematurely.	none
cat_features	List of categorical feature indices in the data.	none
verbose	Level of verbosity during training.	none
random_seed	A random seed in the data.	none

- **Random Forest (RF)**

Its principle is to generate several trees from a set of random data for training and to perform a weighted average of the results predicted by each tree. The figure III. 18 shows schema principle of Random Forest.

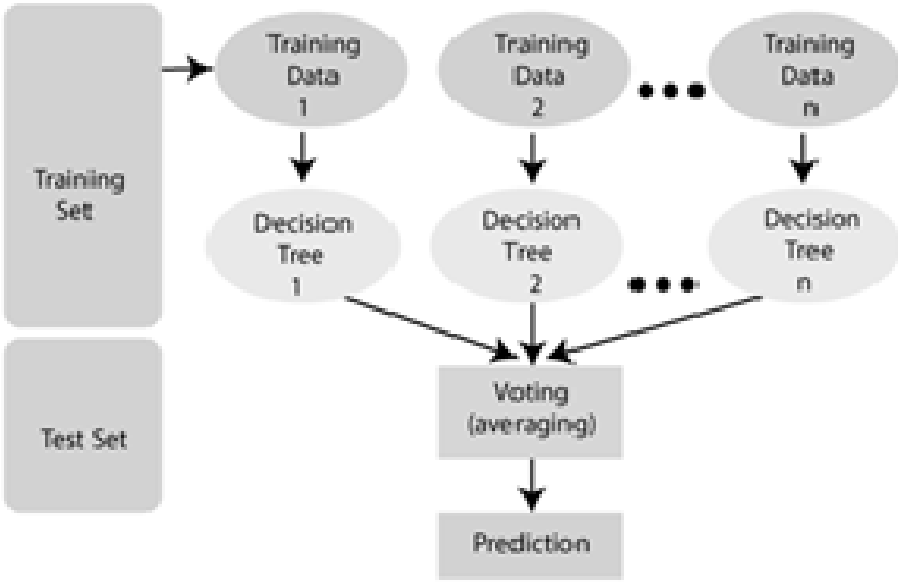

Figure III.18: Schema Principle of Random Forest[135]

These features are specified for the model in the table 10 lists the specific Random Forest model parameters along with an explanation of each one.

Table III.10: Specific parameters of the RF model.

Name parameter	Explain	Value in the model adopted
n_estimators	The number of decision trees in the forest.	100
criterion	The function for measuring the quality of a division (usually "gini" for Gini index or "entropy" for entropy).	MSE
max_depth	Maximum depth of decision trees.	30
min_samples_split	The minimum number of samples required to split an internal node.	2
min_samples_leaf	Minimum number of samples required in a leaf.	1
max_features	The number of features to consider when searching for the best split.	auto
bootstrap	Whether samples are drawn with replacement (True) or without replacement (False) when building trees.	true
random_state	A random seed for reproducibility.	0
class_weight	Class weights for unbalanced classification problems.	none
n_jobs	The number of parallel tasks to be executed during training.	none
verbose	Level of verbosity during training.	0
warm_start	Whether training should start from the previous model (True) or not (False).	false
oob_score	Whether the out-of-bag sampling error should be calculated.	false

- **Extremely Randomized Trees (Extra Tree)**

Extra Trees is a tree-based ensemble machine learning algorithm, part of the same family of methods as random forests. However, Extra Trees injects additional randomness when generating individual decision trees compared to random forests: -Extra Trees selects split features and thresholds fully at random when splitting a tree node. -Meanwhile, random forests randomly subsets the features and chooses the best split from those. -So Extra Trees adds extra randomization into the tree construction. This means Extra Trees exhibits higher tree diversity than basic random forests. Having varied trees via injected randomness allows the ensemble to capture more interactions and achieve better generalization ability. The particular parameters of the Extra Tree model are listed in the table 11.

Table III.11: Specific parameters of the Extra Tree model.

Name parameter	Explain	Value in the model adopted
n_estimators	The number of trees to be built in the model. The higher the number of trees, the more complex the model can capture in the data. However, it also increases training time.	100
max_features	This determines the maximum number of features to be considered when searching for the best split at each tree node. A lower value may increase diversity between trees and potentially reduce overfitting.	auto
max_depth	The maximum depth limits the depth of each tree in the forest. This can help prevent overfitting. If set to "None" (default), trees are expanded until all nodes contain a minimum number of samples.	none
min_samples_split	This is the minimum number of samples required for a node to be split into two subnodes. This can help control tree growth and prevent overfitting.	2
min_samples_leaf	This is the minimum number of samples required for a leaf to be considered valid. Used to control the size of tree leaves and potentially reduce overfitting.	1
bootstrap	If enabled (default), each tree is built using bootstrap sampling of the data. If disabled, trees are built on the full data set.	false
criterion	You can choose between "gini" (Gini index) and "entropy" (entropy) as a splitting criterion to measure the quality of splits.	squared_error
random_state	This is the random seed used to initialize random number generation. Setting this value allows results to be reproduced.	none
n_jobs	Specifies the number of CPU cores to be used for training and prediction. A value of -1 means use all available cores.	none
warm_start	If this option is enabled, you can add additional trees to an already trained model (useful for incremental learning).	false

III.4.3.4 Kernel-Based models

Kernel-Based models are a powerful approach to solving classification and regression problems by converting input data into higher-dimensional spaces, where linear models can be used to accomplish tasks that would be difficult to perform in the original space. The principal steps in a kernel-based model are shown in the following diagram (Figure III.19).

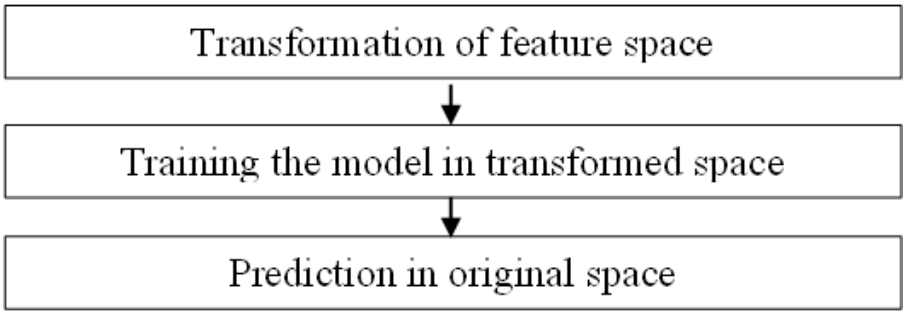

Figure III.19: Kernel-based model step-by-step diagram.

- **Support Vector Regression (SVR)**

Inspired by support vector machines (SVMs), SVRs are particularly well suited to the task of predicting continuous values rather than discrete classes. Their approach is based on the search for a hyper plane in a feature space, which maximizes the margin around data points, while limiting prediction errors. The SVR model has the following features (Table 12):

Table III.12: Specific parameters of the SVR model.

Name parameter	Explain	Value in the model adopted
Kernel	The kernel used to transform data into a higher dimensional space	sigmoid
C	Regularization parameter, controlling the trade-off between fitting the training data and reducing the complexity of the model.	3
Epsilon	Acceptable margin around the target value within which no penalty is applied to the prediction.	0.1
Degree	Degree of the polynomial for the polynomial kernel.	0
Gamma	Scaling parameter for the rbf kernel.	scale
Coef0	Constant term in polynomial and sigmoidal kernels.	0
Shrinking	Whether support vectors are used to shrink (True) or not (False) to improve efficiency.	True
Cache_size	Size of the memory cache for storing kernel values.	200
Tol	Shutdown tolerance.	1e-3
Verbose	Level of verbosity during training.	False
Max_iter	Maximum number of iterations to solve the optimization problem.	1
Kernel_params	Additional parameters for the kernel (if applicable).	

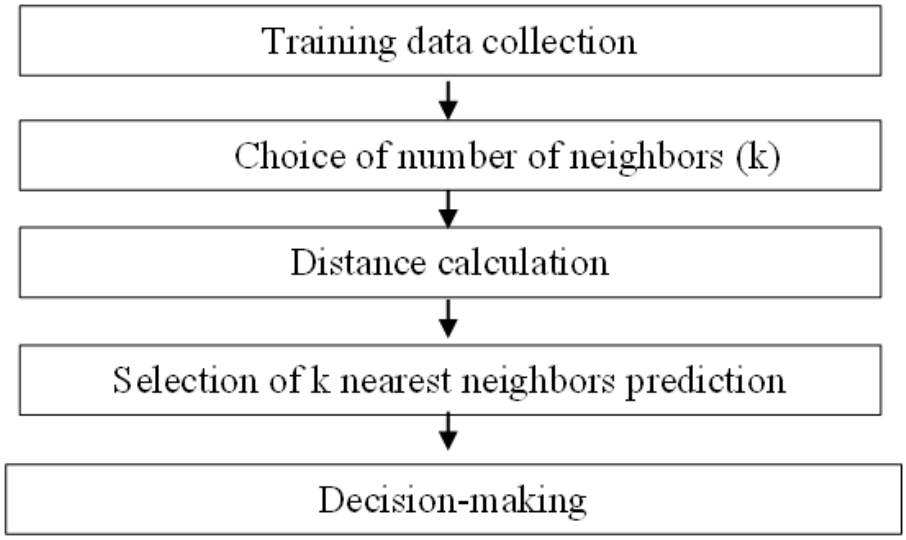

Figure III.20: Selection of K Neighbors.

- **K-Nearest Neighbors (KNN)**

Is a simple and intuitive supervised learning method used for classification and regression. KNN is non-parametric, assuming no particular shape for the data distribution. The basic operating principle of the KNN is illustrated as follows (Figure III.20):

The KNN model has the following characteristics (Table 13).

Table III.13: Specific parameters of the KNN model.

Name parameter	**Explain**	**Value in the model adopted**
k (number of neighbors)	It determines the number of nearest training samples to be taken into account when making a prediction.	5
Distance metric	KNN is based on calculating the distance between data points.	minkowski
Neighbors' weight	Some KNN algorithms assign different weights to neighbors according to their proximity. Closer neighbors may have a higher weight in the prediction.	uniform
Size reduction	Reducing the dimensionality of the feature space, especially when the number of features is high. This can help improve the efficiency and performance of the KNN model.	30
Neighbor search algorithm	To find the k nearest neighbors, different data structures can be used to speed up the search. The KD tree (multidimensional search tree) is one of the most commonly used structures.	Auto
Characteristic standardization	Since KNN is based on the distance between points, it is generally recommended to standardize features so that they have comparable scales.	None

III.4.4 Hybrid models

In this study, we explored the use of hybrid models for predicting global solar radiation over a horizontal surface. Five basic models were combined: arithmetic mean, harmonic mean, geometric mean, weighted mean and majority vote. These models were chosen for their complementarity and their ability to capture different characteristics of the data. The arithmetic mean provides a simple estimate, while the harmonic mean gives more weight to low values. The geometric mean is sensitive to the products of the values, and the weighted mean allows different weights to be assigned to each model according to their performance. Finally, majority voting selects the most frequent prediction among the different models.

III.4.4.1 Averaging

It is a straightforward mathematical approach where the predictions from multiple models are averaged to yield a more resilient and dependable final prediction. This method mitigates the risk of over-fitting by combining predictions from independently trained models. The outcome is a more reliable prediction that is less susceptible to variations in individual models.

$$\text{Ari\_mean} = \frac{x_1 + x_2 + \ldots + x_n}{n} \tag{III.8}$$

$$\text{Geo\_mean} = \sqrt[n]{x_1 \cdot x_2 \cdot \ldots \cdot x_n} \tag{III.9}$$

$$\text{Har\_mean} = \frac{1/x_1 + 1/x_2 + \ldots + 1/x_n}{n} \tag{III.10}$$

Such as : x :the output of the second prediction model.
n :number of models predicted.

III.4.4.2 Weighted averaging

The weighting of each model consists in assigning more weight or significance to certain models that have proved more effective or are deemed more reliable.

$$\text{FinalPrediction} = \sum_i \text{weight}_i \times \text{Prediction}_i \tag{III.11}$$

Where:
Final prediction : the combined final prediction of the base models.
Prediction_i:the prediction of a specific base model.
weight_i : the weight assigned to the prediction of the specific base model, with weights < 1.

III.4.4.3 Majority voting

Majority voting is one of ensemble model , it comprises five fundamental phases, which are outlined below:

Phase 1: Model training Different models are developed on the same training dataset. Each model is developed with different parameters.

Phase 2: Prediction Predictions are made on a new dataset.

Phase 3: Aggregate predictions: The forecasts generated in the preceding step are consolidated, and the chosen prediction is the one endorsed by the majority of the models.

Phase 4: Majority vote For every prediction, compute the count of models that made that specific prediction. The final prediction is determined by selecting the one with the highest number of votes.

Phase 5: Evaluation The final prediction is analyzed using evaluation metrics.

III.5 Results and discussions

For our work, several models selected for the prediction of global solar radiation on a horizontal surface for Batna city. The models used are a varied collection of predictors from different intelligent, classical, individual and hybrid families. The data used for prediction were obtained from the Helio-Clim1 site over a ten-year period (1996-2005) and, after replacing missing data, classified and ordered in the adjacent columns of an Excel file containing data on climatic variables for the city of Batna (Algeria). After collecting and pre-processing the data from the above-mentioned site, these data were structured by dividing them into two categories: one for the seven-year learning (1996-2002) and the other for the three-year test (2003-2005).

Model evaluation plays a pivotal role in the process of model validation. It serves as a critical step in assessing the performance and reliability of a given model. This step involves systematically assessing how well the model aligns with the real-world data it is intended to predict. Through various metrics, statistical analyses and comparisons with observed outcomes, model evaluation helps gauge the accuracy, precision and overall effectiveness of the model. This process not only verifies the model's ability to generalize to new, unseen data but also informs potential improvements or adjustments to enhance its predictive capabilities. In essence, model evaluation is an indispensable aspect of ensuring the validity and practical applicability of predictive models across diverse fields and applications.

III.5.1 Evaluation

Modeling is often linked to a process of evaluating these models using statistical criteria. These criteria provide quantified, objective measures of the performance of one or more models, facilitating decision-making and enabling continuous improvements in accuracy and robustness. These evaluations help researchers to compare models, to determine which is

best suited to their needs and to optimize their features on the basis of the results obtained. The statistical evaluation criteria used are :

- **Mean Square Error (MSE)**

The arithmetic mean of the squared deviations from model predictions and observations.

$$MSE = \frac{1}{m}\sum_{i=1}^{m}(G_{im} - G_{ie})^2 \tag{III.12}$$

Such as:G_im :Measured solar irradiation G_ie : Estimated solar irradiation.

- **The root mean square error (RMSE)**

It is commonly used to determine the performance of a predictive model. It evaluates the average magnitude of differences between predicted and actual values in a data set. The RMSE is calculated as the square root of the average of the squares of the differences between predicted and actual values.

$$RMSE = \sqrt{\frac{1}{m}\sum_{i=1}^{m}(G_{im} - G_{ie})^2} \tag{III.13}$$

- **Mean Absolute Error (MAE)**

Is a metric used to evaluate the performance of a predictive model or estimator. It measures the average magnitude of the differences between the predicted values and the actual values in a dataset. It is a measure of the quality of a predictive model or estimator. It measures the average magnitude of discrepancies between predicted and actual values in a data set. Unlike root mean square error (RMSE), MAE does not require differences to be squared, making it more understandable and less sensitive to outliers. Unlike the Root Mean Square Error (RMSE), the MAE does not involve squaring the differences, which makes it more interpretable and less sensitive to outliers.

$$MAE = \frac{1}{m}\sum_{i=1}^{m}|(G_{im} - G_{ie})| \tag{III.14}$$

- **The Pearson correlation coefficient (R2)**

It is used to calculate the fraction of data variance explained by the model. It is graduated from 0 to 1, with a value close to 1 indicating a better match between the model and the data. It is given by the following formula:

$$R^2 = \frac{\sum_{i=1}^{m}(G_{ie} - \bar{G}_{ie}) \times (G_{im} - \bar{G}_{im})}{\sqrt{\sum_{i=1}^{m}(G_{ie} - \bar{G}_{ie})^2 \times \sum_{i=1}^{m}(G_{im} - \bar{G}_{im})^2}} \tag{III.15}$$

For each family of models, we will present the results of the different models using the statistical criteria described above.

III.5.2 Classical models

III.5.2.1 Regression models

In this work, sixteen regression models are adopted and developed: four linear, five first-orders non-linear, three second-order non-linear and finally four regularized regression models to predict daily global solar radiation on a horizontal surface. The mathematical equations applied for the modeling are described in the table 1. Each regression model is distinguished by its numerical coefficients, which are related to the measured values and must be calculated separately for each group of regression models .

The coefficients a, b and c of the first group (basic models) are constants determined by the method of least squares and their values are given in the table 14.

Table III.14: Regression coefficients of the empirical models

Model	a	b	c
Basic regression			
Angstrom-Prescott	0.938	0.037	/
Exponential	-1.000	0.979	/
Exponent	0.801	0.909	/
Logarithmic	-0.108	0.937	/
Polynomial regression First-order			
Model with T	0.388	0.115	0.007
Model with Hu	0.692	0.280	-0.005
Model with Pr	-8.463	-0.240	0.010
Model with R	0.747	-0.152	-0.038
Model with W	0.678	-0.166	-0.023
Polynomial regression Second-order			
Quadratic_SS0	-0.389	0.262	0.545
Quadratic_T	-1.435e-04	0.088	-13.042
Quadratic_Hu	-4.3601e-06	-0.002	0.722

The evaluation of regression models developed using statistical criteria offers several advantages for assessing the effectiveness and performance of these models. After application of the preceding mathematical equations on MTALAB, results obtained by evaluating the performance of empirical models for testing years which are presented in the table 15.

By testing regression models on test years using statistical criteria, valuable information is obtained about the ability of these models to generalize beyond the training data and make accurate predictions under real-world conditions. The following table shows the evaluation of the empirical models for the three years of testing (2003, 2004 and 2005).

Table III.15: Performance metrics for different regression models.

Model	MSE	MAE	RMSE	R2
Linear	40.880	5.393	6.394	0.651
Exponential	22.503	3.530	4.744	0.789
Exponent	41.258	5.375	6.423	0.670
Logarithmic	45.619	4.945	6.754	0.756
REG_T	17.742	3.325	4.212	0.826
REG_Hu_	17.787	3.325	4.217	0.825
REG_Pr	19.528	3.537	4.419	0.808
REG_Ws	19.133	3.497	4.374	0.812
REG_R	19.116	3.491	4.372	0.812
Quadratic_SS0	19.633	3.534	4.431	0.806
Quadratic_T	17.712	3.310	4.209	0.826
Quadratic_Hu	17.698	3.305	4.207	0.826
Ridge Regression	10.691	2.469	3.269	0.808
Lasso Regression	10.897	2.500	3.301	0.804
Elastic Net Regression	11.074	2.528	3.327	0.801
Logistic Regression	20.021	3.183	4.474	0.736

The table 15 shows various models and their corresponding performance metrics, including Mean Squared Error (MSE), Mean Absolute Error (MAE), Root Mean Square Error (RMSE) and R-squared (R2) values.

- Based on the R^2 value (which measures how well the model fits the data), the models "REG_T", "REG_Hu", "Quadratic_T" and "Quadratic_Hu" have the highest R^2 values, indicating a better fit to the data compared to other models.
- The "Linear',' "Exponent',' and "Logarithmic" models are non-linear and have relatively high RMSE values compared to models like "Exponential", "REG_T" and "REG_Hu".
- "Lasso Regression","Ridge Regression" and "Elastic Net Regression" show lower MSE and RMSE values compared to some non-linear models, suggesting that regularization techniques help in reducing prediction errors.
- The "Logistic Regression" model has relatively high prediction errors (MSE and RMSE) compared to other models, indicating that it might not be well-suited for this regression task.
- "REG_T", "REG_Hu", "REG_Pr", "REG_Ws" and "REG_R" all have similar performance metrics, indicating that they might be capturing different aspects of the same underlying relationship.

Based on the above observation, we can distinguish the impact of meteorological parameters and their influence on the estimation of global solar radiation for the city of Batna, and order the parameters according to their dominance as follows: temperature, humidity, precipitation, wind direction and pressure.

III.5.3 Intelligent models

III.5.3.1 Fuzzy logic models

- **Models of first group**

A quick reminder about models of the first fuzzy group, which have two inputs: one is S/S_0 and the second is the season. The Table 16 illustrates the assessment of the performance of the proposed fuzzy systems for estimating global solar irradiation by varying the number and type of membership functions. Specifically, transition from the trapezoid model to the triangle model and subsequently to the Gaussian model should be examined and analyzed.

Table III.16: Performance metrics for fuzzy models.

Model	MSE	MAE	RMSE	R2
Fuzzy_3_TRA	20.600	3.706	0.276	0.813
Fuzzy_3_TRI	20.775	3.771	0.277	0.812
Fuzzy_3_Gauss	20.366	3.708	0.274	0.817
Fuzzy_7_TRA	18.970	3.365	0.265	0.812
Fuzzy_7_TRI	18.149	3.329	0.259	0.822
Fuzzy_7_Gauss	18.201	3.342	0.259	0.822

The table 16 illustrate various predictors using fuzzy logic and their corresponding performance metrics, including Mean Squared Error (MSE), Mean Absolute Error (MAE), Root Mean Square Error (RMSE) and R-squared (R2) values.

- ◇ All the fuzzy logic models, whether using 3 or 7 triangles (TRI) or trapezoids (TRA) or Gaussian functions have relatively similar performance metrics.
- ◇ The R-squared (R2) values for all fuzzy logic models are relatively consistent ranging from 0.812 to 0.822. This indicates that the models explain a similar proportion of the variance in the data and that the fuzzy logic models are capable of capturing a substantial proportion of the variance in the data and can be considered reasonable models for the given task.
- ◇ The fuzzy logic models have relatively low RMSE and MAE values, which indicates good predictive accuracy and a good fit to the data.

- **Models of second group**

In this section we present the results of the second group of fuzzy models (Table 17):

Table III.17: Comparison of Fuzzy Models for Various Parameters

Model	MSE	MAE	RMSE	R2
Temperature				
Fuzzy_3_TRA	19,850	3,563	4,455	0,807
Fuzzy_3_TRI	19,138	3,513	4,375	0,813
Fuzzy_3_Gauss	**18,909**	3,529	**4,348**	**0,816**
Fuzzy_7_TRA	21,104	3,542	4,594	0,799
Fuzzy_7_TRI	21,055	3,497	4,589	0,808
Fuzzy_7_Gauss	20,324	**3,450**	4,508	0,812
Humidity				
Fuzzy_3_TRA	21,788	3,845	4,668	0,805
Fuzzy_3_TRI	**21,249**	**3,814**	**4,610**	**0,809**
Fuzzy_3_Gauss	21,622	3,844	4,650	0,806
Fuzzy_7_TRA	33,932	4,690	5,825	0,672
Fuzzy_7_TRI	36,500	4,875	6,041	0,646
Fuzzy_7_Gauss	39,222	5,068	6,263	0,630
Pressure				
Fuzzy_3_TRA	22,841	3,928	4,779	**0,797**
Fuzzy_3_TRI	**22,037**	3,885	4,694	0,806
Fuzzy_3_Gauss	23,469	3,576	4,845	0,786
Fuzzy_7_TRA	22,838	3,864	4,779	0,785
Fuzzy_7_TRI	22,945	3,842	4,790	0,778
Fuzzy_7_Gauss	22,628	**3,820**	**4,757**	0,786
Wind-speed				
Fuzzy_3_TRA	21,916	3,859	4,681	0,807
Fuzzy_3_TRI	**21,526**	**3,840**	**4,640**	**0,810**
Fuzzy_3_Gauss	21,719	3,854	4,660	0,808
Fuzzy_7_TRA	32,071	4,510	5,663	0,687
Fuzzy_7_TRI	32,092	4,535	5,665	0,689
Fuzzy_7_Gauss	32,035	4,541	5,660	0,692
Rain-full				
Fuzzy_3_TRA	21,427	**3,813**	4,629	**0,808**
Fuzzy_3_TRI	**21,417**	3,816	**4,628**	**0,808**
Fuzzy_3_Gauss	21,805	3,867	4,670	**0,808**
Fuzzy_7_TRA	24,408	4,023	4,940	0,775
Fuzzy_7_TRI	25,543	4,168	5,054	0,784
Fuzzy_7_Gauss	42,482	5,462	6,518	0,747

The results of the preceding table 17 shown for different fuzzy sets and different weather parameters (Temperature, Humidity, Pressure, Wind-speed and Rainfall). The following discussion will be done for every climatic parameter :

Temperature:

- ◇ The RMSE (Root Mean Square Error) for all fuzzy sets is relatively low, indicating that the fuzzy models perform well in predicting operation.
- ◇ Fuzzy_3_Gauss has the lowest RMSE (4.348) and the highest R-squared value (0.816), suggesting it is the most accurate model for Temperature prediction among the three sets.
- ◇ Fuzzy_7_TRI also performs well with a high R-squared value (0.808).

Humidity:

- ◇ The RMSE for Fuzzy_7_Gauss is the highest (6.263), indicating it may not be the best model for predicting.
- ◇ Fuzzy_3_TRA, Fuzzy_3_TRI, and Fuzzy_3_Gauss have similar RMSE and R-squared values, suggesting they perform similarly in predicting using humidity.
- ◇ Fuzzy_7_TRA and Fuzzy_7_TRI have the lowest R-squared values, indicating they are less accurate for predicting based on humidity.

Pressure:

- ◇ Fuzzy_3_TRI has the lowest RMSE (4.694) and the highest R-squared value (0.806) for predicting using pressure, making it the most accurate model among the three sets.
- ◇ Fuzzy_7_TRI has a slightly higher RMSE and lower R-squared value compared to Fuzzy_3_TRI, suggesting it is less accurate for predicting operation.
- ◇ Fuzzy_7_Gauss has the highest RMSE (4.845), indicating it may not be the best model for solar radiation prediction.

Wind-speed:

- ◇ Fuzzy_3_TRA, Fuzzy_3_TRI, and Fuzzy_3_Gauss have similar RMSE and R-squared values for predicting using wind-speed.
- ◇ Fuzzy_7_TRA, Fuzzy_7_TRI, and Fuzzy_7_Gauss have higher RMSE values and lower R-squared values, indicating that they are less accurate for predicting based on wind-speed compared to the Fuzzy_3 sets.

Rainfall:

- ◇ Fuzzy_3_TRA, Fuzzy_3_TRI, and Fuzzy_3_Gauss have similar RMSE and R-squared values for predicting using rainfall.
- ◇ Fuzzy_7_TRA and Fuzzy_7_TRI have higher RMSE values and lower R-squared values, indicating they are less accurate for predicting based on rainfall.
- ◇ Fuzzy_7_Gauss has the highest RMSE (6.518) and the lowest R-squared value (0.747), suggesting it is the least accurate model for solar radiation prediction using rainfall among

the three sets.

In summary, the selection of the best fuzzy set for a specific weather parameter depends on the desired trade-off between accuracy and complexity. Fuzzy_3 sets generally perform well, while Fuzzy_7 sets tend to be less accurate in most cases.

- **Models of third group**

Remember that the fuzzy models of the third type have two inputs: season and one of the meteorological parameters. The results of the third group of fuzzy models presented in the table 18 reflect their performance.

Table III.18: Prediction of Solar Radiation by Fuzzy Models Third Group .

Model	MSE	MAE	RMSE	R^2
Temperature				
Fuzzy_ 3_TRA	20,650	3,695	4,544	0,809
Fuzzy_ 3_TRI	**18,809**	3,513	**4,337**	**0,820**
Fuzzy_3_Gauss	20,769	3,662	4,557	0,807
Fuzzy_7_TRA	21,953	3,779	4,685	0,799
Fuzzy _7_TRI	20,434	**3,454**	4,520	**0,820**
Fuzzy_ 7_Gauss	20,656	3,692	4,545	0,808
Humidity				
Fuzzy_ 3_TRA	20,798	3,765	4,561	0,810
Fuzzy_ 3_TRI	20,951	3,789	4,577	0,811
Fuzzy_3_Gauss	21,242	3,814	4,609	0,808
Fuzzy_7_TRA	19,269	**3,447**	4,390	0,810
Fuzzy_7_TRI	**18,680**	3,449	**4,322**	**0,819**
Fuzzy_ 7_Gauss	18,781	3,454	4,334	0,818
Pressure				
Fuzzy_ 3_TRA	22,841	3,928	4,779	0,797
Fuzzy_ 3_TRI	22,037	3,885	4,694	0,806
Fuzzy _3_Gauss	23,469	3,576	4,845	0,786
Fuzzy_7_TRA	22,838	3,864	4,779	0,785
Fuzzy _7_TRI	18,501	3,396	4,301	0,817
Fuzzy_ 7_Gauss	**18,129**	**3,356**	**4,258**	**0,822**
Wind-speed				
Fuzzy_ 3_TRA	20,977	3,788	4,580	0,813
Fuzzy_ 3_TRI	20,733	3,768	**4,553**	**0,816**
Fuzzy _3_Gauss	**20,728**	**3,772**	**4,553**	**0,816**
Fuzzy_7_TRA	25,789	4,098	5,078	0,764
Fuzzy _7_TRI	23,693	3,952	4,868	0,781
Fuzzy_ 7_Gauss	23,741	3,962	4,872	0,782
Rain-full				
Fuzzy_ 3_TRA	21,377	3,811	4,624	0,808
Fuzzy_ 3_TRI	19,240	3,519	4,386	0,810
Fuzzy_3_Gauss	21,621	3,846	4,650	0,807
Fuzzy_7_TRA	19,299	3,464	4,393	0,815
Fuzzy_7_TRI	18,042	**3,386**	4,248	**0,824**
Fuzzy_7_Gauss	**18,009**	3,397	**4,244**	**0,824**

The observations from the provided errors (Table 18)on different fuzzy models for various weather parameters.

◇ **Model Comparison for Temperature Parameter:**

- Among the fuzzy models used for Temperature prediction, "Fuzzy 3_TRI" performs the best with the lowest Mean Squared Error (MSE) of 18,809 and the highest R-squared (R2) value of 0.820.
- "Fuzzy 3_TRA" and "Fuzzy 3_Gauss" are also competitive models for solar radiation prediction using Temperature.
- All three models for 3 membership functions show similar performance in terms of MSE, MAE, RMSE, and R2 values.

◇ **Model Comparison for Humidity Parameter:**

- Similar to Temperature, "Fuzzy 3_TRI" performs the best for solar prediction using humidity with the lowest MSE (20,951) and the highest R2 value (0.811).
- "Fuzzy 3_Gauss" and "Fuzzy 3_TRA" are also good choices for prediction based on humidity.
- The number of membership functions (3 in this case) seems to yield better results for solar radiation prediction using humidity.

◇ **Model Comparison for Pressure Parameter:**

- For prediction using pressure , "Fuzzy 3_TRI" and "Fuzzy 3_Gauss" models exhibit the lowest MSE values, indicating good performance.
- The "Fuzzy 7_TRI" and "Fuzzy 7_Gauss" models perform well, especially in terms of R-squared values.
- Solar radiation prediction based on pressure is generally more challenging, as indicated by higher MSE values compared to Temperature and humidity.

◇ **Model Comparison for Wind Speed Parameter:** - "Fuzzy 3_TRA" and "Fuzzy 3_TRI" are the top-performing models for solar radiation prediction, with low MSE and high R2 values.
- The "Fuzzy 7_TRA" and "Fuzzy 7_TRI" models also provide reasonable predictions, although with slightly higher MSE values.

◇ **Model Comparison for Rainfall Parameter:** - "Fuzzy 3_TRA" and "Fuzzy 3_TRI" models show the best performance for prediction based on rainfall, with low MSE and high R2 values.
-"Fuzzy 7_TRA" and "Fuzzy 7_TRI" models also perform well for this parameter.

Overall, it appears that the selection of the number of membership functions (3 or 7) and the specific fuzzy model (e.g., TRI, GAUSS, or TRA) can have a significant impact on the performance of the fuzzy system for solar radiation prediction based on the weather parameters. It's essential to consider both MSE and R^2 values when evaluating model performance, as they provide complementary information about prediction accuracy and goodness of fit. Additionally, it's advisable to further investigate the data and domain-specific factors to select the most suitable fuzzy model for a particular weather parameter.

- **Models of four group**

The findings of the four group of fuzzy models are shown in the table 19 and represent their performance in solving the given problem.

Table III.19: Performance Metrics for Different Models

Parameter	Model	MSE	MAE	RMSE	R2
Temperature					
Fuzzy_3_TRA	19.609	3.518	4.428	0.807	
Fuzzy_3_TRI	18.862	3.483	4.343	0.815	
Fuzzy_3_Gauss	18.770	3.509	4.332	0.817	
Fuzzy_7_TRA	19.320	3.437	4.395	0.813	
Fuzzy_7_TRI	18.500	3.376	4.301	0.818	
Fuzzy_7_Gauss	18.473	3.377	4.298	0.818	
Humidity					
Fuzzy_3_TRA	21.133	3.787	4.597	0.809	
Fuzzy_3_TRI	20.981	3.790	4.581	0.812	
Fuzzy_3_Gauss	21.249	3.813	4.610	0.809	
Fuzzy_7_TRA	19.514	3.457	4.417	0.807	
Fuzzy_7_TRI	18.680	3.449	4.322	0.819	
Fuzzy_7_Gauss	18.781	3.454	4.334	0.818	
Pressure					
Fuzzy_3_TRA	19.955	3.660	4.467	0.817	
Fuzzy_3_TRI	20.349	3.733	4.511	0.819	
Fuzzy_3_Gauss	20.216	3.701	4.496	0.814	
Fuzzy_7_TRA	18.766	3.400	4.332	0.814	
Fuzzy_7_TRI	18.169	3.359	4.262	0.821	
Fuzzy_7_Gauss	18.129	3.356	4.258	0.822	
Wind-speed					
Fuzzy_3_TRA	20.169	3.678	4.491	0.815	
Fuzzy_3_TRI	20.665	3.760	4.546	0.815	
Fuzzy_3_Gauss	20.644	3.754	4.544	0.815	
Fuzzy_7_TRA	20.296	3.611	4.505	0.801	
Fuzzy_7_TRI	19.371	3.559	4.401	0.812	
Fuzzy_7_Gauss	19.487	3.571	4.414	0.811	
Rain-full					
Fuzzy_3_TRA	21.383	3.810	4.624	0.808	
Fuzzy_3_TRI	19.640	3.595	4.432	0.809	
Fuzzy_3_Gauss	21.598	3.842	4.647	0.807	
Fuzzy_7_TRA	19.431	3.461	4.408	0.810	
Fuzzy_7_TRI	18.042	3.386	4.248	0.824	
Fuzzy_7_Gauss	18.009	3.397	4.244	0.824	

The observations from the provided errors(Table 19) on different fuzzy models for various weather parameters:

◇ **Temperature parameter:**
-Fuzzy 7_TRI model has the lowest MSE (18,500) and RMSE (4,301), indicating it performs the best for predictions solar radiation based Temperature.
-Fuzzy 3_Gauss model has the highest R2 value (0.817), showing a good fit to the errors.

◇ **Humidity parameter:**
- Fuzzy 7_TRI model has the lowest MSE (18,680) and RMSE (4,322), suggesting it provides the best predictions with humidity.
-Fuzzy 7_TRI also has the highest R2 value (0.819), indicating a strong fit.

- **Pressure parameter:**
- Fuzzy 7_Gauss model has the lowest MSE (18,129) and RMSE (4,258), making it the top performer for solar radiation predictions based pressure.
-Fuzzy 7_TRI has the highest R2 value (0.822), indicating an excellent fit to the results.

- **Wind-speed parameter:** -Fuzzy 3_TRA model has the lowest MSE (20,169) and RMSE (4,491), performing well for predictions.
-The R2 values for wind-speed predictions are relatively consistent across models, ranging from 0.801 to 0.815.

- **Rainfall parameter:**
-Fuzzy 7_TRI model has the lowest MSE (18,042) and RMSE (4,248), making it the most accurate for solar radiation predictions.
-Fuzzy 7_Gauss also has a high R2 value (0.824), indicating a strong fit.

Model synthesis is useful for consolidating knowledge, opening up new research perspectives and improving overall understanding of solar radiation prediction. A detailed analysis of the performance of various fuzzy logic models for the prediction of global solar radiation of the city of Batna with meteorological parameters, such as temperature, humidity, atmospheric pressure, wind speed and precipitation is carried out for the last three study groups.

To demonstrate the influence of meteorological parameters on solar radiation prediction, this analysis of these variables in relation to variations in solar radiation will be carried out.This study will seek to establish correlations, assess the relative importance of each parameter, and quantify their direct impact on the accuracy of solar radiation predictions. We've excluded the first group because it's a basic group containing two s/s0 entries and the season.Key metrics, including mean square error (MSE), mean absolute error (MAE), root mean

square error (RMSE) and coefficient of determination (R2), were evaluated in three groups (GR2, GR3, GR4) for each climate parameter. This analysis reveals general(see Table 20) trends in performance, identifies the best-performing models for each factor, and offers recommendations for guiding the choice of models according to specific environmental prediction requirements.

	GR2					GR3					GR4				
Feather	Model	MSE	MAE	RMSE	R2	Model	MSE	MAE	RMSE	R2	Model	MSE	MAE	RMSE	R2
T	3_Gauss	18,909	3,529	4,348	0.816	3_TRI	18,809	3,513	4,337	0.820	7_TRI	18,500	3,376	4,301	0.818
Hum	3_TRI	21,249	3,814	4,610	0.809	7_TRI	18,680	3,449	4,322	0.819	7_TRI	18,680	3,449	4,322	0.819
Pr	3_TRA	22,841	3,928	4,779	0.797	3_TRA	22,841	3,928	4,779	0.797	7_Gauss	18,129	3,356	4,258	0.822
Ws	3_TRI	21,526	3,840	4,640	0.810	3_Gauss	20,728	3,772	4,553	0.816	3_Gauss	20,644	3,754	4,544	0.815
R	3_TRI	21,417	3,816	4,628	0.808	7_Gauss	18,009	3,397	4,244	0.824	7_Gauss	18,009	3,397	4,244	0.824

Table III.20: Performance Comparison of Fuzzy Logic Models for Meteorological Parameters

- **Overall Model Performance:**
  -The models generally perform well, with R2 values ranging from 0.797 to 0.824 across different groups and environmental factors.

- **Consistency Across groups:** -For T (Temperature), GR3 with Fuzzy_3_TRI has the highest R2 (0.820), while for other factors, GR4 with Fuzzy_7_Gauss has the highest R2 (0.822-0.824).

- **Temperature (T):**
  -Best Model: Fuzzy_3_TRI at GR3 has the highest R2 (0.820).
  - Consistency: Fuzzy_3_TRI performs consistently well across GR2, GR3 and GR4.

- **Humidity (Hu):**
  -Best Model: Fuzzy_7_TRI at GR3 has the highest R2 (0.819).
  -Consistency: Fuzzy_7_TRI performs consistently well across GR2, GR3 and GR4.

- **Pressure (Pr):**
  -Best Model: Fuzzy_7_Gauss at GR4 has the highest R2 (0.822).
  -Consistency: Fuzzy_3_TRA performs consistently well across GR2 and GR3.

- **Wind Speed (Ws):**
  -Best Model: Fuzzy_3_TRI at GR3 has the highest R2 (0.810).
  -Consistency: Fuzzy_3_TRI performs consistently well across GR2, GR3 and GR4.

- **Rainfall (R):**
  -Best Model: Fuzzy_7_Gauss at GR4 has the highest R2 (0.824).
  -Consistency: Fuzzy_7_Gauss performs consistently well across GR2, GR3 and GR4.
  Consider Fuzzy_3_TRI as a robust choice for Temperature and wind speed predictions. For humidity, Fuzzy_7_TRI at GR3 seems to be a reliable option. Pressure predictions are well-captured by Fuzzy_7_Gauss at GR4. Fuzzy_7_Gauss at GR4 is recommended for rainfall prediction.

III.5.3.2 ANN-Based models

In this section, ANN-based models are analyzed to assess their performance and ability to predict daily global solar radiation on a horizontal surface for the city of Batna.

- **MLP**

The table 21 provides the evaluation metrics for various models denoted by different

combinations of variables (T for temperature, Hu for humidity, Pr for pressure, Ws for wind speed, Wd for wind direction, and R for some other variable)and including Mean Squared Error (MSE), Mean Absolute Error (MAE), Root Mean Square Error (RMSE) and R-squared (R2) values. These metrics are often used to assess the performance of predictive models. Here are some insights from the provided data:

Table III.21: Performance Metrics for Different MLP Models

Model	MSE	MAE	RMSE	R2
MLP	18.022	3.349	4.245	0.824
MLP_T	15.884	3.076	3.986	0.847
MLP_Hu	10.998	2.538	3.316	0.897
MLP_Pr	16.286	3.024	4.036	0.843
MLP_Ws	16.810	3.114	4.100	0.839
MLP_Wd	9.477	2.272	3.079	0.912
MLP_R	13.109	2.689	3.621	0.877
MLP_T_Hu	10.668	2.429	3.266	0.900
MLP_T_Pr	15.257	2.960	3.906	0.855
MLP_T_Pr	15.257	2.960	3.906	0.855
MLP_T_Ws	16.102	3.095	4.013	0.846
MLP_T_Wd	15.658	3.042	3.957	0.849
MLP_T_R	10.451	2.249	3.233	0.906
MLP_Hu_Pr	10.246	2.392	3.201	0.904
MLP_Hu_Ws	10.485	2.463	3.238	0.902
MLP_Hu_Wd	10.456	2.425	3.234	0.902
MLP_Hu_R	9.825	2.216	3.134	0.911
MLP_Pr_Ws	16.297	3.051	4.037	0.847
MLP_Pr_R	11.154	2.402	3.340	0.899
MLP_Ws_Wd	17.149	3.146	4.141	0.835
MLP_Ws_R	10.396	2.359	3.224	0.904
MLP_Wd_R	11.148	2.412	3.339	0.900
MLP_T_Hu_Pr	10.225	2.348	3.198	0.905
MLP_T_Hu_Pr_Ws	18.001	3.217	4.243	0.825
MLP_T_Hu_Pr_Wd	10.249	2.323	3.201	0.905
MLP_T_Hu_Pr_Ws_Wd_R	9.014	2.180	3.002	0.918

◇ **Performance Variation:**

The models exhibit significant variation in their performance. The two less effectives models are the MLP and MLP_Pr_R, with the same metric values: MSE=18,022, MAE=3,349, RMSE=4,245 and R2=0,824. On the other hand, the better effectives model is the MLP T_Hu_Pr_Ws_Wd, with the following values: MSE=9,014, MAE=2,180, RMSE=3,002 and R2=0,918. We can therefore see that the MLP model T_Hu_Pr_Ws_Wd performs best in terms of R2, which means that it is the best to predict the solar radiation. The MLP model and MLP_Pr_R perform the worst in terms of MSE, MAE and

RMSE, which means that it is the least accurate and reliable.

◇ **Feature Importance:**

It appears that including more variables or features in the model does not always result in better predictive performance. Some models with fewer variables outperform those with more, suggesting that feature selection and engineering play a crucial role in model accuracy. The characteristics influencing the prediction of daily global solar radiation on a horizontal surface in the case of the city of Batna are: temperature, humidity and wind speed.

Overall, the MLP_T_Hu_Pr_Wd model performed the best, with the lowest MSE, MAE, and RMSE, and the highest R2. This suggests that this model is the most accurate and reliable of the models tested.The MLP_T and MLP_Hu models also performed well, with MSE, MAE, and RMSE values lower than the baseline MLP model. This suggests that adding temperature feature (MLP_T) and humidity parameter (MLP_Hu) can improve the performance of MLP models. The MLP_Wd model performed particularly well on the R2 metric, with the highest value of 0.912. This suggests that this model is good at explaining the variation in the target variable.If the goal is to achieve the best possible accuracy and reliability, the MLP_T_Hu_Pr_Wd model should be used. If the goal is to explain the variation in solar radiation, the MLP_Wd model should be considered. If the model is over fitting the training data, rain full parameter (MLP_R) can be added to improve the generalization ability of the model.

- **RNN,CNN and LSTM**

The results obtained by applying statistical criteria to evaluate the performance of three predictors based ANN which are: RNN, CNN and LTSM, are shown in the following table 22:

Table III.22: Performance Metrics for Different Models

Model	MSE	MAE	RMSE	R2
RNN	8.88	2.21	2.91	0.84
CNN	8.96	2.12	2.99	0.83
LSTM	**7.74**	**2.04**	**2.78**	**0.86**

The following observations are based on the supplied errors on three deep learning models for various weather parameters:

◇ The LSTM predictor looks to have the greatest prediction among the predictors. LSTM based model This implies that LSTM based model is the best model for estimating daily global sun irradiance in Batna with, MAE=2,04, MSE=7,74 and R2 = 0,86.

◇ Both CNN and RNN predictors operate slightly higher RMSEs and MAEs respectively and marginally worse, with MSE=8,96 and MSE=8,88 and slightly higher MAE and

RMSE, respectively. However, their R2 remains high, which demonstrating that the both predictors explain a significant percentage of the variability in the data.

Models based on artificial neural networks are proving extremely effective for solar radiation prediction, demonstrating remarkable accuracy in forecasting solar radiation levels thanks to their ability to capture complex, non-linear relationships in meteorological data.

III.5.3.3 Tree-Based models

Tree-based models are widely used in solar radiation prediction because of their ability to capture complex non-linear relationships between meteorological variables and solar radiation. The models, developed for the prediction of daily global solar radiation on a horizontal surface for the city of Batna are:Decision Tree (DT), Models-5 Tree (M5), Gradient Boosting Decision Trees(GBDT), XGBoost, CatBoost and Random Forest(RF).
The following table 23 shows the results of applying statistical criteria to evaluate the performance of tree based models:

Table III.23: Performance Metrics for Different Tree Based Models

Model	MAE	RMSE	R2
DT	2.267	3.132	0.829
M5	2.479	3.385	0.801
GBDT	1.992	2.779	0.861
XGBOOST	2.067	2.935	0.849
CatBoost	**1.979**	**2.755**	**0.863**
RF	2.020	2.831	0.856

The following observations are based on the errors reported by tree based models for different weather parameters:

- All models are performing well and their correlation rate is above 80%.
- According to the results of performance evaluation with the statistical criteria of the models developed in the previous table 23, we note the effectiveness of following algorithms, which are ordered according to the correlation rate: CatBoost, GBDT, RF, XGBOOST DT and M5.
- The model based on the XGBOOST algorithm was the model that provided the highest correlation rate (MAE=0.004, RMSE=0.006 and R2=0.999) for the training.
- The model based on CATBOOST algorithm is the best model for solar radiation prediction with the following statistical error values: MAE=1.979, RMSE=2.755 and R2=0.863.
- The DT, M5 models have relatively fast formation times of less than 0.019.
- GBDT, XGBoost and Catboost have longer training times greater than 1,840 due to their iterative training approach.

- RF provided relatively high performance (MAE=220, RMSE=2.831 and R2=0.856) due to its ability to reduce over-learning and handle missing data.
- GBDT, XGBoost and Catboost also have high performance above 84.9% due to their iterative training approach.
- DT and M5 can be prone to over-learning, which can affect performance.
- During the implementation of the adopted models it was found that:
◇ RF can require a significant amount of memory space to store large data sets.
◇ GBDT, XGBoost and Catboost may also require a large amount of memory space due to their iterative training approach.
◇ DT and M5 require less memory space because they are based on a single decision rule.

III.5.3.4 Kernel-Based models

Kernel-based models, such as support vector machines (SVMs) with adapted kernels, have demonstrated their effectiveness in predicting solar radiation, exploiting the ability of these approaches to capture complex relationships between meteorological variables and radiation levels. Two models have been developed to predict solar radiation in Batna: SVR and KNN. The following table 24 shows the results of applying statistical criteria to evaluate the performance of the tree based models:

Table III.24: Performance metrics for SVR and KNN models.

Model	MSE	MAE	RMSE	R2
SVR	1878.695	33.054	43.343	0.752
KNN	**12.584**	**2.637**	**3.547**	**0.774**

- The MSE measures the mean square of the prediction errors, with lower values indicating better performance. Thus, KNN (12.584) has a lower MSE than SVR (1878.695), suggesting better accuracy for the KNN model.
- The MAE measures the mean of the absolute values of the errors, and here too, the KNN (2.637) shows a more accurate performance compared to the SVR (33.054).
- RMSE is the square root of MSE and measures the standard deviation of errors. Similarly, KNN (3.547) has a lower RMSE than SVR (43.343), indicating better accuracy for KNN.
- The R-squared (R2) measures the proportion of variance in the dependent variable explained by the model. Both models have fairly close R2 values, but the KNN (0.774) shows a slight improvement over the SVR (0.752), suggesting a better fit of the KNN model to the data.

In summary, on the basis of these metrics, the KNN model appears to offer better prediction performance than the SVR model for the solar radiation prediction task.

III.5.3.5 Hybrid models

The enhancement of predictive models for more dependable outcomes constitutes a crucial aspect of scientific research across various domains. Hybrid models represent a strategic approach aimed at optimizing the efficacy of predictors.These models amalgamate distinct features and strengths from various methodologies, striving to attain predictions that are not only more reliable but also more resilient. The primary hurdle faced by hybrid models lies in effectively leveraging the unique strengths of each approach to yield predictions of heightened reliability. Drawing on our theoretical investigation, hybrid models encompass methodologies such as averaging, weighted averaging and majority voting.

- **Averaging**

The use of techniques in the hybridization process is particularly beneficial for improving the accuracy of solar radiation forecasts. Its advantage is that it can reduce individual biases and compensate for fluctuations in predictions.

- **Weighted averaging**

The advantage of using the weighted average is that it favors the best-performing models, resulting in more accurate and robust predictions.

- **Majority voting**

Majority voting serves as an effective and straightforward approach, engineered to mitigate individual biases and foster a more robust prediction by harnessing the diversity inherent in various models.

The methods mentioned above are implemented on the foundational models through the application of respective calculations. The table 25 represents the quality of different hybrid models with different clustering strategies.

Table III.25: Performance metrics for various models in solar radiation prediction.

Model	MSE	MAE	RMSE	R2
Avr-mean	8.120	2.107	2.849	0.854
Avr-geo	15.008	2.908	3.874	0.730
Avr-harm	8.382	2.125	2.895	0.849
Weight-avr	**7.703**	**2.029**	**2.775**	**0.861**
Maj-Vote	8.120	2.107	2.849	0.854

- The weight-avr model performs best on all 4 criteria. It is therefore the model that best fits the data.
- The Avr-geo model performs least well, with the highest MSE, MAE and RMSE and the lowest R2. It is less accurate at modeling the data.

- The other 3 models have similar intermediate performances.

In conclusion, the weight-avr model seems the most appropriate according to these error and data fit metrics.

III.6 Conclusion

In conclusion, this chapter offers a thorough examination of various AI-based models employed and suggested for forecasting global solar radiation on a horizontal surface, specifically tailored for the city of Batna. The analysis encompasses an evaluation of their performance, limitations, followed by a comparative assessment among the different models and other relevant works.The second section of the chapter provides a detailed description of the study site, setting the context for the subsequent analyses. The third section elucidates the meticulous process of collecting meteorological data, which serves as the foundation for training and testing the devised models.Moving forward, the fourth and fifth sections delineate the methodologies underlying the approaches used, offering insights into the techniques applied to predict solar radiation accurately. Finally, the chapter concludes with a comprehensive discussion of the results, synthesizing the findings from the various models and shedding light on their implications for solar radiation prediction in the specific context of Batna. Through this comprehensive approach, the chapter not only contributes to advancing the understanding of AI-based solar radiation prediction models but also provides valuable insights for potential applications and future research endeavors.

GENERAL CONCLUSION

Forecasting daily solar radiation is an important task for many applications, including solar energy production, power grid management and outdoor activity planning. Artificial intelligence (AI) methods offer considerable potential for improving the accuracy and reliability of these forecasts. The ultimate aim is to improve the accuracy of daily solar radiation forecasts using these artificial intelligence methods, enabling more efficient planning of solar energy systems, better management of energy resources and smoother integration of renewable energies into electricity grids.

This study elucidates the entire process, encompassing the design, implementation, and comparison phases, and provides a comprehensive analysis of the development, execution, and performance evaluation of prediction models that are classified into two main groups: Classical Models and Intelligent Models. Classical Model fall under the umbrella of traditional techniques and include one subcategory: Regression. These models rely on statistical approaches and historical data patterns to forecast solar radiation. On the other hand, Intelligent Models encompass more advanced methodologies and are further divided into two subcategories: Individual and Hybrid. Within the Individual Models subgroup, four distinct types are explored:

- **Fuzzy Logic Models:** These models utilize fuzzy logic principles to handle uncertainty and imprecise data, offering a more adaptable approach to solar radiation prediction.
- **ANN-Based Models (Artificial Neural Network-Based):** These models leverage the neural network architecture to learn complex patterns in solar radiation data, enabling them to capture nonlinear relationships and dependencies more accurately.
- **Tree-Based Models:** This category involves decision tree algorithms such as Random Forest or Decision Trees that segment data hierarchically, aiding in the precise prediction of solar radiation by partitioning the input space effectively.
- **Kernel-Based Models:** are used for their ability to manage complex data and capture non-linear relationships between environmental variables.
- **Hybrid models:** The essence of hybrid modeling lies in combining the distinctive characteristics and advantages of various models to attain predictions that are not only more accurate but also robust.

The models are formulated with eleven inputs, encompassing a combination of atmospheric and meteorological variables. Atmospheric parameters are:

- **Duration of Insolation (S):** The amount of time during which solar radiation is received.
- **Time between Sunset and Sunrise (S0):** The duration of darkness or nighttime.
- **Daily Mean of Irradiation at the Top of the Atmosphere (G0):** The solar

radiation that would be received at the top of the atmosphere under clear sky conditions. Meteorological parameters are :

- **Temperature (T):** Ambient air temperature.
- **Humidity (Hu):** Amount of moisture present in the air.
- **Pressure (Pr):** Atmospheric pressure.
- **Wind Speed (Ws):** Speed of the wind.
- **Rainfall (R):** Amount of rainfall.

The single Output of all models is predicted solar radiation. Each model type within these categories demonstrates unique strengths and applications in predicting daily solar radiation, providing a comprehensive toolkit for enhancing the accuracy and reliability of solar radiation forecasts. This diverse range of models allows for a more holistic exploration of predictive capabilities, ensuring a robust approach to harnessing solar energy efficiently.

In this study, which focused on the prediction of daily solar radiation using artificial intelligence methods, several crucial aspects were explored and evaluated. This study conducts simulations of all models using two programming languages, Python and Matlab. The data-set utilized for implementing the simulated models is sourced from the Helio-Clim1 website, ensuring comprehensive and reliable data for the analytical processes.

The results of the model performance tests demonstrate the robustness and accuracy of the simulated models in various evaluation measures. These measures include [Mean Square Error (MSE), Root Mean Square Error (RMSE), Mean Absolute Error (MAE) and the Pearson correlation coefficient (R2)], revealing information about the predictive capabilities of the models and their suitability for the intended application. Comparative analysis highlights the strengths and potential areas for improvement of each model, making it easier to select the most effective approach for the given task and reveal the following observations:

- Regression, as a classical method, offers a sound statistical approach by modeling linear relationships between variables. In our study, the correlation rate was 0.826 for the models (REG_T, Quadratic_T and Quadratic_Hu).
- Fuzzy logic-based models exploit conceptual flexibility to deal with the uncertainty and variability inherent in solar radiation data, offering a robust approach under changing conditions. These models show a correlation rate equal to 0.824 for the models (Fuzzy_7_TRI and Fuzzy_7_Gauss).
- Models based on artificial neural networks (ANNs) (MLP,RNN,CNN and LSTM) demonstrate their ability to learn complex, non-linear patterns, delivering high predictive accuracy. At the same time, models based on decision trees provide an intuitive and interpretable approach, suitable for decomposing complex patterns, with a correlation rate of 0.860, notably for the LSTM model.

- Kernel-based models (SVR and KNN) harness the power of nonlinear transformations, achieving a correlation rate of 0.774 with the KNN model.
- Hybrid models combine the advantages of different approaches for improved performance,recording a correlation rate of 0.861 for Hyb-weight-avr.

The thesis concludes that AI offers a promising approach to solar radiation forecasting and the integration of hybrid models, skilfully combining statistical approaches, complex meteorological data and machine learning techniques, offers a promising and accurate method for predicting solar radiation, opening up crucial prospects for sustainable and efficient energy exploitation of solar resources.The models developed through this research have shown a significant ability to process complex data sets, take into account the variability of environmental conditions and provide reliable forecasts of solar radiation on a daily basis. This increased accuracy in solar radiation prediction is of paramount importance for the optimal integration of solar energy systems into power grids, energy planning and resource management. All in all, this study opens up exciting prospects for the use of artificial intelligence methods in solar radiation prediction. It underlines the importance of continuing research and development in this field in order to exploit the full potential of solar energy, thereby contributing to a more sustainable and efficient energy transition.

Solar radiation prediction using artificial intelligence (AI) offers a vast field of perspectives that can be meaningfully addressed by exploring different ideas here are some of them:

- Exploring others AI Methods by enriching the palette of AI methods used for solar radiation prediction.
- The possibility of hybridizing different AI techniques: For example, a model might combine weather data with solar collector data.
- Extend the scope of the models developed by applying them to other cities.
- Integrate other relevant data sources to improve prediction accuracy for example, incorporate geo-spatial data.

Bibliography

Bibliography

[1] image1 Source of Image 1 - URL: https://t3.gstatic.com/licensed-image?q=tbn:ANd9GcRcf9FiFK243A65CF7cgZJWygno8HBu3vGP1w64W4Dq-W2BGK7h1YoR5fSsjWbkM_sC

[2] image2 Source of Image 2 - URL: https://www.google.com/search?sca_esv=601771759&rlz=1C1GCEA_enDZ1069DZ1069&sxsrf=ACQVn09yxlho_idcbzMRINSM7_GXLnB1vA:1706296805006&q=Types+of+solar+radiation&tbm=isch&source=lnms&sa=X&sqi=2&ved=2ahUKEwiBicb34vuDAxXhQEEAHcQtDbgQ0pQJegQIDBAB#imgrc=B667ad4Slsj1HM

[3] https://weather.com/en-IN/india/news/news/2021-06-21-summer-solstice-longest-day-of-the-year-and-start-of-dakshinayan

[4] earthorbit Earth's Orbit - URL: https://en.wikipedia.org/wiki/Earth%27s_orbit

[5] azimuthangle Definition of the Sun's Azimuth Angle - URL:https://www.nicepng.com/ourpic/u2e6t4e6t4r5i1r5_altitude-describes-how-high-the-sun-is-and/

[6] altitudeazimuth Azimuth and Altitude for Northern Latitudes - URL:https://www.researchgate.net/figure/Azimuth-and-altitude-for-northern-latitudes_fig2_327941333

[7] altitude Altitude - URL: https://www.e-education.psu.edu/meteo300/node/683

[8] incidentradiation Calculating Incident Solar Radiation on an Inclined Surface - URL: http://synergyfiles.com/2015/10/calculating-incident-solar-radiation-on-inclined-surface-easy-method/

[9] solarradiation What is Solar Radiation? - URL: https://planetfacts.org/what-is-solar-radiation/

[10] @miscsource,title = Irradiation globale journalière sur plan horizontal en décembre, howpublished = https://www.researchgate.net/publication/338817741, year = 2022, note = Accessed on: September 18, 2024

[11] Angstrom, A. (1924) Solar and Terrestrial Radiation. Quarterly Journal of the Royal Meteorological Society, 50, 121-126.

[12] Guy Stewart Callendar et Charles David Keeling équations du bilan radiatif calculer les variations du rayonnement solaire sur Terre wiki

[13] ellers, P. J., S. I. Rasool, et H-J. Bolle. « A Review of Satellite Data Algorithms for Studies of the Land Surface ». Bulletin of the American Meteorological Society 71, no 10 (octobre 1990): 1429 47.

[14] Mefti, A., M.Y. Bouroubi, et A. Adane. « Generation of Hourly Solar Radiation for Inclined Surfaces Using Monthly Mean Sunshine Duration in Algeria ». Energy Conversion and

Management 44, no 19 (novembre 2003): 3125 41.

[15] chatten, Kenneth. « Solar Activity Prediction: Timing Predictors and Cycle 24 ». Journal of Geophysical Research: Space Physics 107, no A11 (novembre 2002).

[16] Theodor Landscheidt, « Solar Forcing of El Niño and La Niña»,The solar cycle and terrestrial climate, Solar and space weather Euroconference (1 : 2000 : Santa Cruz de Tenerife, Tenerife, Spain).

[17] Nishizuka, N., K. Sugiura, Y. Kubo, M. Den, et M. Ishii. « Deep Flare Net (DeFN) Model for Solar Flare Prediction ». The Astrophysical Journal 858, no 2 (14 mai 2018): 113. https://doi.org/10.3847/1538-4357/aab9a7.

[18] Upendran, Vishal, Mark C. M. Cheung, Shravan Hanasoge, et Ganapathy Krishnamurthi. « Solar Wind Prediction Using Deep Learning ». Space Weather 18, no 9 (septembre 2020): e2020SW002478.

[19] Nwokolo, Samuel Chukwujindu, et Julie C. Ogbulezie. « A Qualitative Review of Empirical Models for Estimating Diffuse Solar Radiation from Experimental Data in Africa ». Renewable and Sustainable Energy Reviews 92 (septembre 2018): 353 93.

[20] Almorox, Javier, Cyril Voyant, Nadjem Bailek, Alban Kuriqi, et J.A. Arnaldo. « Total Solar Irradiance's Effect on the Performance of Empirical Models for Estimating Global Solar Radiation: An Empirical-Based Review ». Energy 236 (décembre 2021): 121486.

[21] Suganthi, L., S. Iniyan, et Anand A. Samuel. « Applications of Fuzzy Logic in Renewable Energy Systems – A Review ». Renewable and Sustainable Energy Reviews 48 (août 2015): 585 607.

[22] Sridharan, M. « Short Review on Various Applications of Fuzzy Logic-Based Expert Systems in the Field of Solar Energy ». International Journal of Ambient Energy 43, no 1 (31 décembre 2022): 5112 28.

[23] Shah, D., K. Patel, et M. Shah. « Prediction and Estimation of Solar Radiation Using Artificial Neural Network (ANN) and Fuzzy System: A Comprehensive Review ». International Journal of Energy and Water Resources 5, no 2 (juin 2021): 219 33.

[24] Patel, Daxal, Shriya Patel, Poojan Patel, et Manan Shah. « Solar Radiation and Solar Energy Estimation Using ANN and Fuzzy Logic Concept: A Comprehensive and Systematic Study ». Environmental Science and Pollution Research 29, no 22 (mai 2022): 32428 42.

[25] Chellali, Farouk, Kabouche Nourdine, et Abdelmadjid Recioui. « A Review on Solar Radiation Assessment and Forecasting in Algeria (Part 1: Solar Radiation Assessment) ». Algerian Journal of Signals and Systems 6, no 2 (30 juin 2021): 75 97.

[26] Kabouche, Nourdine, Farouk Chellali, et Aem Recioui. « A Review on Solar Radiation Assessment and Forecasting in Algeria: (Part 2; Solar Radiation Forecasting) ». Algerian Journal of Signals and Systems 6, no 3 (30 septembre 2021): 130 46.

[27] Voyant, Cyril, Gilles Notton, Soteris Kalogirou, Marie-Laure Nivet, Christophe Paoli, Fabrice Motte, et Alexis Fouilloy. « Machine Learning Methods for Solar Radiation Forecasting: A Review ». Renewable Energy 105 (mai 2017): 569 82.

[28] Gupta, Shubham, Amit Kumar Singh, Sachin Mishra, Pradeep Vishnuram, Nagaraju Dharavat, Narayanamoorthi Rajamanickam, Ch. Naga Sai Kalyan, Kareem M. AboRas, Naveen Kumar Sharma, et Mohit Bajaj. « Estimation of Solar Radiation with Consideration of Terrestrial Losses at a Selected Location—A Review ». Sustainability 15, no 13 (22 juin 2023): 9962.

[29] Kumari, Pratima, et Durga Toshniwal. « Deep Learning Models for Solar Irradiance Forecasting: A Comprehensive Review ». Journal of Cleaner Production 318 (octobre 2021): 128566.

[30] Nawab, Faisal, Ag Sufiyan Abd Hamid, Adnan Ibrahim, Kamaruzzaman Sopian, Ahmad Fazlizan, et Mohd Faizal Fauzan. « Solar Irradiation Prediction Using Empirical and Artificial Intelligence Methods: A Comparative Review ». Heliyon 9, no 6 (juin 2023): e17038.

[31] ssaf, Abbas Mohammed, Habibollah Haron, Haza Nuzly Abdull Hamed, Fuad A. Ghaleb, Sultan Noman Qasem, et Abdullah M. Albarrak. « A Review on Neural Network Based Models for Short Term Solar Irradiance Forecasting ». Applied Sciences 13, no 14 (19 juillet 2023): 8332.

[32] Ajith, Meenu, et Manel Martínez-Ramón. « Deep Learning Algorithms for Very Short Term Solar Irradiance Forecasting: A Survey ». Renewable and Sustainable Energy Reviews 182 (août 2023): 113362.

[33] Quej, Victor H., Javier Almorox, Mirzakhayot Ibrakhimov, et Laurel Saito. « Estimating Daily Global Solar Radiation by Day of the Year in Six Cities Located in the Yucatán Peninsula, Mexico ». Journal of Cleaner Production 141 (janvier 2017): 75 82.

[34] Quej, Victor H., Javier Almorox, Mirzakhayot Ibrakhimov, et Laurel Saito. « Empirical Models for Estimating Daily Global Solar Radiation in Yucatán Peninsula, Mexico ». Energy Conversion and Management 110 (février 2016): 448 56.

[35] Hassan, Muhammed A., A. Khalil, S. Kaseb, et M.A. Kassem. « Independent Models for Estimation of Daily Global Solar Radiation: A Review and a Case Study ». Renewable and Sustainable Energy Reviews 82 (février 2018): 1565 75.

[36] Feng, Yu, Daozhi Gong, Qingwen Zhang, Shouzheng Jiang, Lu Zhao, et Ningbo Cui. « Evaluation of Temperature-Based Machine Learning and Empirical Models for Predicting Daily Global Solar Radiation ». Energy Conversion and Management 198 (octobre 2019): 111780.

[37] Voyant, Cyril, Gilles Notton, Jean-Laurent Duchaud, Javier Almorox, et Zaher Mundher Yaseen. « Solar Irradiation Prediction Intervals Based on Box–Cox Transformation and

Univariate Representation of Periodic Autoregressive Model ». Renewable Energy Focus 33 (juin 2020): 43 53.

[38] Dhakal, Sandeep, Yogesh Gautam, et Aayush Bhattarai. « Evaluation of Temperature-Based Empirical Models and Machine Learning Techniques to Estimate Daily Global Solar Radiation at Biratnagar Airport, Nepal ». Advances in Meteorology 2020 (16 septembre 2020): 1 11.

[39] Asri, Rishal, Koko Friansa, et Sefrani Siregar. « Predicting Solar Irradiance Using Regression Model (Case Study: ITERA Solar Power Plant) ». IOP Conference Series: Earth and Environmental Science 830, no 1 (1 septembre 2021): 012080.

[40] Acharya, Bishwa B., Yugal K. Shrestha, Sandeep Dhakal, Usha Joshi, et Khem N. Poudyal. « Prediction of Daily Global Solar Radiation Using Different Empirical Models at Eastern Subtropical Region, Nepal », 22 janvier 2021.

[41] Bounoua, Zineb, Laila Ouazzani Chahidi, et Abdellah Mechaqrane. « Estimation of Daily Global Solar Radiation Using Empirical and Machine-Learning Methods: A Case Study of Five Moroccan Locations ». Sustainable Materials and Technologies 28 (juillet 2021): e00261.

[42] Oyewola, Olanrewaju M., Tchilabalo E. Patchali, Olusegun O. Ajide, Satyanand Singh, et Olaniran J. Matthew. « Global Solar Radiation Predictions in Fiji Islands Based on Empirical Models ». Alexandria Engineering Journal 61, no 11 (novembre 2022): 8555 71.

[43] Li, Qi, Miloud Bessafi, et Peng Li. « Mapping Prediction of Surface Solar Radiation with Linear Regression Models: Case Study over Reunion Island ». Atmosphere 14, no 9 (23 août 2023): 1331.

[44] Zeynab Ramedani a, Mahmoud Omid b, Alireza Keyhani b, Benyamin Khoshnevisan b, Hadi Saboohi,"A comparative study between fuzzy linear regression and support vector regression for global solar radiation prediction in Iran", Solar Energy 109 (2014) 135–143.

[45] Rizwan, M., Majid Jamil, SheerazKirmani, et D.P. Kothari. « Fuzzy Logic Based Modeling and Estimation of Global Solar Energy Using Meteorological Parameters ». Energy 70 (juin 2014): 685 91. https://doi.org/10.1016/j.energy.2014.04.057.

[46] Remus St. Boata, Paul Gravila ," Functional fuzzy approach for forecasting daily global solar irradiation", Atmospheric Research 112 (2012) 79–88

[47] Remus Boata," Modeling of daily global solar irradiation in Timisoara by using a fuzzy approach", Annals of west university of Timisoara physics ;Vol. LX, 2018.

[48] Dept. of Computer Science, College of Science, University of Duhok, Kurdistan Region-Iraq, et Jwan Abdulkhaliq Mohammed. « THE PREDICTION OF SOLAR RADIATION USING FUZZY LOGIC: A CASE STUDY ». The Journal of The University of Duhok 21, no 2 (27 novembre 2018): 34 44.

[49] Mehta, Sahil, et Prasenjit Basak. « Solar Irradiance Forecasting Using Fuzzy Logic and Multilinear Regression Approach: A Case Study of Punjab, India ». International Journal of Advances in Applied Sciences 8, no 2 (1juin 2019): 125.

[50] Bahani, Khalid, Hamza Ali-Ou-Salah, Mohammed Moujabbir, Benyounes Oukarfi, et Mohammed Ramdani. « A Novel Interpretable Model for Solar Radiation Prediction Based on Adaptive Fuzzy Clustering and Linguistic Hedges ». In Proceedings of the 13th International Conference on Intelligent Systems: Theories and Applications, 1 6. Rabat Morocco: ACM, 2020.

[51] Abdulhamid, Idris A Masoud, Ahmet Sahiner, et Murat Ozturk. « Temperature And Pressure Based Estimation Of Daily Global Solar Radiation Over Turkey Using Fuzzy Logic Modeling », s. d.

[52] Al-Kaissi, Shahad M., et Osama T. Al-Taai. «Prediction of Global Solar Irradiation by Using Fuzzy Logic». In 2021 1st Babylon International Conference on Information Technology and Science (BICITS), 9297. Babil,Iraq:IEEE,2021.

[53] Sridharan, M. « Generalized Regression Neural Network Model Based Estimation of Global Solar Energy Using Meteorological Parameters ». Annals of Data Science, 3 janvier 2021.

[54] Silva, Maurício Bruno Prado da, João Francisco Escobedo, Taiza Juliana Rossi, CíceroManoeldosSantos, etSílvia Helena ModeneseGorladaSilva. « Performance of the Angstrom-Prescott Model (A-P) and SVM and ANN Techniques to Estimate Daily Global Solar Irradiation in Botucatu/SP/Brazil». Journal of Atmospheric and Solar-Terrestrial Physics 160 (juillet2017):11 23.

[55] Sivaneasan, B., C.Y. Yu, et K.P. Goh. « Solar Forecasting Using ANN with Fuzzy Logic Pre-Processing ». Energy Procedia 143 (décembre 2017): 727 32. https://doi.org/10.1016/j.egypro.2017.12.753.

[56] Guariso, Giorgio, Giuseppe Nunnari, et Matteo Sangiorgio. « Multi-Step Solar Irradiance Forecasting and Domain Adaptation of Deep Neural Networks ». Energies 13, no 15 (2 août 2020): 3987.

[57] Pang, Zhihong, Fuxin Niu, et Zheng O'Neill. « Solar Radiation Prediction Using Recurrent Neural Network and Artificial Neural Network: A Case Study with Comparisons ». Renewable Energy 156 (août 2020): 279 89.

[58] Haider, Syed Altan, Muhammad Sajid, Hassan Sajid, Emad Uddin, et Yasar Ayaz. « Deep Learning and Statistical Methods for Short- and Long-Term Solar Irradiance Forecasting for Islamabad ». Renewable Energy 198 (octobre 2022): 51 60.

[59] Liao, Xuan, Rui Zhu, et Man Sing Wong. « Simplified Estimation Modeling of Land Surface Solar Irradiation: A Comparative Study in Australia and China ». Sustainable Energy Technologies and Assessments 52 (août 2022): 102323.

[60] Alzahrani, Ahmad. « Short-Term Solar Irradiance Prediction Based on Adaptive Extreme Learning Machine and Weather Data ». Sensors 22, no 21 (27 octobre 2022): 8218.

[61] Gao, Yuan, Shohei Miyata, et Yasunori Akashi. « Multi-Step Solar Irradiation Prediction Based on Weather Forecast and Generative Deep Learning Model ». Renewable Energy 188 (avril 2022): 637 50.

[62] Tajjour, Salwan, Shyam Singh Chandel, Majed A. Alotaibi, Hasmat Malik, Fausto Pedro García Márquez, et Asyraf Afthanorhan. « Short-Term Solar Irradiance Forecasting Using Deep Learning Techniques: A Comprehensive Case Study ». IEEE Access 11 (2023): 119851 61.

[63] Tolun, Gülizar-Gizem, et Yusuf-Alper Kaplan. « Development Of Backpropagation Algorithm For Estimating Solar Radiation: A Case Study In Turkey ». Revue Roumaine Des Sciences Techniques — Série Électrotechnique Et Énergétique 68, no 3 (12 octobre 2023): 313 16.

[64] Benali L, Notton G, Fouilloy A, Voyant C, et Dizene R. « Solar Radiation Forecasting Using Artificial Neural Network and Random Forest Methods: Application to Normal Beam, Horizontal Diffuse and Global Components ». Renewable Energy 132 (mars 2019): 871 84.

[65] Liu, J, M Y Cao, D Bai, et R Zhang. « Solar Radiation Prediction Based on Random Forest of Feature-Extraction ». IOP Conference Series: Materials Science and Engineering 658, no 1 (1 octobre 2019): 012006.

[66] Srivastava, Rachit, A.N. Tiwari, et V.K. Giri. « Solar Radiation Forecasting Using MARS, CART, M5, and Random Forest Model: A Case Study for India ». Heliyon 5, no 10 (octobre 2019): e02692.

[67] Wu, Wei, Xiaoping Tang, Jiake Lv, Chao Yang, et Hongbin Liu. « Potential of Bayesian Additive Regression Trees for Predicting Daily Global and Diffuse Solar Radiation in Arid and Humid Areas ». Renewable Energy 177 (novembre 2021): 148 63.

[68] Fan, Junliang, Lifeng Wu, Fucang Zhang, Huanjie Cai, Wenzhi Zeng, Xiukang Wang, et Haiyang Zou. « Empirical and Machine Learning Models for Predicting Daily Global Solar Radiation from Sunshine Duration: A Review and Case Study in China ». Renewable and Sustainable Energy Reviews 100 (février 2019): 186 212.

[69] Alizamir Meysam, Sungwon Kim, Ozgur Kisi, et Mohammad Zounemat-Kermani. « A Comparative Study of Several Machine Learning Based Non-Linear Regression Methods in Estimating Solar Radiation: Case Studies of the USA and Turkey Regions ». Energy 197 (avril 2020): 117239.

[70] Arora, Isha, Jaimala Gambhir, et Tarlochan Kaur. « Solar Irradiance Forecasting Using Decision Tree and Ensemble Models ». In 2020 Second International Conference on Inven-

tive Research in Computing Applications (ICIRCA), 675 81. Coimbatore, India: IEEE, 2020.

[71] Jumin Ellysia, Basaruddin Faridah Bte, Yusoff Yuzainee Bte. Md, Latif Sarmad Dashti, et Ahmed Ali Najah. « Solar Radiation Prediction Using Boosted Decision Tree Regression Model: A Case Study in Malaysia ». Environmental Science and Pollution Research 28, no 21 (juin 2021): 26571 83.

[72] Kor Hakan. « Global Solar Radiation Prediction Model with Random Forest Algorithm ». Thermal Science 25, no Spec. issue 1 (2021): 31 39.

[73] Rahul, Gupta Aakash, Bansal Ankur et Roy Kshitij. « Solar Energy Prediction Using Decision Tree Regressor ». In 2021 5th International Conference on Intelligent Computing and Control Systems (ICICCS), 489 95. Madurai, India: IEEE, 2021.

[74] Wu, Wei, Xiaoping Tang, Jiake Lv, Chao Yang, et Hongbin Liu. « Potential of Bayesian Additive Regression Trees for Predicting Daily Global and Diffuse Solar Radiation in Arid and Humid Areas ». Renewable Energy 177 (novembre 2021): 148 63.

[75] Sehrawat, Neha, Sahil Vashisht, et Amritpal Singh. « Solar Irradiance Forecasting Models Using Machine Learning Techniques and Digital Twin: A Case Study with Comparison ». International Journal of Intelligent Networks 4 (2023): 90 102.

[76] Alzahrani, Ahmad, Pourya Shamsi, Cihan Dagli, et Mehdi Ferdowsi. « Solar Irradiance Forecasting Using Deep Neural Networks ». Procedia Computer Science 114 (2017): 304 13.

[77] Hassan Muhammed A, Khalil A, Kaseb S, et Kassem M.A « Potential of Four Different Machine-Learning Algorithms in Modeling Daily Global Solar Radiation ». RenewableEnergy 111 (octobre 2017): 52 62.

[78] Khosravi, A., R.N.N. Koury, L. Machado, et J.J.G. Pabon. « Prediction of Hourly Solar Radiation in Abu Musa Island Using Machine Learning Algorithms ». Journal of Cleaner Production 176 (mars 2018): 63 75.

[79] Fan, Junliang, Xiukang Wang, Lifeng Wu, Hanmi Zhou, Fucang Zhang, Xiang Yu, Xianghui Lu, et Youzhen Xiang. « Comparison of Support Vector Machine and Extreme Gradient Boosting for Predicting Daily Global Solar Radiation Using Temperature and Precipitation in Humid Subtropical Climates: A Case Study in China ». Energy Conversion and Management 164 (mai 2018): 102 11.

[80] Javed Abeera, Bakhtiar Khan Kasi, et Faisal Ahmad Khan. « Predicting Solar Irradiance Using Machine Learning Techniques ». In 2019 15th International Wireless Communications & Mobile Computing Conference (IWCMC), 1458 62. Tangier, Morocco: IEEE, 2019.

[81] Bellido-Jiménez, Juan Antonio, Javier Estévez Gualda, et Amanda Penélope García-Marín.

« Assessing New Intra-Daily Temperature-Based Machine Learning Models to Outperform Solar Radiation Predictions in Different Conditions ». Applied Energy 298 (septembre 2021): 117211.

[82] Jia, Dongyu, Liwei Yang, Tao Lv, Weiping Liu, Xiaoqing Gao, et Jiaxin Zhou. « Evaluation of Machine Learning Models for Predicting Daily Global and Diffuse Solar Radiation under Different Weather/Pollution Conditions ». Renewable Energy 187 (mars 2022): 896 906.

[83] Nematchoua Modeste Kameni, Orosa José A, et Afaifia Marwa. « Prediction of Daily Global Solar Radiation and Air Temperature Using Six Machine Learning Algorithms; a Case of 27 European Countries ». Ecological Informatics 69 (juillet 2022): 101643.

[84] Demir, Vahdettin, et Hatice Citakoglu. « Forecasting of Solar Radiation Using Different Machine Learning Approaches ». Neural Computing and Applications 35, no 1 (janvier 2023): 887 906.

[85] Chen, Chao-Rong, et Unit Kartini. « K-Nearest Neighbor Neural Network Models for Very Short-Term Global Solar Irradiance Forecasting Based on Meteorological Data ». Energies 10, no 2 (8 février 2017): 186.

[86] Khosravi, A., R.N.N. Koury, L. Machado, et J.J.G. Pabon. « Prediction of Hourly Solar Radiation in Abu Musa Island Using Machine Learning Algorithms ». Journal of Cleaner Production 176 (mars 2018): 63 75.

[87] Zhang, Yixuan, Ningbo Cui, Yu Feng, Daozhi Gong, et Xiaotao Hu. « Comparison of BP, PSO-BP and Statistical Models for Predicting Daily Global Solar Radiation in Arid Northwest China ». Computers and Electronics in Agriculture 164 (septembre 2019): 104905.

[88] Ozoegwu, Chigbogu Godwin. « Artificial Neural Network Forecast of Monthly Mean Daily Global Solar Radiation of Selected Locations Based on Time Series and Month Number ». Journal of Cleaner Production 216 (avril 2019): 1 13.

[89] Gouda, Shaban G., Zakia Hussein, Shuai Luo, et Qiaoxia Yuan. « Model Selection for Accurate Daily Global Solar Radiation Prediction in China ». Journal of Cleaner Production 221 (juin 2019): 132 44.

[90] Zang, Haixiang, Lilin Cheng, Tao Ding, Kwok W. Cheung, Miaomiao Wang, Zhinong Wei, et Guoqiang Sun. « Estimation and Validation of Daily Global Solar Radiation by Day of the Year-Based Models for Different Climates in China ». Renewable Energy 135 (mai 2019): 984 1003.

[91] Lubbe, Foster, Jacques Maritz, et Thomas Harms. « Evaluating the Potential of Gaussian Process Regression for Solar Radiation Forecasting: A Case Study ». Energies 13, no 20 (21 octobre 2020): 5509. https://doi.org/10.3390/en13205509.

[92] Brahma, Banalaxmi, et Rajesh Wadhvani. « Solar Irradiance Forecasting Based on Deep Learning Methodologies and Multi-Site Data ». Symmetry 12, no 11 (5 novembre 2020):

1830.

[93] Araujo, Jose Manuel Soares De. « Combination of WRF Model and LSTM Network for Solar Radiation Forecasting—Timor Leste Case Study ». Computational Water, Energy, and Environmental Engineering 09, no 04 (2020): 108 44.

[94] Rai, Amit, Ashish Shrivastava, et Kartick C Jana. « A CNN-BILSTM Based Deep Learning Model for Mid-term Solar Radiation Prediction ». International Transactions on Electrical Energy Systems 31, no 9 (septembre 2021).

[95] Zang, Haixiang, Ling Liu, Li Sun, Lilin Cheng, Zhinong Wei, et Guoqiang Sun. « Short-Term Global Horizontal Irradiance Forecasting Based on a Hybrid CNN-LSTM Model with Spatiotemporal Correlations ». Renewable Energy 160 (novembre 2020): 26 41.

[96] Liu, Yanfeng, Yong Zhou, Yaowen Chen, Dengjia Wang, Yingying Wang, et Ying Zhu. « Comparison of Support Vector Machine and Copula-Based Nonlinear Quantile Regression for Estimating the Daily Diffuse Solar Radiation: A Case Study in China ». Renewable Energy 146 (février 2020): 1101 12.

[97] Ali-Ou-Salah, Hamza, Benyounes Oukarfi, Khalid Bahani, et Mohammed Moujabbir. « A New Hybrid Model for Hourly Solar Radiation Forecasting Using Daily Classification Technique and Machine Learning Algorithms ». Édité par Shigeyuki Hamori. Mathematical Problems in Engineering 2021 (15 mars 2021): 1 12.

[98] Zhao, Shuting, Lifeng Wu, Youzhen Xiang, Jianhua Dong, Zhen Li, Xiaoqiang Liu, Zijun Tang, et al. « Coupling Meteorological Stations Data and Satellite Data for Prediction of Global Solar Radiation with Machine Learning Models ». Renewable Energy 198 (octobre 2022): 1049 64.

[99] Ghimire, Sujan, Ravinesh C. Deo, David Casillas-Pérez, Sancho Salcedo-Sanz, Ekta Sharma, et Mumtaz Ali. « Deep Learning CNN-LSTM-MLP Hybrid Fusion Model for Feature Optimizations and Daily Solar Radiation Prediction ». Measurement 202 (octobre 2022): 111759.

[100] Ghimire, Sujan, Thong Nguyen-Huy, Ravinesh C Deo, David Casillas-Pérez, et Sancho Salcedo-Sanz. « Efficient Daily Solar Radiation Prediction with Deep Learning 4-Phase Convolutional Neural Network, Dual Stage Stacked Regression and Support Vector Machine CNN-REGST Hybrid Model ». Sustainable Materials and Technologies 32 (juillet 2022): e00429.

[101] Sehrawat, Neha, Sahil Vashisht, et Amritpal Singh. « Solar Irradiance Forecasting Models Using Machine Learning Techniques and Digital Twin: A Case Study with Comparison ». International Journal of Intelligent Networks 4 (2023): 90 102.

[102] Liu, Jingxuan, Haixiang Zang, Fengchun Zhang, Lilin Cheng, Tao Ding, Zhinong Wei, et Guoqiang Sun. « A Hybrid Meteorological Data Simulation Framework Based on Time-

Series Generative Adversarial Network for Global Daily Solar Radiation Estimation ». Renewable Energy 219 (décembre 2023): 119374.

[103] Irshad, Kashif, Nazrul Islam, Abdullatif A. Gari, Salem Algarni, Talal Alqahtani, et Binash Imteyaz. « Arithmetic Optimization with Hybrid Deep Learning Algorithm Based Solar Radiation Prediction Model ». Sustainable Energy Technologies and Assessments 57 (juin 2023): 103165.

[104] Abdallah, Mohammed, Babak Mohammadi, Hamid Nasiri, Okan Mert Katipoğlu, Modawy Adam Ali Abdalla, et Mohammad Mehdi Ebadzadeh. « Daily Global Solar Radiation Time Series Prediction Using Variational Mode Decomposition Combined with Multi-Functional Recurrent Fuzzy Neural Network and Quantile Regression Forests Algorithm ». Energy Reports 10 (novembre 2023): 4198 4217.

[105] Goliatt, Leonardo, et Zaher Mundher Yaseen. « Development of a Hybrid Computational Intelligent Model for Daily Global Solar Radiation Prediction ». Expert Systems with Applications 212 (février 2023): 118295.

[106] Alizamir, Meysam, Jalal Shiri, Ahmad Fakheri Fard, Sungwon Kim, AliReza Docheshmeh Gorgij, Salim Heddam, et Vijay P. Singh. « Improving the Accuracy of Daily Solar Radiation Prediction by Climatic Data Using an Efficient Hybrid Deep Learning Model: Long Short-Term Memory (LSTM) Network Coupled with Wavelet Transform ». Engineering Applications of Artificial Intelligence 123 (août 2023): 106199.

[107] Xing, Liwen. « Predicting Daily Solar Radiation Using a Novel Hybrid Long Short-Term Memory Network across Four Climate Regions of China ». Computers and Electronics in Agriculture, 2023.

[108] Lu, Yunbo, Lunche Wang, Canming Zhu, Ling Zou, Ming Zhang, Lan Feng, et Qian Cao. « Predicting Surface Solar Radiation Using a Hybrid Radiative Transfer–Machine Learning Model ». Renewable and Sustainable Energy Reviews 173 (mars 2023): 113105.

[109] Neshat, Mehdi, Meysam Majidi Nezhad, Seyedali Mirjalili, Davide Astiaso Garcia, Erik Dahlquist, et Amir H. Gandomi. « Short-Term Solar Radiation Forecasting Using Hybrid Deep Residual Learning and Gated LSTM Recurrent Network with Differential Covariance Matrix Adaptation Evolution Strategy ». Energy 278 (septembre 2023): 127701.

[110] Ouali, K., et R. Alkama. « A New Model of Global Solar Radiation Based on Meteorological Data in Bejaia City (Algeria) ». Energy Procedia 50 (2014): 670 76.

[111] Mecibah, Mohamed Salah, Taqiy Eddine Boukelia, Reda Tahtah, et Kacem Gairaa. « Introducing the Best Model for Estimation the Monthly Mean Daily Global Solar Radiation on a Horizontal Surface (Case Study: Algeria) ». Renewable and Sustainable Energy Reviews 36 (août 2014): 194 202.

[112] Belaid, S., et A. Mellit. « Prediction of Daily and Mean Monthly Global Solar Radiation

Using Support Vector Machine in an Arid Climate ». Energy Conversion and Management 118 (juin 2016): 105 18.

[113] Achour, Lazhar, Malek Bouharkat, Ouarda Assas, et Omar Behar. « Smart Model for Accurate Estimation of Solar Radiation ». Frontiers in Energy 14, no 2 (juin 2020): 383 99.

[114] Smaili, K, N Kasbadji Merzouk, et M Merzouk. « Atlas Climatiques de l'Irradiation Solaire Journalière en Algérie », 2018.

[115] Marif, Y, B Hebbal, et R Maouedj. « Empirical Models for Estimating Solar », s. d.

[116] Rabehi, Abdelaziz, Mawloud Guermoui, et Djemoui Lalmi. « Hybrid Models for Global Solar Radiation Prediction: A Case Study ». International Journal of Ambient Energy 41, no 1 (2 janvier 2020): 31 40.

[117] Guermoui, Mawloud, Farid Melgani, et Céline Danilo. « Multi-Step Ahead Forecasting of Daily Global and Direct Solar Radiation: A Review and Case Study of Ghardaia Region ». Journal of Cleaner Production 201 (novembre 2018): 716 34.

[118] Benatiallah, Djelloul, Ali Benatiallah, Kada Bouchouicha, Messaoud Hamouda, et Bahous Nasri. « An Empirical Model for Estimating Solar Radiation in the Algerian Sahara », 030031. Beirut, Lebanon, 2018.

[119] Benatiallah, Djelloul, Kada Bouchouicha, Ali Benatiallah, Abdelkader Harrouz, Bahous Nasri, . « Forecasting of Solar Radiation Using an Empirical Model ». Algerian Journal of Renewable Energy and Sustainable Development 01, no 02 (15 décembre 2019): 212 19.

[120] Benmouiza, K. Hourly solar irradiation forecast using hybrid local gravitational clustering and group method of data handling methods. Environ Sci Pollut Res 29, 60792–60810 (2022).

[121] Ahlam, Senouci, Maouedj Rachid, Benatiallah Ali, Benatiallah Djelloul, et Bouchouicha Kada. « Enhanced Daily Global Solar Radiation Prediction Through Hybrid Artificial Neural Network and Adaptive Neuro-Fuzzy Inference System with Meta-Heuristic Algorithm Integration ». Instrumentation Mesure Métrologie 22, no 6 (27 décembre 2023): 241 51.

[122] Dhiaeddine, Mostefaoui Mohamed, Benmouiza Khalil, et Oubbati Youcef. « Optimal Artificial Neural Network Configurations for Hourly Solar Irradiation Estimation ». International Journal of Electrical and Computer Engineering (IJECE) 13, no 5 (1 octobre 2023): 4878.

[123] Djeldjli, Halima, Djelloul Benatiallah, Camel Tanougast, et Ali Benatiallah. « Solar Radiation Forecasting Based on ANN, SVM and a Novel Hybrid FFA-ANN Model: A Case Study of Six Cities South of Algeria ». AIMS Energy 12, no 1 (2024): 62 83.

[124] Yahiaoui, Samah, et Ouarda Assas. « Comparison of Solar Radiation Models Using Me-

teorological Parameters ». Energy Systems, 5 juillet 2023.

[125] Yahiaoui, Samah, et Ouarda Assas. « Smart Prediction of Global Solar Radiation for the City of Batna Using Fuzzy Logic ».2nd International Conference on Computational & Applied Physics - ICCAP 2023 ,October 08 a 10, 2023. https://univ-blida.dz/iccap-blida1/.

[126] Yahiaoui, Samah, et Ouarda Assas.«Friendly Deep Learning Model for Estimating Daily Global Solar Radiation ».IEEE Commenincation .November 2023.Conference: 2023 International Conference on Electrical Engineering and Advanced Technology (ICEEAT).

[127] https://www.soda-pro.com/web-services/radiation/helioclim-1.

[128] https://www.soda-pro.com/web-services/meteo-data/merra

[129] Mamdani, E.H. and Assilan, S.,"An experiment in linguistic synthesis with a fuzzy controller". Int. J. Man Mach.Stud.1975,7(1),1–13.

[130] https://aiml.com/what-is-the-basic-architecture-of-an-artificial-neural-network-ann/

[131] https://www.simplilearn.com/tutorials/deep-learning- tutorial/rnn

[132] https://www.geeksforgeeks.org/introduction-convolution-neural-network/.

[133] https://stackoverflow.com/questions/55385906/whats-the-input-of-each-lstm-layer-in-a-stacked-lstm-network.

[134] https://www.javatpoint.com/machine-learning-decision-tree-classification-algorithm.

[135] https://en.wikipedia.org/wiki/Random-forest*.